



University  
of Glasgow

<https://theses.gla.ac.uk/8351/>

This is a digitised version of the original print thesis.

Copyright and moral rights for this work are retained by the author

A copy can be downloaded for personal non-commercial research or study, without prior permission or charge

This work cannot be reproduced or quoted extensively from without first obtaining permission in writing from the author

The content must not be changed in any way or sold commercially in any format or medium without the formal permission of the author

When referring to this work, full bibliographic details including the author, title, awarding institution and date of the thesis must be given

Enlighten:Theses  
<http://theses.gla.ac.uk/>  
theses@gla.ac.uk

ProQuest Number: 10391164

All rights reserved

INFORMATION TO ALL USERS

The quality of this reproduction is dependent upon the quality of the copy submitted.

In the unlikely event that the author did not send a complete manuscript and there are missing pages, these will be noted. Also, if material had to be removed, a note will indicate the deletion.



ProQuest 10391164

Published by ProQuest LLC (2017). Copyright of the Dissertation is held by the Author.

All rights reserved.

This work is protected against unauthorized copying under Title 17, United States Code  
Microform Edition © ProQuest LLC.

ProQuest LLC.  
789 East Eisenhower Parkway  
P.O. Box 1346  
Ann Arbor, MI 48106 – 1346

# **Inducible Nitric Oxide Synthase Gene Targeting**

BY

Xiao-qing Wei

A thesis submitted for the degree of Doctor of Philosophy  
to the Faculty of Science, University of Glasgow

Department of Immunology,  
Western Infirmary,  
University of Glasgow,  
Glasgow G11 6NT

X.Q.WEI, December, 1995

Theris  
10330  
Copy 2



# CONTENTS

	<u>Page No.</u>
<b>Title</b>	<b>1</b>
<b>Contents</b>	<b>2</b>
<b>Table of Contents</b>	<b>3</b>
<b>List of Figures</b>	<b>9</b>
<b>List of Tables</b>	<b>12</b>
<b>Abbreviations</b>	<b>13</b>
<b>Acknowledgements</b>	<b>16</b>
<b>Declaration</b>	<b>17</b>
<b>Summary</b>	<b>18</b>
<b>Chapter 1</b> <u>General Introduction</u>	<b>21</b>
<b>Chapter 2</b> <u>Materials and Methods</u>	<b>42</b>
<b>Chapter 3</b> <u>Inducible Nitric Oxide Synthase cDNA Clone</u>	<b>71</b>
<b>Chapter 4</b> <u>Inducible Nitric Oxide Synthase Gene Targeting</u>	<b>87</b>
<b>Chapter 5</b> <u>Biological Phenotypes of iNOS Mutant Mice</u>	<b>120</b>
<b>Chapter 6</b> <u>General Discussion</u>	<b>141</b>
<b>Bibliography</b>	<b>160</b>

# Table of Content

## Chapter 1

### General Introduction

<b>Part I. Cytokine Inducible Nitric Oxide Synthase</b>	<b>22</b>
<b>1.1. Nitric oxide (NO) and nitric oxide synthase</b>	<b>22</b>
1.1.1. Historical perspective	22
1.1.2. Characteristic of three forms of nitric oxide synthase	23
1.1.3. The functions of NO	24
<b>1.2. Inducible nitric oxide synthase (iNOS)</b>	<b>26</b>
1.2.1. iNOS cDNA cloning from mouse and human libraries	26
1.2.2. iNOS expression	26
1.2.3. Regulation of biosynthesis of nitric oxide from iNOS	27
<b>1.3. The role of iNOS</b>	<b>29</b>
1.3.1. Non-specific defence	29
1.3.2. Inflammation	31
1.3.3. Autoimmunity	31
<b>Part II. Gene Targeting in Mice</b>	<b>32</b>
<b>1.4. New strategies in animal genetics</b>	<b>32</b>
<b>1.5. Gene targeting in mice</b>	<b>34</b>
1.5.1. Homologous recombination	34
1.5.2. Design of a gene targeting construct	35
1.5.3. Embryonic stem (ES) cells	37
1.5.4. Screening the genetic mutation in ES cells	38
1.5.5. Introducing the mutated gene into mice	39
<b>1.6. Summary and rational of the project</b>	<b>40</b>

## Chapter 2

### Materials and Methods

2.1. Lambda phage	43
2.2. Library screening	43
2.3. Double stranded DNA probe labelling	44
2.4. Lambda phage DNA purification	44
2.5. Excision of the pBluescript from the lambda ZAPII vector	45
2.6. DNA restriction enzymes digestion	46
2.7. Dephosphorylation of DNA fragment ends	46
2.8. Agarose gel electrophoresis	47
2.9. Purification of DNA fragments from agarose gels	47
2.10. DNA ligation.	48
2.11. Transformation of bacterial strains	48
2.12. Isolation of plasmid DNA	50
2.13. DNA sequencing	51
2.14. Introduction of synthetic oligonucleotide into plasmid vector	53
2.15. Southern blot analysis of Lambda phage DNA and genomic DNA	53
2.16. Isolation of total cellular RNA	55
2.17. Isolation of polyadenylated messenger RNA (poly A <sup>+</sup> mRNA)	56
2.18. Reverse transcribed polymerase chain reaction (RT-PCR)	56
2.19. ES cell culture	57
2.20. Purification and linearisation of the gene targeting vector	58
2.21. Electroporation of ES cells	58
2.22. Neomycin (G418) resistance colonies selection	58
2.23. Preparation of Low temperature agarose ES cell plugs	58
2.24. Restriction digestion of DNA in plugs	59
2.25. Screening G418 resistant colonies	59

2.26. Freezing, storage, and thawing of ES cell lines	59
2.27. Blastocyst injection and the production of chimeras	60
2.28. Germline transmission and the generation of heterozygous mice	60
2.29. DNA isolation from mice tails	61
2.30. Elicitation and culture of peritoneal macrophages	61
2.31. Greiss reaction for NO <sub>2</sub> measurement	61
2.32. Northern blotting	62
2.33. iNOS Western blotting	62
2.34. Growth and maintenance of <i>Leishmania major</i>	62
2.35. <i>Leishmania major</i> infection	63
2.36. Preparation of parasite antigens	64
2.37. Parasite quantitation in footpads	64
2.38. ELISA for IL-4 and IFN- $\gamma$	65
2.39. Measurement of specific antibody responses	65
2.40. Antigen specific proliferation <i>in vitro</i>	66
2.41. Carrageenan inflammation mouse model	66
2.42. LPS mouse shock model	66
2.43. T-cell proliferation assays	67
2.44. T-cell phenotyping	67

### Chapter 3

#### Inducible Nitric Oxide Synthase cDNA Clone

3.1. Introduction	72
3.2. $\lambda$ Phage cDNA library Screening	72
3.3. cDNA subclones	73
3.4. Sequencing of subclones	73
3.5. Making a full-length murine iNOS cDNA clone	75
3.6. Double strand cDNA sequencing for the J774 iNOS cDNA	75
3.7. Summary	81

## Chapter 4

### Inducible Nitric Oxide Synthase Gene Targeting

<b>4.1. Introduction</b>	<b>88</b>
<b>4.2. Mouse iNOS genomic DNA cloning and gene mapping</b>	<b>88</b>
<b>4.3. Positive-negative selection constructs</b>	<b>94</b>
<b>4.4. No detectable inducible nitric oxide synthase in ES cell</b>	<b>97</b>
<b>4.5. A large deletion positive selection construct</b>	<b>98</b>
<b>4.6. The design of 5' and 3' specific external probes</b>	<b>98</b>
<b>4.7. Selection and screening of ES cell lines for iNOS gene targeting</b>	<b>101</b>
<b>4.8. Production of chimeras and germ line transmission to offspring</b>	<b>106</b>
<b>4.9. Segregating genotypes</b>	<b>107</b>
<b>4.10. Investigation of the homozygous embryos during development</b>	<b>107</b>
<b>4.11. Identification of the homozygous mice by back crossing</b>	<b>109</b>
<b>4.12. iNOS gene duplication after gene targeting</b>	<b>109</b>
<b>4.13. The expected deletion had not occurred</b>	<b>111</b>
<b>4.14. The murine iNOS gene rearrangement and mutation</b>	<b>112</b>
<b>4.15. The iNOS transposition and replacement events may have occurred in the same locus</b>	<b>115</b>
<b>4.16. No detectable iNOS protein in homozygous mice by Western blot</b>	<b>115</b>
<b>4.17. Culture supernatant NO<sub>2</sub><sup>-</sup> measurement by the Greiss method</b>	<b>115</b>
<b>4.18. Summary</b>	<b>118</b>

## Chapter 5

### Biological Phenotypes of iNOS Mutant Mice

<b>5.1. Introduction</b>	<b>121</b>
<b>5.2. Mice lacking iNOS have normal T cell functions</b>	<b>121</b>
5.2.1. Spleen cells proliferation after ConA stimulation	121
5.2.2. Analysis of spleen cells from immunologically naive mice	122
5.2.3. IFN- $\gamma$ and IL-4 produced by spleen cells <i>in vitro</i>	122
<b>5.3. Mice lacking iNOS fail to control a <i>Leishmania major</i> infection</b>	<b>126</b>
5.3.1. The lesion of a <i>L. major</i> infection	126
5.3.2. Parasite load of infected footpads	126
5.3.3. T cell analysis of mice infected with <i>L. major</i>	128
5.3.4. Spleen cell proliferation of mice infected with <i>L. major</i>	129
5.3.5. IFN- $\gamma$ and IL-4 production after stimulation with <i>L. major</i> antigen <i>in vitro</i>	129
5.3.6. Serum IgG types of mice infected with <i>L. major</i>	129
<b>5.4. Response to local inflammation</b>	<b>132</b>
5.4.1. Reduced inflammation to carrageenin in mutant mice	132
5.4.2. T cell analysis after injection with carrageenin	132
5.4.3. Spleen cells of mutant mice had higher proliferation	134
5.4.4. IFN- $\gamma$ and IL-4 produced after ConA stimulation <i>in vitro</i>	134
<b>5.5. Mice lacking iNOS are more resistant to LPS-included loss of mass and mortality than wild type mice</b>	<b>134</b>
5.5.1. Reduced loss of mass during LPS-induced shock	134
5.5.2. Mutant mice survived from endotoxin-induced shock	138
<b>5.6. Summary</b>	<b>138</b>

## Chapter 6

### General Discussion

<b>6.1. The 5' murine iNOS gene structural organisation</b>	<b>142</b>
<b>6.2. The optimum gene targeting strategy</b>	<b>143</b>
6.2.1. Maximising efficient homologous recombination	143
6.2.2. Enrichment for targeted clones in culture	145
<b>6.3. The iNOS gene mutation</b>	<b>146</b>
6.3.1. iNOS gene is not duplication in wild-type mice	146
6.3.2. End extension of the targeting construct	146
6.3.3. Targeted iNOS gene	147
6.3.4. The larger mutant mRNA	147
6.3.5. Abrogation of iNOS protein translation	149
6.3.6. Detectable nitrite production after prolonged culture period	149
<b>6.4. The role of iNOS in host defence</b>	<b>152</b>
6.4.1. iNOS is important against leishmania infection	152
6.4.2. Possible mechanisms of altered immune response in iNOS mutant mice	153
6.4.3. iNOS may not be involved in parasite growth control by <i>Nramp</i> gene	154
<b>6.5. The roles of iNOS in acute inflammation and LPS-induced death</b>	<b>155</b>
<b>6.6. Conclusions</b>	<b>156</b>
<b>6.7. Future work for iNOS mutant mice</b>	<b>157</b>
6.7.1. Analysis of recombination events	157
6.7.2. Human iNOS (hiNOS) transgenic mice	157
6.7.3. Phenotypic analysis of iNOS deficient mice	159

## List of Figures

Page No.

### Chapter 1

- Figure 1.1** Binding sites of cofactors (NADPH, FMN and FAD) on ncNOS  
ecNOS, iNOS and P450 reductase 25
- Figure 1.2** The generation of NO and the possible mechanism of its anti-  
microbial effects 30
- Figure 1.3** Gene inactivation by homologous recombination with an insertion  
and a replacement 36
- Figure 1.4** Major steps of the procedures involved in the generation of gene  
targeting mice 41

### Chapter 3

- Figure 3.1** Cloning map of J774 iNOS cDNA's 74
- Figure 3.2** Construct of Full-length J774 iNOS cDNA (pFLJ7) 76
- Figure 3.3** The map of J774 iNOS cDNA antisense sequencing 77
- Figure 3.4** Theoretical size of recombinant proteins 82
- Figure 3.5** Schematic representation of the iNOS protein encoded by the J774  
iNOS cDNA 83
- Figure 3.6** The sequence of J774 iNOS cDNA 84

## **Chapter 4**

<b>Figure 4.1</b>	The location of 5' end probe in iNOS cDNA	<b>89</b>
<b>Figure 4.2</b>	The restriction enzymes mapping and four overlapping genomic DNA clones of murine iNOS	<b>91</b>
<b>Figure 4.3</b>	The location of exons 1 to 8 and the subclones	<b>92</b>
<b>Figure 4.4</b>	The first eight exons contribute 937bp of 4117bp of iNOS cDNA	<b>93</b>
<b>Figure 4.5</b>	The double selection gene replacement constructs for PCR screening	<b>96</b>
<b>Figure 4.6</b>	The steps of making iNOS gene replacement construct	<b>99</b>
<b>Figure 4.7</b>	Southern blot analyses to select functional external probes	<b>100</b>
<b>Figure 4.8</b>	Southern blot analyses to select a specific external probe for the 3'- targeting event	<b>102</b>
<b>Figure 4.9</b>	Southern blot by using a 300bp PCR fragment as a 3' end external probe	<b>103</b>
<b>Figure 4.10</b>	The strategy of iNOS gene disruption	<b>104</b>
<b>Figure 4.11</b>	Southern blot analysis for gene targeting event screening	<b>105</b>
<b>Figure 4.12</b>	The map of the flanking of homologous arms from using both 5' and 3' specific external probes	<b>114</b>
<b>Figure 4.13</b>	Southern blot, Northern blot, western blot and nitric measurement for the iNOS deficient	<b>116</b>
<b>Figure 4.14</b>	iNOS Western blot using polyclonal antibodies	<b>117</b>

## **Chapter 5**

<b>Figure 5.1</b>	Proliferation of spleen cells from wild type and mutant mice	<b>123</b>
<b>Figure 5.2</b>	Spleen T cells population of the wild type and mutant mice	<b>124</b>
<b>Figure 5.3</b>	IFN- $\gamma$ and IL-4 production of spleen cells from wild type and mutant mice	<b>125</b>
<b>Figure 5.4</b>	Footpads swelling differences at weeks after <i>L. major</i> infection	<b>127</b>
<b>Figure 5.5</b>	IFN- $\gamma$ and IL-4 production of spleen cells from infected wild type, heterozygous and homozygous mutant mice with <i>L. major</i>	<b>130</b>
<b>Figure 5.6</b>	Serum IgG types of mice infected with <i>L. major</i>	<b>131</b>
<b>Figure 5.7</b>	Footpad swelling differences in the mice with carrageenin injection	<b>133</b>
<b>Figure 5.8</b>	Proliferation of spleen cells from the mice with carrageenin injection	<b>135</b>
<b>Figure 5.9</b>	IFN- $\gamma$ and IL-4 production of spleen cells from the mice with carrageenin injection	<b>136</b>
<b>Figure 5.10</b>	The loss of mass and mortality of LPS induced shock	<b>137</b>

## **Chapter 6**

<b>Figure 6.1</b>	End extension model by homologous recombination	<b>148</b>
<b>Figure 6.2</b>	The map of possibility of duplication exons in the mutant mice	<b>150</b>
<b>Figure 6.3</b>	The map of possibility of fusion messenger in the mutant mice	<b>151</b>

<b>List of Tables</b>	<b>Page No.</b>
 <b><u>Chapter 2</u></b>	
<b>Table 2.1</b> Buffer composition used in restriction enzyme digests	<b>69</b>
<b>Table 2.2</b> Restriction endonucleases used and their recognition sites	<b>70</b>
 <b><u>Chapter 3</u></b>	
<b>Table 3.1</b> The list of deleted cDNA clones and locations	<b>78</b>
 <b><u>Chapter 4</u></b>	
<b>Table 4.1</b> The intron-exon junctions of murine iNOS genome	<b>94</b>
<b>Table 4.2</b> The genotypes of embryos from F2 heterozygous mice mating	<b>108</b>
<b>Table 4.3</b> The genotypes of the offsprings from F2 back-cross	<b>109</b>
<b>Table 4.4</b> The restriction fragments of hybridising bands with 5' and 3' external probes	<b>111</b>
 <b><u>Chapter 5</u></b>	
<b>Table 5.1</b> Content of <i>L. major</i> in the infected footpad	<b>128</b>
<b>Table 5.2</b> T-cell analysis of spleen cells from mice infected with <i>L. major</i>	<b>128</b>
<b>Table 5.3</b> Spleen cell proliferation after stimulation with <i>L. major</i> antigen and Con A	<b>129</b>
<b>Table 5.4</b> T-cell analysis of the mice after injection with carrageenin	<b>132</b>

## ABBREVIATIONS

AP	Alkaline phosphatase
BCIP	5-bromo-4-chloro-3-indo phosphate
bp	Base pair
BSA	Bovine serum albumin
cmp	Counts per minute
Con A	Concanavalin A
dATP	2'-Deoxyadenosine 5'-triphosphate
dCTP	2'-Deoxycytidine 5'-triphosphate
ddH <sub>2</sub> O	Double distilled water
dGTP	2'-Deoxyguanosine 5'-triphosphate
dH <sub>2</sub> O	Distilled water
DIA	differentiation inhibitory activity
DMF	Dimethylformamide
DMSO	Dimethyl sulphoxide
DNA	Deoxyribose nucleic acid
dNTPs	2'-Deoxyribonuceoside 5'-triphosphates
ds	Double stranded
DTT	1,4-dithiothreitol
dTTP	2'-Deoxythymidine 5'-triphosphate
EDTA	Ethylene diamino tetraacetic acid
ELISA	Enzyme linked immunosorbent assay
ES cell	Embryonic stem cell
FACS	Fluorescence-activated cell sorter
FAD	Flavin adenine dinucleotide
FCS	Foetal calf serum
FIAU	1-(2-deoxy,2-fluoro-b-d-arabinofuranosyl)-5-iodouracil
FITC	Fluorescein isothithere
Ganciclovir	9-(1,3-dihydroxy-2-propoxymethyl) guanine)

GTE	Glucose-Tris-EDTA buffer
Hb	haemoglobin
HRP	Horseradish peroxidase
HSV-tk	Herpes simplex virus thymidine kinase
IFN	Interferon
Ig	Immunoglobulin
IL	Interleukin
IPTG	Isopropylthio-b-D-galactoside
LB	Luria-Bertani Medium
LIF	Leukaemia inhibitory factor
LPS	Lipopolysaccharide
MF1	
mRNA	Messenger ribonucleic acid
NADPH	b-Nicotinamide adenine dinucleotide phosphate
NBT	p-nitroblue tetrazolium chloride
<i>Neo</i> gene	neomycin resistance encoding gene
NO	Nitric oxide
NO <sub>2</sub> <sup>-</sup>	Nitrite
NO <sub>3</sub> <sup>-</sup>	Nitrate
OD	Optical density
PBS	Phosphate-buffered saline
PCR	Polymerase chain reaction
PE	Phycoerythrin
PEG	Polyethylene Glycol
QBT	QIAGEN Equilibrate buffer
QC	QIAGEN Wash buffer
QF	QIAGEN Elution buffer
RNA	Ribonucleic acid
RNasin	Ribonuclease inhibitor

rpm	Revolutions per minute
rRNA	Ribosomal ribonucleic acid
RT	Reverse transcription
RT-PCR	Reverse transcription polymerase chain reaction
SM	Sodium-Magnesium buffer
SSC	Sodium-Citrate buffer
T-cell	Thymus derived lymphocyte
Taq	Thermus aquaticus
TBE	Tris-borate/EDTA electrophoresis buffer
TBS	Tris-buffered saline
TCR	T-cell receptor
TE	Tris-EDTA buffer
TGF	Transforming growth factor
Th	Helper T-lymphocyte
TMB	Tris-Magnesium buffer
Tris	Tris (hydroxymethyl) methylamine
tRNA	Transfer ribonucleic acid
U	Units
v/v	Volume per volume
X-gal	5-bromo-4-chloro-3-indolyl-b-D-galactoside
YT	Yeast-Tryptone Medium.

## ACKNOWLEDGEMENTS

Firstly, I wish to express many thanks to Professor Foo Y. Liew, Dr. Ian G. Charles and Dr. Austin Smith for providing me the opportunity to carry this study and for their constant encouragement throughout this work. I am also grateful to the World Health Organisation for financial support.

My sincere thanks also to all colleagues in the Department of Immunology, University of Glasgow; the Department of Cell Biology, Wellcome Research Laboratories, and the Gene Targeting Group, Centre for Genome Research, University of Edinburgh. In particular, I like to thank Dr. John Ansell, Dr. Jan Ure and Dr. Meng Li for their kindness and assistance throughout the gene targeting work.

I would like to thank Dr. Werner Müller (the Institute for genetics, University of Cologne) and Dr. David Moss (the Department of Cell Biology, Wellcome Research Laboratory) for their advice. I am grateful to Dr. Fang Ping Huang and Dr. Damo Xu for assistance and helpful discussion.

Finally, I would like to express my love, appreciation and gratitude to my wife and laboratory partner, Dr. Gui-jie Feng, and my son, Ran Wei, for their understanding, enthusiastic support and encouragement.

Xiao-qing Wei

December, 1995

## **Declaration**

These studies represent original work carried out by the author, and have not been submitted in any form to any other University. Where use has been made of materials provided by others, due acknowledgement has been made.

Xiao-qing Wei

December, 1995

## SUMMARY

Nitric oxide (NO) is a critical mediator of a variety of biological functions, including vascular and muscle relaxation, platelet aggregation, neuronal-cell function, microbicidal and tumoricidal activity, and a range of immunopathologies. NO is derived from L-arginine and molecular oxygen in a reaction catalysed by NO synthase (NOS). Three isoforms of NOS have been identified: neuronal constitutive NOS (ncNOS), endothelial constitutive NOS (ecNOS), and inducible NOS (iNOS). ncNOS and ecNOS are calcium-dependent, present constitutively in a variety of tissues and produce physiological concentrations of NO. However, large amounts NO are produced by iNOS which are expressed in cells such as macrophage after stimulation with a number of cytokines, including interferon-gamma (IFN- $\gamma$ ), tumour necrosis factor-alpha (TNF- $\alpha$ ), and bacterial lipopolysaccharide (LPS). Findings of iNOS biological functions are based mainly on experiments using L-arginine analogues such as L-N<sup>G</sup> monomethyl arginine (L-NMMA) which competitively inhibits NO Synthase. These inhibitors are not NOS isoform selective and have differential bioavailability, and hence often render interpretation of results difficult. To directly define the iNOS biological functions, I constructed a strain of iNOS gene targeted mice.

The first step of a gene targeting experiment is typically cDNA cloning and sequencing. A cDNA library was constructed in the vector  $\lambda$  ZAPII using mRNA isolated from J774 macrophages activated with IFN- $\gamma$  and LPS. Six independent positive colonies were found in the screen with both 5' and 3' specific probes and were subcloned in pBluescript. A full-length iNOS cDNA was constructed using the clones isolated from the library. Double strand cDNA sequence analysis showed that the J774 iNOS clone was identical to that of the Raw 264.7 macrophages iNOS cDNA sequence.

A replacement-type targeting construct was prepared from 129/sv genomic DNA. A single targeted clone was identified amongst 636 screened after two independent electroporations of the CGR8 embryonic stem cell line. Gene replacement was detected by

both 5' and 3' specific external probes. Five of ten chimeras generated gave germ line transmission. No homozygous mice were found by Southern blot analysis with 5' and 3' external probe in the offspring from heterozygous mice (F1) breedings. The iNOS gene had been altered by replacement with gene targeting construct and 5' iNOS gene translocation which could be detected by internal probe Southern blot analysis. Using the internal probe, mutant homozygous, heterozygous and wild-type mice were found in the offspring from heterozygous breedings. The ratio of these three genotypes was 21:47:25. Northern blot analysis with 5' iNOS cDNA probe showed that a large messenger appeared in the macrophages of homozygous mice when the cells were activated with IFN- $\gamma$  and LPS *in vitro*. However there was no detectable iNOS protein translation by western blot analysis using monoclonal or polyclonal anti-iNOS antibodies. No nitrite (NO<sub>2</sub><sup>-</sup>) was produced from macrophages of iNOS mutant mice 24 hours after stimulation with IFN- $\gamma$  and LPS. By 72 hours, however, a low level of nitrite was detectable in the supernatant of cells from the mutant mice. This may reflect the upregulation of constitutive NOS by LPS.

The homozygous mice are viable, fertile and without evident histopathological abnormalities. Spleen cells from iNOS mutant mice had similar proportion of T cells compared with wild-type mice and also gave similar levels of IFN- $\gamma$  and IL-4 production and proliferations after stimulation with concanavalin A. The wild-type and heterozygous mice were highly resistant to *Leishmania major* infection, and all animals achieved spontaneous healing after footpad infection. In contrast, the iNOS mutant mice were uniformly susceptible to the infection. Spleen cells from mutant mice infected with *L. major* contained a significantly higher proportion of CD3<sup>+</sup> and CD3<sup>+</sup>CD4<sup>+</sup> T cells and produced more IFN- $\gamma$  but less IL-4 than those from similarly infected wild-type or heterozygous mice.

The capacity of these mice to develop local inflammation was also investigated. The mutant mice developed significantly less footpad swelling than wild-type mice after injection with carrageenin. Spleen cells from carrageenin-treated mutant mice also had a

higher proportion of CD3<sup>+</sup>, CD3<sup>+</sup>CD4<sup>+</sup> and CD3<sup>+</sup>CD8<sup>+</sup> T cells than those from similarly treated wild-type mice. They also had a higher proliferation rate and produced more IFN- $\gamma$  than those from the wild-type mice when stimulated with concanavalin A *in vitro*.

The mutant mice were more resistant to LPS-induced death than wild-type mice, which developed severe loss of mass when injected intraperitoneally with LPS. The mutant mice showed a transient loss of mass but no further sign of ill health. In contrast, wild-type mice underwent substantial loss of mass with about 50% mortality by 72 hours after injection with 12.5 mg/kg body mass.

Mice deficient in iNOS provide a powerful tool that will not only facilitate formal demonstration of the effect or roles of NO in microbicidal and tumoricidal activity, transplantation and in a range of immunopathologies, but also help to define the involvement of NO in immune regulation, immunological tolerance and antigen processing and presentation. This is highlighted by the recent demonstration that human monocyte/macrophages expressed iNOS and generated NO in quantities sufficient to kill *Leishmania* parasites.

# **Chapter 1**

## **General Introduction**

## Part I. Cytokine Inducible Nitric Oxide Synthase

### 1.1. Nitric oxide (NO) and nitric oxide synthase

#### 1.1.1. The historical perspective

The quest to identify the so-called endothelium-derived relaxing factor (EDRF) (Furchgott, *et al.*, 1980) led to the discovery in the vasculature of an enzyme, nitric oxide synthase (NOS) (reviewed in Moncada, *et al.*, 1993). The early studies on EDRF demonstrated that EDRF was a very short-lived substance, with half-life of only seconds in oxygenated physiological salt solutions (Griffith, *et al.*, 1984; Cocks, *et al.*, 1985). The effects of EDRF were shown to be inhibited by haemoglobin (Hb), methylene blue (Martin, *et al.*, 1985) and other agents such as dithiothreitol and hydroquinone (Griffith, *et al.*, 1984) and to be mediated by stimulation of the soluble guanylate cyclase with the consequent elevation of intracellular cyclic GMP (cGMP) levels (Rapoport, *et al.*, 1983). Superoxide anions ( $O_2^-$ ) contribute to the instability of EDRF, because the effects of EDRF were prolonged by the addition of SOD (Gryglewski, *et al.*, 1986a; Rubanyi, *et al.*, 1986) and inhibited by  $Fe^{2+}$  (Gryglewski *et al.*, 1986b). In 1987, Palmer and Ignarro independently suggested that endothelium-derived relaxing factor (EDRF) was either NO or an NO-related molecule. The first direct demonstration of the release of NO by mammalian cells was in experiments on vascular tone and platelet aggregation (Palmer, *et al.*, 1987; Moncada, *et al.*, 1990).

Meanwhile, an independent line of scientists found that when human were fed a low nitrite diet, endogenously synthesized  $NO_3^-$  was excreted (Green, *et al.*, 1981). Similar results were obtained with germ-free rats, thus ruling out the participation of gut microflora in the reaction. During the course of the human experiments, one of the subjects coincidentally became ill and showed a large increase in urinary  $NO_3^-$  excretion. Subsequent experiments in rats showed that the urinary  $NO_3^-$  levels could be elevated about tenfold when fever was induced by an intraperitoneal injection of *Escherichia Coli* (*E. coli*) lipopolysaccharide (LPS). These findings suggested that this elevated synthesis

might be related to the immunostimulation known to be brought about by LPS. The LPS-induced synthesis NO *in vivo* was then reproduced by stimulation of murine peritoneal macrophages in culture (Stuehr, *et al.* 1985). Some cytokines could also stimulate macrophages to carry out this synthesis. Subsequent experiments showed that the major lymphokine involved in the synthesis response was interferon- $\gamma$  (IFN- $\gamma$ ) (Stuehr, *et al.* 1987). The stimulatory effects of LPS and IFN- $\gamma$  were synergistic and a elevator of murine macrophage cell that were found to respond in a similar way to LPS and IFN- $\gamma$  (reviewed in Marletta, *et al.*, 1989). Subsequent studies showed that NO is synthesised from the semi-essential amino acid L-arginine by NO synthase (Hibbs, *et al.* 1987; Stuehr, *et al.* 1987; Iyengar, *et al.* 1987; Palmer, *et al.* 1988). This process can be inhibited by certain guanidino-substituted arginine analogues, including N<sup>G</sup>-monomethyl-L-arginine (L-NMMA) (Hibbs, *et al.*, 1987).

#### 1.1.2. Characteristic of three forms of nitric oxide synthase

There are at least three distinct forms of NO synthase: One is the inducible nitric oxide synthase (iNOS) which was first found in the murine macrophages. Under basal conditions, iNOS activity in macrophages is negligible, while on stimulation with IFN- $\gamma$  and LPS, macrophages can produce massive enhancement of NO synthase in a few hours (Nathan and Hibbs, 1991). iNOS (NOS-II) is independent of Ca<sup>2+</sup>. The other two forms of NOS were identified in blood vessels and neurones, they are constitutively expressed and their activity depends on elevated levels of Ca<sup>2+</sup>. Recently they have been named eNOS (NOS-III) and nNOS(NOS-I) (reviewed by Nathan and Xie, 1994). All three NO synthases are flavoproteins containing bound flavin mononucleotide (FMN) and flavin adenine dinucleotide (FAD). They are dependent on NADPH as a co-factor and tetrahydrobiopterin (BH<sub>4</sub>) enhances enzyme activity (Palmer, *et al.*, 1989; Hevel, *et al.* 1991; Mayer, *et al.*, 1991; Schmidt, *et al.*, 1992; Brecht, *et al.*, 1992; Tayeh, *et al.*, 1989; Kwon, *et al.*, 1989) The derived sequence of nNOS from rat brain was the first to note that the C terminus showed a significant homology to NADPH cytochrome P-450 reductase (Brecht, *et al.*, 1991). The nucleotide binding sequence as well as those

sequences associated with FAD and FMN binding were highly conserved when compared with P-450 reductase from rat liver. This same homology has been observed in all the reported NOS sequences (Fig.1.1). The N terminus in all sequences of three forms shows a great deal of similarity suggesting a common functional role, most likely related to the arginine binding site and catalysis (reviewed by Marletta, 1993). A comparison with other arginine binding enzymes, however, has not provided any answers (Lowenstein, et al. 1992).

So far, genes encoding the three distinct NOS isoforms have been cloned and located to different human chromosomes (ncNOS: 12q24.2; ecNOS: 7q35-36; iNOS: 17cen-q12) (reviewed by Nathan and Xie, 1994). Expressions of three genes are vary in subcellular location, ncNOS was found originally in neuro-systems but also in extraneuronal sites such as skeletal muscle, pancreas, and kidney (Kobzik, *et al.*, 1994; Lukic, *et al.*, 1991; Mundel, *et al.*, 1992; Imai, *et al.*, 1992). The isoform first purified and cloned from endothelial cells is also expressed in neurons (Dinerman, *et al.*, 1994). The isoform first purified and cloned from macrophages is inducible in cell types from all branches of the histogenetic tree, among them neurons and endothelial cells (Oswald, *et al.*, 1994). Recent reports showed that one or more isoforms could also express in the same cell type (Reiling, *et sl.*, 1994; Dusting, *et al.*, 1995).

### 1.1.3. The functions of NO

Small amounts of NO are generated by the two constitutively expressed NOS (ncNOOS and neNOS) enzymes, while high levels of NO are produced by inducible NOS. NO produced from the NOS enzymes have manifold functions. In many systems, NO derives from two or more different cellular sources, forming networks of paracrine communication. Neurones produce NO to regulate transmitter release of adjacent neurones and also to match cerebral blood flow with neuronal activity. Endothelium-derived NO is vasoprotective by potentially antagonizing smooth muscle contraction and all stages of platelet activation. NO is a double-edged sword, it is essential as a messenger or modulator, and for host defence against pathogens. However, in excessive amounts it can

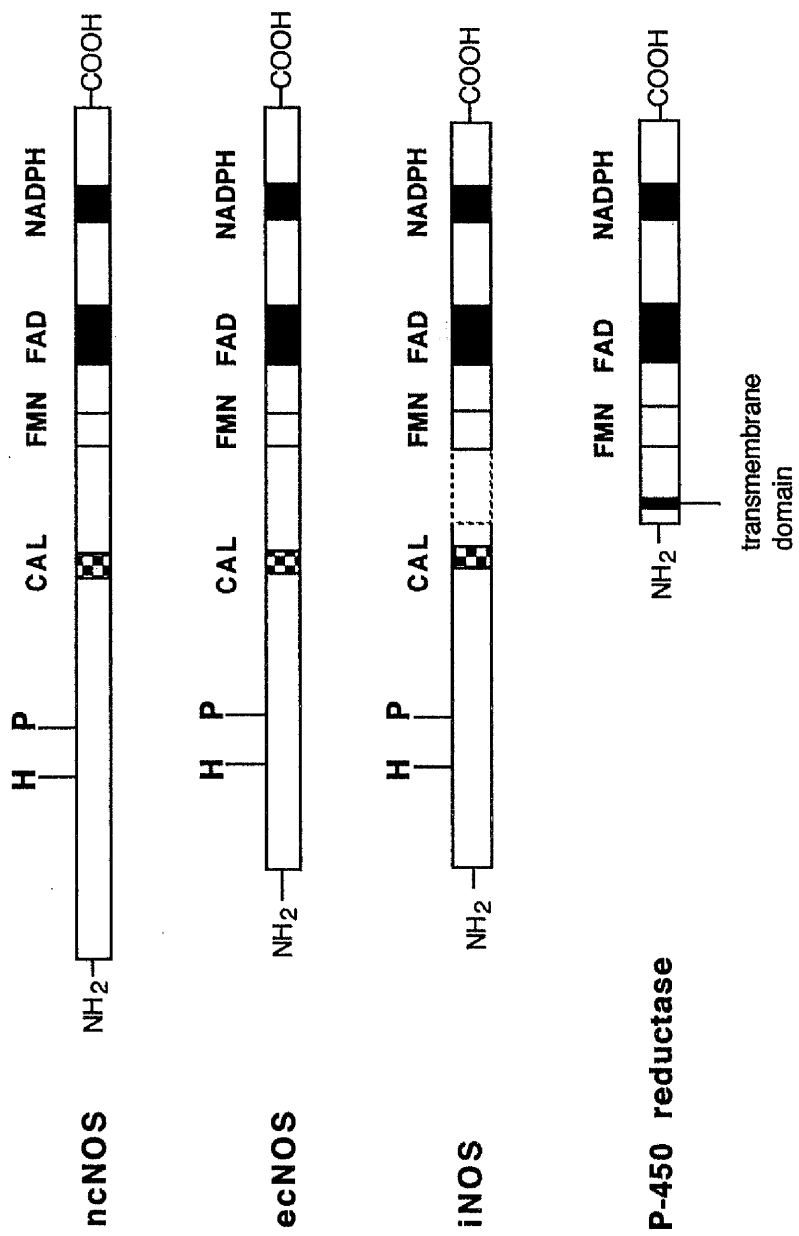


Fig 1.1. Binding sites for cofactors (NADPH, FMN and FAD) on ncNOS, ecNOS, iNOS and P-450 reductase. Calmodulin binding (CAL), protein phosphorylation (P) and consensus site for heme binding (H) are also shown.

also lead to a range of immunopathologies. In this study, I shall concentrate on the iNOS using gene-targeting to demonstrate its role in number of biological functions.

## **1.2. Inducible nitric oxide synthase (iNOS)**

### 1.2.1. iNOS cDNA cloning from mouse and human

At the beginning of this study, several groups reported iNOS cDNA molecular cloning from murine macrophage RAW 264.7 cells (Xie, *et al.*, 1992; Lyons, *et al.*, 1992; and Lowenstein, *et al.*, 1992) and also from rat vascular smooth muscle cells (Nunokawa, *et al.*, 1993). Human iNOS from different cell types (chondrocyte, hepatocyte, and smooth muscle) have also been subsequently cloned (Charles, *et al.*, 1993; Geller, *et al.*, 1993; Sherman, *et al.*, 1993). During this study, I cloned the iNOS cDNA from murine macrophage J774 cells (Moss, *et al.*, 1995).

### 1.2.2. iNOS expression

Although resting unstimulated cells express little iNOS, the capacity to express this enzyme exists in nearly every tissue in the body. The list of cell types capable of expressing iNOS now includes macrophages, neutrophils, keratinocytes, respiratory epithelium, retinal pigment epithelium, renal tubular epithelium, myoepithelium, adenocarcinomas, hepatocytes, pancreatic islet cells, endothelium, endocardium, mesangial cells, cardiac myocytes, vascular smooth muscle, uterine and fallopian tube smooth muscle, fibroblasts, chondrocytes, osteoclasts, neurons and astrocytes (Lorsbach, *et al.*, 1993; Cunha, *et al.*, 1993; Geller, *et al.*, 1993; Nussler, *et al.*, 1992; Wood, *et al.*, 1993; Eizirik, *et al.*, 1993; Corbett, *et al.*, 1993; Nakayama, *et al.*, 1992; Koide, *et al.*, 1993; Galea, *et al.*, 1992; Goureau, *et al.*, 1993; Heck, *et al.*, 1992). Many agents have the ability to induce iNOS expression in various cell types to different levels. Most of these described so far are microbes, microbial products, or inflammatory cytokines, and there is often strong synergy between these agents. For example, murine macrophages express high levels of iNOS upon exposure to LPS and this is elevated by the addition of IFN- $\gamma$  or TNF- $\alpha$  (Hibbs, *et al.*, 1990).

### 1.2.3. Regulation of the biosynthesis of nitric oxide from iNOS

Biosynthesis of NO from iNOS is regulated at different levels: genomic level, transcriptional control, post-transcriptional/translational control, and post-translational control.

Genomic level. So far, naturally occurring defects of the iNOS gene have not been reported. One observation showed that the chromosomal position of human iNOS is syngenic to a region of rat chromosome 10 implicated in spontaneous hypertension (P.A. Marsden, *et al.*, 1994). A phenotypic deficiency in iNOS expression resulting from disrupting each of three other genes has been reported: IFN- $\gamma$  (Dalton, *et al.*, 1993), one chain of the IFN- $\gamma$  receptor (Huang, *et al.*, 1993) and interferon regulatory factor-1 (Kamijo, *et al.*, 1994). However, IFN- $\gamma$  is not the only stimulator for the induction of iNOS gene expression. Knowledge on the regulation of iNOS expression at a genomic level is currently obscure.

Transcriptional control. Both mouse and human iNOS promoters have been identified (Xie, *et al.*, 1993; Lowenstein, *et al.*, 1993, Chartrain, *et al.*, 1994). By transfection of murine macrophage RAW 264.7 cells with the promoter-reporter gene cassettes, the function of promoter/enhancer elements was shown for both murine (Xie, *et al.*, 1993) and human genes (reviewed by Marris, *et al.*, 1994). In the murine iNOS promoter, there are at least 24 oligonucleotide elements homologous to consensus sequences for the binding of transcription factors involved in the inducibility of other genes by cytokines or bacterial products. Transcription factors are translocated and phosphorylated before binding on the iNOS promoter. IRF-1 is one of the crucial transcription factors

Post-transcriptional and translational control. Stability of mRNA is a major control point in the regulation of iNOS. For example, TGF- $\beta$  suppresses macrophage iNOS expression via decreased iNOS mRNA stability and translational efficiency and by decreased stability of iNOS protein but does not alter iNOS transcription (Vodovotz, *et*

*al.*, 1993). These effects may be cell-type specific, as TGF- $\beta$  attenuates iNOS mRNA induction in RAW 264.7 cells but enhances induction in Swiss 3T3 cells (reviewed by Morris, *et al.*, 1994). Conversely, Cycloheximide markedly stabilises iNOS mRNA in the latter cells (Imai, *et al.*, 1994), while in mouse macrophages, the same protein synthesis inhibitor prevents expression of iNOS mRNA

Post-translational control. Unlike the other two NOSs (ncNOS and ecNOS), iNOS contains calmodulin which is tightly bound to each subunit of the enzyme, so that iNOS is Ca<sup>2+</sup> independent (Stuehr, *et al.* 1991). iNOS protein is phosphorylated after translation, however no effect of phosphorylation on iNOS activity has been reported. L-arginine is the only physiological nitrogen donor for the NOS-catalysed reaction, regulation of availability of this essential substrate by arginine synthesis and uptake could determine cellular rates of NO synthesis (Nussler, *et al.*, 1994, Bogle, *et al.*, 1994). BH<sub>4</sub> is synthesised from GTP. Levels can also be influenced by the activities of recycling or salvage pathways that convert the oxidised forms, quinoid-dihydrobiopterin and dihydrobiopterin, respectively to BH<sub>4</sub>. GTP-cyclohydrolase I (GTP-CH) levels are absent or very low in unstimulated cells, but it is strongly co-induced with iNOS in these cells by cytokines and LPS. However, it is unknown whether the activities of the recycling or salvage pathways for BH<sub>4</sub> synthesis are co-regulated with iNOS expression (reviewed by Morris, *et al.*, 1994). Electrons donated by NADPH are essential for NO formation by NOS. The requirement of NOS for NADPH implies that the activities of metabolic-pathways that generate or compete for this co-factor could play an important role in determining rates of cellular NO production. Although there have been relatively few studies on this point, observations that the activity of the NADPH-generating pentose phosphate pathway, and of the rate-limiting enzyme glucose-6-phosphate dehydrogenase (G-6-PDH), in particular, is correlated with NO production in some cells support this possibility.

### 1.3. The role of iNOS

### 1.3.1. Non-specific defence

It has been known for many years that micro-organisms, or microbial components, can increase host resistance to the growth of tumours by an antigen-specific step that involves sensitised lymphocytes and by a non-specific step that is mediated by activated macrophages (Alexander, *et al.*, 1971; Keller, *et al.*, 1971; Hibbs, *et al.*, 1972). Present evidence suggests that this non-specific immunity is associated with the induction of NOS. If this the case, NO-dependent non-specific immunity is a general phenomenon involving not only the reticuloendothelial system but also nonreticuloendothelial cells such as hepatocytes (Nussler, *et al.*, 1992), vascular smooth muscle (Rees, *et al.*, 1990) and the vascular endothelium (Radomski, *et al.*, 1990), in all of which the inducible NOS has been detected. The role of the lung and liver in NO-dependent non-specific immunity appears to be crucial, since both organs are strategically placed in the circulation to serve as immunologic filters. Lymphocytes release NO (Kirk, *et al.*, 1990), and murine macrophages reduce lymphocyte activation by a NO-dependent mechanism (Hoffman, *et al.*, 1990; Albina, *et al.*, 1991). Furthermore, NO has been shown to be involved in immune rejection of allografted organs (Langrehr, *et al.*, 1991), graft-versus-host disease, and sepsis (reviewed by Schmidt, *et al.*, 1994). These data suggest that NO is involved in specific immunity, but its precise role is not yet clear.

NO has also been shown to be important in parasitic infections and has been most extensively studied in leishmaniasis. Mouse peritoneal macrophages stimulated, *in vitro*, with IFN- $\gamma$  in the presence of LPS are efficient in killing *Leishmania* and this leishmanicidal activity can be completely abrogated by L-NMMA (Fig.1.2) in a dose-dependent manner, but not by its D-enantiomer (D-NMMA) (Green, *et al.*, 1990; Liew, *et al.*, 1990). Furthermore, culture supernatants of macrophages activated by IFN- $\gamma$  contain significantly increased levels of NO<sub>2</sub><sup>-</sup> (Stuehr, *et al.*, 1987; Ding, *et al.*, 1988; Drapier, *et al.*, 1988), the production of which is also inhibited by L-NMMA (Liew, *et al.*, 1990). *Leishmania major* (*L.major*) promastigotes are killed when incubated, *in vitro*, at room

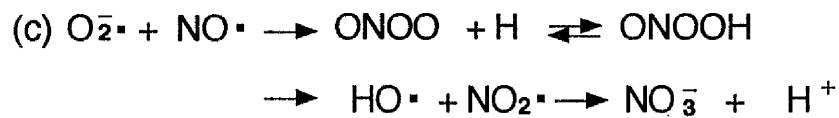
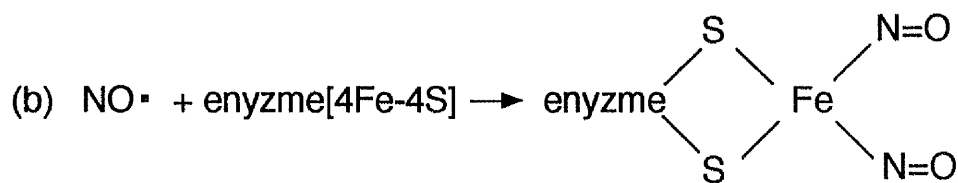
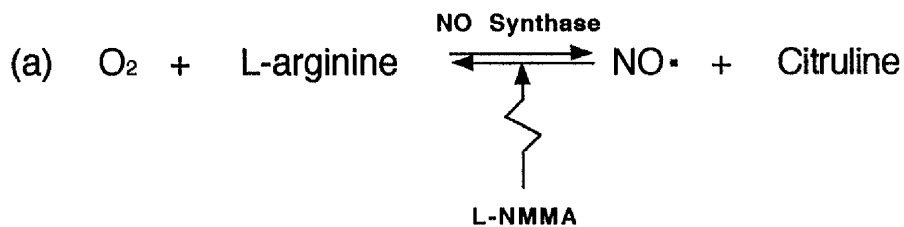


Fig. 1.2. The generation of NO and the possible mechanisms of its anti-microbial effects. (a) NO synthesis is catalysed by NO synthase and can be competitively inhibited by an L-arginine analogue, L-NMMA. (b) NO could react with the Fe-S groups forming an iron-nitrosyl complex causing the inactivation and degradation of the Fe-S prosthetic groups of aconitase and complex I and complex II of the mitochondrial electron transport chain. (c) Alternatively, NO can react with  $O_2^{\bullet -}$  to form  $ONOO^-$  (peroxynitrite) which decays rapidly once protonated to form the highly reactive  $HO^\bullet$ .

temperature in phosphate buffer saline containing NO (Liew, *et al.*, 1990). The importance of NO, *in vivo*, is demonstrated by the finding that disease in CBA mice infected with *L. major* is exacerbated when L-NMMA is injected into the lesions resulting in a 10<sup>4</sup>-fold increase in the number of parasites that can be extracted from the lesions (Liew, *et al.*, 1990).

### 1.3.2. Inflammation

Increasing evidence indicates that NO may play a part in acute and chronic inflammation. Treatment with L-NMMA reduces the degree of inflammation in rats (Ialenti, *et al.*, 1992) with acute inflammation or adjuvant arthritis (Ialenti, *et al.*, 1993) whereas L-arginine enhances it. Immune complex-induced vascular injury in rat lung and dermal vasculature can be attenuated by inhibitors of NOS (Mulligan, *et al.*, 1991). In the carrageenin-induced acute inflammation model, the NO inhibitor (L-NMMA) can reduce inflammation and down-regulate inflammatory cytokines in mice (Ianaro, *et al.* 1994). Furthermore, the colonic synthesis of NO is increased in patients with ulcerative colitis (Middleton, *et al.*, 1993), and inhibitors of NOS ameliorate experimentally induced chronic ileitis (Miller, *et al.*, 1993). In addition, nitrite concentrations in plasma and synovial fluid are increased in patients with rheumatoid arthritis and osteoarthritis (Farrell, *et al.*, 1992). The origin of NO in the inflammatory process is unclear.

### 1.3.3. Autoimmunity

NO may play a part of role in tissue damage, for it may be cytostatic or cytotoxic not only for invading microorganisms but also for the cells that produce it and for neighboring cells (Moncada, 1992). In MRL-lpr/lpr mutant mice, NOS inhibitors prevent anti-DNA immune complex glomerulonephritis and reduce the intensity of inflammatory arthritis (Weinberg, *et al.*, 1994) (MRL-lpr/lpr is a lupus mouse strain which was developed by Murphy and Roths in 1979). Pancreatic  $\beta$  cells have a rather limited capacity for free radical scavenging and are thus highly sensitive to NO cytotoxicity. In pharmacologically induced models of insulin-dependent diabetes mellitus and nonobese

diabetic mice, progressive insulinitis, dysfunction and eventual killing of pancreatic  $\beta$  cells correlate with the induction of iNOS and are, in some reports, abrogated by NOS inhibitors (Lukic, *et al.*, 1991; Kolb. *et al.*, 1991; Green, *et al.*, 1994).

The iNOS is multi-functional. It is essential for the defence against pathogens such as parasites. However, it can also cause tissue injury inducing inflammation and autoimmune diseases. So far, all the evidence of iNOS functions have been demonstrated by using NOS inhibitors, which are analogues of L-arginine and are not NOS isoform specific. To further define the role of iNOS, iNOS gene targeted mice will be very useful.

## **Part II. Gene Targeting in Mice**

### **1.4. New strategies in animal genetics**

It is no accident that our understanding of the development and function of animals of different species parallels the power of methods available for their genetic analysis. Progress has been slower even in the best-understood experimental mammal, the mouse, because genetic analysis is limited by longer generation times, which determine the rate at which information can be accumulated from breeding studies, and larger size, which places a practical limit on the numbers of animals which can be studied. However, a revolution is now sweeping through mammalian genetics. Whereas until recently the discovery of desired mutations was a matter of chance, techniques developed in the mouse and currently being extended to other species make it possible to tailor animals with predetermined alterations in their genome. These techniques have already had an enormous impact on fundamental biology in such areas as the understanding of developmental regulation of gene expression, the study of cell lineage relationships and the investigation of the consequences of altered gene expression and of the ablation of chosen tissues. In biomedicine they offer the opportunities to produce animal models of human disease and to engineer animals that produce proteins of therapeutic importance, and a basis for the development of techniques for human somatic gene therapy.

The first of these techniques of germline manipulation to be developed was the production of transgenic mice, *i.e.* mice carrying additional exogenous DNA sequences in their germline. This can be achieved either by retroviral infection of early embryos or by microinjection of DNA into one pronucleus of the fertilized egg (Jaenisch, 1988). Over the last decade these techniques have made enormous contributions to our understanding. They do, however, have several limitations. They are restricted to the addition, rather than removal or replacement, of DNA sequences, so that it is not possible to produce recessive mutations systematically in a chosen gene. The inserted DNA sequence integrates randomly rather than at the homologous chromosomal site, and frequently in the form of several tandemly arranged copies, and it is not possible to characterise the integration site or determine the copy number prior to producing an animal. Also, the method can only be applied to the study of dominant lethal changes if a way can be found to make them conditional. These limitations do not apply to a more recently developed technique for germline manipulation using embryonal stem cells (ES cells; alternatively designated as embryonic stem cells, embryo-derived stem cells or EK cells).

ES cell lines, which are established from peri-implantation mouse blastocysts (Evans and Kaufman, 1981; Martin, 1981), have many properties in common with embryonal carcinoma (EC) lines established from the malignant stem cells of teratocarcinomas, including the ability to colonize the somatic tissues of chimaeric mice following injection into host blastocysts. However, they have two important advantages over EC cells. First, lines with normal karyotypes can be readily obtained, and second, karyotypically normal ES cells are frequently capable of colonizing the germ-cell lineage of chimaeras (Bradley, *et al.*, 1984). This raises the possibility of using the techniques of somatic cell genetics to isolate ES cells carrying any of a variety of genetic modifications, and then introducing these modifications into the germ line. This approach is particularly well suited to the introduction of recessive mutations, and has become especially powerful as a consequence of recent developments in cell genetics. Homologous recombination between native chromosomal gene and exogenous DNA can be used in culture to modify specifically the target locus (Smithies, *et al.*, 1985). The recombination is a low frequency

event, so that selective techniques or powerful rapid screening methods are required to allow isolation of the recombinant cells, but these can be made independent of the properties of the gene and thus of broad application. This approach, known as gene targeting or targeted mutagenesis, has now been applied to the introduction of substantial number of recessive mutations into the mouse germline. The more detail will be introduced below.

## **1.5. Gene targeting in mice**

### 1.5.1. Homologous recombination

When a fragment of genomic DNA is introduced into a mammalian cell it can locate and recombine with the endogenous homologous sequences. The first experimental evidence for the occurrence of gene homologous recombination was made using a fibroblast cell line with a selectable artificial locus (Lin, *et al.*, 1985) and was subsequently demonstrated to occur at the endogenous  $\beta$ -globin gene in erythroleukaemia cells (Smithies, *et al.*, 1985).

In gene targeting technology, homologous recombination has been exploited to alter endogenous genes by replacing them with homologous recombination constructs in which the gene sequences have been interrupted. Despite the success of the gene targeting technology, mechanisms and cellular enzymes involved in homologous recombination are largely unknown. The understanding of this machinery will be of great value in improving the efficiency of gene targeting. It has been speculated that the physiological role of homologous recombination in cells is the repair of chromosomal breaks and the generation of genetic diversity that propels the evolution of organisms.

In mammalian cells, exogenous DNA is generally integrated randomly at non-specific sites; only rare occasions does the introduced DNA recombine with and replace its chromosomal homologous through homologous recombination. The ratio of homologous recombination events to random integration in mammalian cells is about 1 to 1000 (Thomas, *et al.* 1987). The frequency of homologous recombination seems to be

affected by the extent of homology between the homologous recombination construct and endogenous chromosomal DNA (Thomas, et al 1987), but not by the length of the non-homologous region transferred to the target locus (Mansour, et al. 1990). Neither the copy number of the target DNA sequences present in the genome (Zheng, et al. 1990) nor the number of exogenous DNA molecules introduced into recipient cells (Thomas, 1986) has a significant effect on the frequency of gene targeting. An early study showed that the frequency of homologous recombination is similar in transcriptionally active and in silent  $\beta$ -globin loci (Thomas, et al. 1986). However, transcription activity of the targeted gene has recently been shown to enhance homologous recombination in mammalian cells (Nickiloff, et al. 1990).

#### 1.5.2. Design of a gene targeting construct

There are two types of homologous recombination constructs: firstly, the insertion type that creates a partial duplication of the gene, and secondly, the replacement type that involves two reciprocal recombination events (Fig.1.3). They result in the replacement of the endogenous DNA with an homologous recombination construct, and have both been used to inactivate the targeted gene. The replacement gene construct is commonly used in gene targeting in mice. Considerations for a gene replacement construct should not only be for generating a mutation to disrupt the gene functions, but also for increase homologous recombination efficiency for convenient screening.

Generating the mutation. The deletion should be made as large as possible in the replacement construct to ensure complete disruption of the genes function. If the gene is small, delete the entire gene, or if the gene is large, the important 5' exons. A replacement construct has been designed that causes a deletion of up to 17kb of genomic DNA without a significant decrease in frequency of homologous recombination. (Mombaerts, *et al.* 1991). Disruption of the start coding sequence by a positive selection marker will in most instances ablate a genes function.

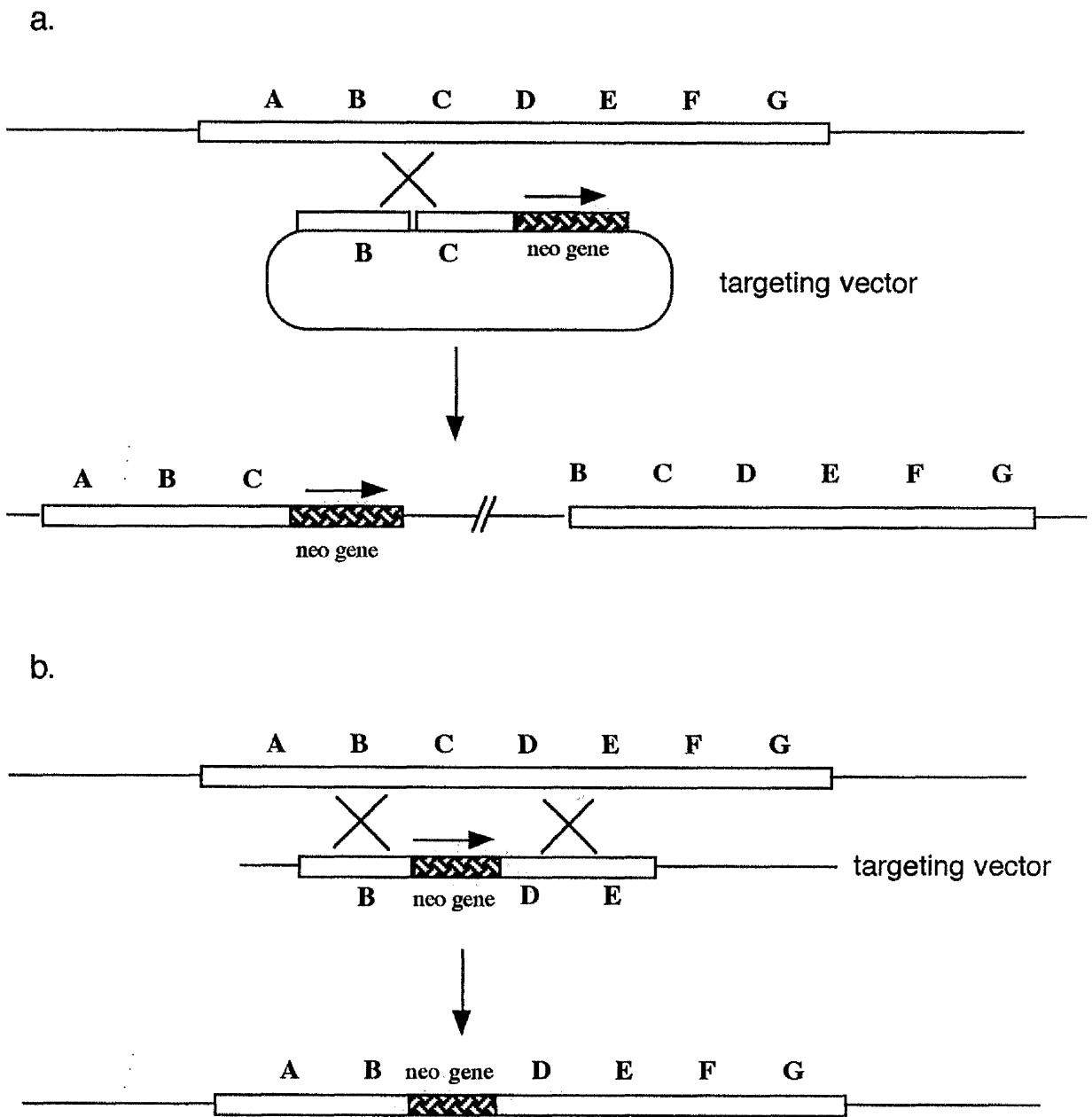


Fig1.3. Gene inactivation by homologous recombination with (a) an insertion construct and (b) a replacement construct. X is the site of homologous recombination.

Efficient homologous recombination. Using isogenic DNA (the genomic DNA from same mouse strain as the ES cells) to construct the targeting vector can result in 20-fold more efficient gene targeting (Riele, et al. 1992). The length of the homologous sequences will affect the targeting frequency. For most vectors the length of homology should be in the range of 5-8 kilobases.

Considerations for the recombination event in screening. If Southern blotting is used, the restriction enzyme sites in the construct should give size changes of hybridisation bands with external or internal probes after gene recombination. The restriction enzymes used for screening should be efficient in digesting the chromosomal DNA. If PCR is to be used to screen for gene replacement events, the positive selection marker should be cloned so that one of homology arms is 0.5-2.0kb.

### 1.5.3. Embryonic stem (ES) cells

Characteristics of ES cells. Murine ES cells are permanent cell lines, established from blastocysts of the inner cell mass of pre-implantation mouse embryos. The pluripotent state of ES cells can be maintained *in vitro* by culturing in medium supplemented with a soluble factor called leukaemia inhibitory factor (LIF) or differentiation inhibiting activity (DIA), or by co-culturing with mitotically inactivated feeder cells, such as embryonic fibroblasts or the fibroblastic STO cell line. When ES cells are returned to the embryonic environment, they can resume normal development and contribute to all cell lineages including the germ line of the resulting chimeric mice. Genetic manipulations that require massive screenings can, therefore, be performed in ES cells *in vitro* and mutant mice generated from the genetically modified ES cells. Isolation from the genetically modified ES cell lines was first demonstrated in 1981 (Evans, and Kaufman, 1981; Martin, *et al.*, 1981). Now a number of ES cell lines have been shown to be capable of germ line transmission. All the existing ES cell lines are derived from male embryos because the XY karyotype appears to be more stable in culture than the XX karyotype. Thus, most of the germ line transmission chimeric mice are males.

Targeted ES cell clones. Using stringent culture conditions, ES cells can maintain their embryonic developmental potential even after many passages. Gene targeting construct can be introduced by either microinjection or electroporation. Electroporation is the fastest and easiest way to introduce the targeting vector with the selection marker. Following the drug resistant selection and genetic mutation screening, cloned ES cells with the targeted mutation are isolated and injected back into mouse blastocysts to generate chimeric mice. In theory, this genetic manipulation technique will allow us to generate any type of mutation in any cloned gene. The mutations that can be created include null mutations, point mutations, deletions of specific functional domains, exchanges of functional domains from related genes, and gain of function mutations in which exogenous cDNA sequences are inserted adjacent to endogenous regulatory sequences.

#### 1.5.4. Screening for a genetic mutation in ES cells

The selection markers. Although different strategies are used to design the gene targeting construct, a positive selection marker is always used in the targeting vector. After the introduction of the targeting vector into the ES cells, all the neomycin analogue (G418)-resistant cells will have the targeting vector in the chromosomal DNA, either by random integration or by homologous recombination. To ensure expression of the marker gene in cells, a strong promoter such as the phosphoglycerate kinase I promoter, the RNA polymerase II promoter, the thymidine kinase promoter from herpes simplex virus or the murine  $\beta$ -actin promoter, is used to drive the expression of the marker gene. Negative selection can also be used to further enrich for cells with homologous recombination events. Toxic genes are used in negative selection by placing them in the gene targeting construct flanking the homologous region, so that the toxic genes will remain in the construct if DNA is randomly integrated into chromosomal DNA, but will be excluded if the construct has undergone homologous recombination with the endogenous gene.

Screening for the homologous targeting events. One of the most important aspects of any gene targeting experiment is to confirm that the desired genetic change has

occurred. This change can be detected with polymerase chain reaction (PCR) or Southern blot. PCR is by far the most sensitive and fastest screening method which can be used for a large number of screenings, but the homologous recombination events normally need to be confirmed by Southern blot. An external probe is normally used in Southern blot screenings, which is generated the flanking sequence of the homologous region in the targeted gene sequences. The external probe does not hybridise with the construct sequence, so that random integration is not detected with external probe. To avoid the insertion event, both external probes from 5' and 3' ends are normally used to confirm the gene replacement event.

#### 1.5.5. Introducing mutated genes into mice

An ES cell line with targeted mutation, normally in one chromosome, is returned to the embryonic environment by injection into a host blastocyst. They can contribute to many kinds of tissues in the resulting chimeras. Some of the chimeras, when mature, will produce sperm derived from the ES cells. These are so called germ-line transmission animals which can be easily detected by the offspring coat colour. Because the ES cells are derived from a mouse homozygous for the agouti coat colour (129/Sv) allele and the recipient blastocyst is derived from a black coat colour mouse (C57 Bl6). The fur of the resulting chimeras has patches of both colours because the mouse contains cells of both genotypes. Breeding of the chimeras to an MF1 albino mouse yields some chinchilla coat colour mice, indicating that the ES cells contributed to the formation of the germ line, but not for the black coat colour progeny. By mating the germ-line transmission chimeras with wild type mice, heterozygous offspring can be generated carrying the mutation in one of two copies of the gene in every cell. These heterozygous mice should be healthy in most instances, because their second, undamaged copy of the gene will still be functioning properly. To identify heterozygous and wild-type mice in this stage, the DNA from tail tipping is examined by Southern blot or PCR. Matings between heterozygous siblings would result in one in four of the offspring having two defective copies of the gene homozygous. Gene mutation analysis by Southern blot will find two targeted

mutation presence in the homozygous mice. The transcription of this targeted gene can be detected by Northern blot or by reverse transcription PCR, and the protein translation can be detected by Western blot. Biological phenotypes can now be investigated. The procedure for constructing gene mutant mice is summarised in Fig1.4.

### **1.6. Summary and rational of the project**

NO is a crucial mediator of a variety of biological functions, including vascular relaxation, platelet aggregation, neurotransmission, tumoricidal and microbicidal activity and immunopathology. There are at least three isoform of NOS, the enzyme generating NO from L-arginine and molecular oxygen. ncNOS and ecNOS are calcium-dependent and expressed constitutively in many mammalian cell types. The cytokine inducible iNOS is calcium independent and is inducible in many mammalian cells. Once induced, iNOS catalyses the production of large amounts of NO which can be cytotoxic. iNOS is therefore important in the hosts' defence against infectious pathogens and tumours, but excessive production of NO generated by iNOS can also lead to a range of important immunopathologies.

The role of iNOS has so far been demonstrated using L-arginine analogues which competitively inhibit all isoforms of NOS. This has led to considerable discrepancy in result interpretation. To define the role of iNOS more precisely, this project was designed to construct iNOS-deficient mice by gene targeting, a technique which has proved invaluable in defining many biological systems.

The specific aims of this project are as follows:

1. Cloning and mapping of the murine iNOS cDNA from J774 cells and genomic DNA from 129s/v ES cells.
2. Constructing iNOS-deficient mice.
3. Investigating the phenotype of iNOS-deficient mice.

Experimental design and results obtained, together with their implications will be presented and discussed in the following chapters.

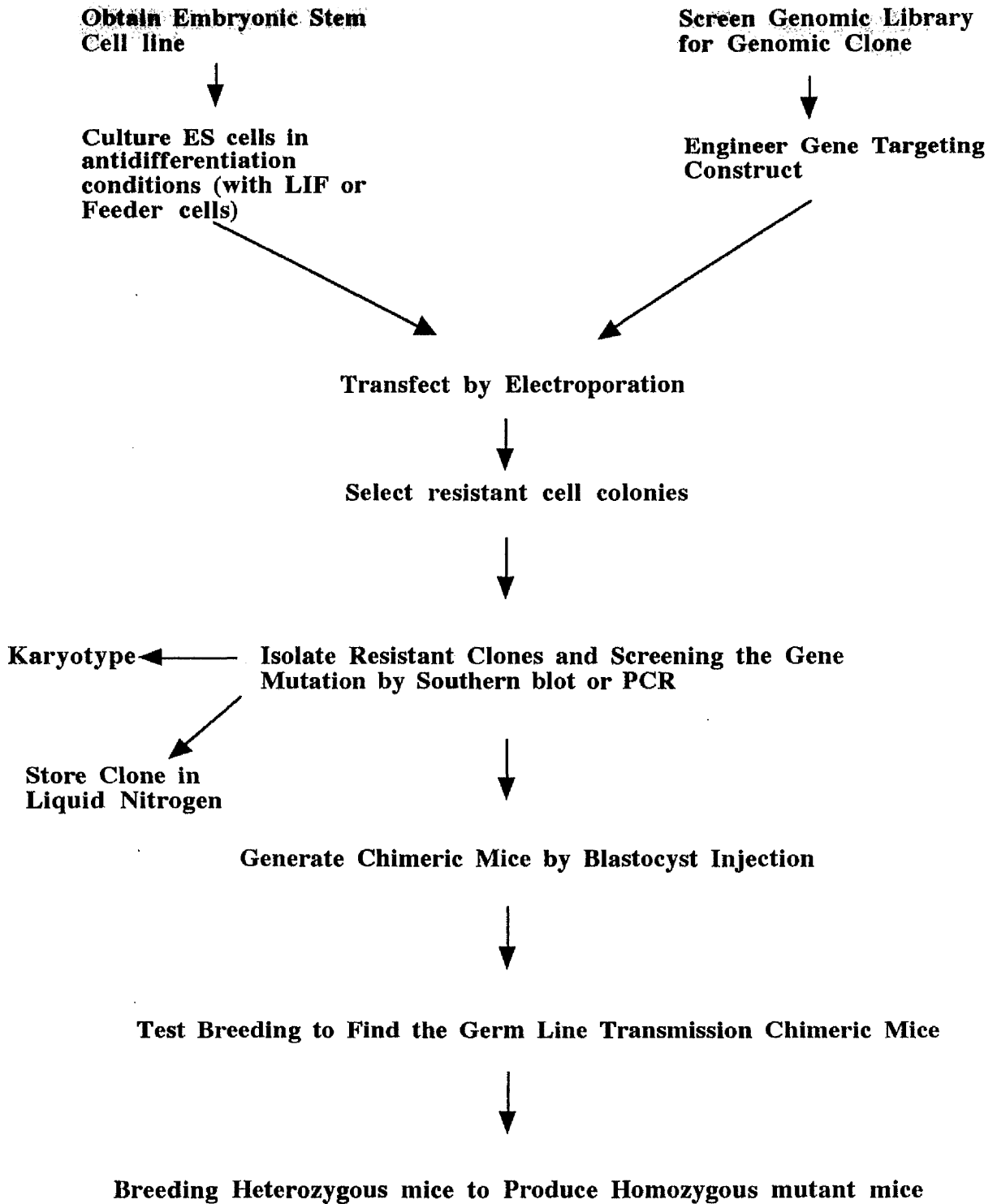


Fig 1.4.. Major steps of the procedures involved in the generation of gene targeting mutant mice.

## **Chapter 2**

### **Materials and Methods**

## **2.1. Lambda phage**

A colony of XL1-Blue (*E.coli*) was added to 10ml LB supplemented with 0.2% maltose and 10mM MgSO<sub>4</sub>. The culture was grown overnight with vigorous shaking at 37°C, and was centrifuged at 2000xg for 10min. The pellet was resuspended in 10ml of 10mM MgSO<sub>4</sub>. Cells were stored on ice prior to use.

Dilute λ ZAPII J774 cytokine induced macrophage cDNA library (which was made by Dr. Ian Charles, Wellcome Research Laboratory, Beckenham, U.K.) to 10<sup>1</sup>, 10<sup>2</sup>, 10<sup>3</sup>, 10<sup>4</sup>, 10<sup>5</sup>, in SM solution (100mM NaCl, 10mM MgSO<sub>4</sub>, 50mM Tris.HCl pH7.5, 0.01% gelatine). 20µl diluted phage was mixed with 200µl treated XL1-Blue cells respectively and incubated at 37°C for 20min. Melt 0.7% top agarose was kept in a 55°C water bath for use. 3ml of warm top agarose was mixed well with infected bacteria and poured on the plates. After the top agarose has set, the plates were incubated in the 37°C incubator for overnight (12-18 hours).

## **2.2. Library screening**

Plates with a good density of plaques (about 200-400 plaques/plate) were selected and placed in the fridge for 2 hours to make the top agarose hard. Plaques were transferred to nitrocellulose (NC) filters (A and B as duplicate). The phage DNA were denatured in the denaturing solution (1.5M NaCl, 0.5N NaOH) for 5 min. Neutralisation was carried with the neutralisation solution (1.5M NaCl, 0.5M Tris·Cl pH 8.0) for 7 min. Finally the filters were rinsed in the rinse solution (0.2M Tris·Cl pH7.5, 2xSSC) for 30 seconds. The filters were dried at room temperature and baked at 80°C for 2 hours. 20xSSC is 3M NaCl, 0.3M Sodium Citrate pH 7.5.

The filters were placed in a plastic box, 100ml pre-hybridisation solution (6xSSC, 3.3%SDS, 20mM NaH<sub>2</sub>PO<sub>4</sub>, 100µg/ml tRNA) was added and shaken at 65°C for 2 hours for pre-hybridisation. The radioactivated probe was added to the pre-hybridisation solution and hybridisation carried out overnight.

The filters were washed at room temperature twice with 2xSSC, 0.1%SDS for 15 minutes each. They were then washed with 0.5xSSC, 0.1% SDS at 65°C for 30 minutes. (if the background was high, the filters were washed again with 0.1xSSC, 0.1 SDS). The filters were exposed to X-omat AR auto radiography film (Kodak) for 4-8 hours at -70°C in cassettes fitted with Kronex intensifying screens (Kodak). The film was developed with an automatic X-ray developer (Kodak).

### **2.3. Double stranded DNA probe labelling**

Double stranded DNAs were labelled with  $\alpha$ -<sup>32</sup>P-dATP using a commercially available random priming kit (Gibco BRL). The DNA was heated to 96°C for 10 minutes in a 1.5ml screw tube and chilled on ice. Samples of 25ng-50ng DNA was mixed with 2 $\mu$ l each of 0.5mM dCTP, 0.5mM dGTP and 0.5mM dTTP, 15 $\mu$ l of concentrated random primer reaction buffer, 5 $\mu$ l (50 $\mu$ Ci) of  $\alpha$ -<sup>32</sup>P-dATP (Amersham), 1 $\mu$ l Klenow DNA polymerase (Exonuclease-free, 2units/ $\mu$ l) and distilled H<sub>2</sub>O was added to 50 $\mu$ l. The reaction was allowed to proceed at 37°C for at least 30 minutes and stopped by the addition of 50 $\mu$ l of TE buffer (10mM Tris.HCl, pH7.5, 1mM EDTA).

The Nick Column (Pharmacia) was pre-equilibrated with 2ml of TE buffer and 100 $\mu$ l reaction mixture loaded onto the top of the gel bed and allowed to enter into the gel completely. 400 $\mu$ l of TE buffer was supplied to the column. The DNA probe was eluted with another 500 $\mu$ l of TE buffer and collected in a 1.5ml screw cap tube. Un-incorporated  $\alpha$ -<sup>32</sup>P-dATP was retained in the column which was discarded. The labelled cDNA was denatured by heating at 96°C for 10 min and chilled on ice prior to addition into the pre-hybridisation solution.

### **2.4. Lambda phage DNA purification**

The genomic libraries of two strains of mice, B6 and 129/sv, have been made in a  $\lambda$  EMBL phage vector and a  $\lambda$  DASH vector respectively, so the lambda DNA containing the iNOS-specific inserts has to be purified in order to carry out the gene mapping and subcloning experiments.

A total of  $10^{10}$  plating cells were infected with a single plaque in a 10 ml L-broth culture and left shaking at 37°C overnight. This culture was used as phage stock for making DNA.

1ml of phage stock was used to inoculate 200ml of L-broth containing 10mM MgSO<sub>4</sub> and left overnight at 37°C with vigorous shaking. The culture was checked for lysis the next day and was completed by the addition of 1ml of chloroform with vigorous shaking at 37°C for a further 10 minutes. The bacterial debris was then pelleted out at 15,000xg for 10 minutes at 4°C. The supernatant was treated with RNase and DNase (each at a final concentration of 10mg/ml) at 37°C for 1 hr. The phage were precipitated by adding an equal volume of 20% PEG, 2M NaCl on ice for 1-2 hr and pelleted by centrifugation for 30mins at 8000xg, 4°C. The pellet was drained well, resuspended in 10ml of SM buffer (0.1M NaCl, 50mM MgSO<sub>4</sub>, 50mM TrisHCl pH 7.5, 0.01% gelatine) and extracted 3-4 times with chloroform to remove traces of PEG. Phage DNA was then extracted by adding 0.5ml 0.5M EDTA (pH 8.0), 1ml 5M NaCl and mixing with TE-buffered phenol followed by centrifugation for 10mins. The phenol extraction was repeated and the aqueous phase was re-extracted twice with chloroform. Phage DNA was precipitated with 2.5 volumes of ethanol, washed in 70% ethanol and air dried before resuspending in TE.

### **2.5. Excision of pBluescript from the lambda ZAPII vector**

The mouse J774 macrophage cDNA library was constructed in the lambda ZAPII vector (Stratagene) by Dr. Ian Charles, (Department of Cell Biology, Wellcome Research Laboratories). The mRNA was isolated from J774 macrophages activated with 10ng/ml LPS and 100units/ml IFN- $\gamma$ . When the host strain XL1-Blue was co-infected with the recombinant lambda ZAPII and helper phage, the phagemid was formed by excision of the pBluescript. The XL1-Blue was subsequently infected with this phagemid and grown in ampicilin medium, the pBluescript plasmid was amplified. In this way, cloned cDNA were effectively subcloned in plasmid directly from lambda phage.

An XL1-Blue colony was inoculated in 60ml LB containing 0.2% maltose, 10mM MgSO<sub>4</sub> at 37°C overnight with vigorous shaking. At the end of the growth, a 10ml sample of the bacterial culture was pipetted into a 50ml tube and centrifuged at 4000xg for 20min at 4°C. The bacterial pellet was resuspended in 10ml chilled 10mM MgSO<sub>4</sub> and kept on ice for use as competent cells. For a typical excision experiment, 200µl the above XL1-Blue competent cells, 200µl λ ZAPII phages carrying the iNOS cDNA fragment and 1µl of R408 helper phage were mixed in a 50ml tube and incubated at 37°C for 15 minutes. 5ml of 2xYT media (10g NaCl, 10g Yeast Extract and 16g Bactarial tryptone in 1 litre dH<sub>2</sub>O) was added and incubated at 37°C for 3 hours with vigorous shaking. The culture was heated at 70°C for 20 minutes and centrifuged at 8000xg for 5 minutes. The supernatant (containing phagemid) was decanted into a sterile tube. 10µl of phagemid and 20µl 1/100 2xYT diluted phagemid were mixed with 200µl of the above XL1-Blue respectively and the mixture was incubated at 37°C for 15 minutes. 20µl and 100µl of the culture respectively were placed on the LB agar plates containing 100µg/ml ampicillin. The plates were incubated at 37°C overnight.

## **2.6. DNA restriction enzymes digestion**

In this study, a range of different buffer systems and restriction endonucleases (both from Boehringer Mannheim) were used to digest DNA into required fragments. Five different buffer (A, B, L, M, H) were supplied suitable for different restriction enzyme reactions (Table 2.1). All the restriction endonuclease digestion of double stranded DNA was carried out at 37°C. In general, for the cloned and purified DNA, up to 1µg of DNA was digested in the presence of 10-20 units of the enzymes in a volume of 20-50µl for 1-4 hours. The purified genomic DNA from ES cells and mouse tails were digested with more enzyme (60 units) and longer time (overnight) in 100µl total volume.

## **2.7. Dephosphorylation reaction of DNA fragment ends**

To avoid the self ligation of plasmid vector, the digested plasmid vector was normally dephosphorylated on the 5' phosphate residue by the addition of 1µl (1unit/µl)

calf intestine alkaline phosphatase (Boehringer Mannheim). This was included in the restriction endonuclease digest reaction. As an alternative, the phosphatase buffer and phosphatase were used directly after the enzyme digestion step.

## **2.8. Agarose gel electrophoresis**

Nucleic acids were routinely analysed by electrophoresis through agarose gels. In this study, gels were made at a range of concentrations from 0.6% to 1.0% depending on the size of the fragment and amount of DNA. For plasmid subcloned DNA digestion and analysis of PCR products, the 0.8%-1.0% agarose gels were used. However, for  $\lambda$  phage DNA and genomic DNA digestion, 0.6%-0.7% agarose gels were used. Gels were made by dissolving the required amount of dry agarose powder (Gibco BRL) in 1 X TBE buffer or 0.5 X TBE buffer from 10xTBE stock buffer [200mM TrisHCl pH 8.0, 900mM Boric acid, 25mM Ethylenediamine tetra-acetic acid (EDTA)] by boiling or in microwave oven. The melted gels were allowed to cool to 45°C and ethidium bromide (Sigma) was added to the final concentration of 10ng/ml. Gels were cast in tanks with combs where they were allowed to set. After setting space, gels were submerged in TBE buffer and the well-forming combs were removed. The samples of the DNA and 1kb DNA ladder (Gibco BRL) were mixed with loading buffer (6xloading buffer: 0.25% bromophenol blue, 150mM Tris.HCl pH8.0, 10mM EDTA, 40% sucrose) and loaded into the relevant wells on the gel. Gels were electrophoresed at a constant current of 10mA/cm gel-length or a constant voltage of 1-5V/cm of gel-length until the bromophenol blue had migrated the required distance. Gels were then analysed under ultra-violet light and photographed if necessary.

## **2.9. Purification of DNA fragments from agarose gels**

DNA bands were visualised with Ethidium Bromide by short-wave UV illumination. The relevant band was excised with a clean scalpel and placed in a Eppendorf tube. 1.5ml of Freeze-Squeeze buffer (25mM Tris, 0.3M Sodium Acetate, 1mM EDTA pH7.0) was added and the sample kept in the dark at room temperature for

15 minutes. The buffer was then discarded and the Eppendorf tube with the agarose inside was placed in dry ice for 10 minutes. The frozen gel slice was then rapidly transferred to a Spin X centrifuge filter tube (Costar) and centrifuged for 15 minutes at 15,000xg. The agarose in the filter was discarded and the DNA solution was extracted with phenol/chloroform and chloroform before precipitation with ethanol.

### **2.10. DNA ligation**

Following restriction digestion and purification, the DNA fragments with compatible sticky ends or those with blunt ends were ligated using DNA ligase isolated from the bacteriophage T4 (Gibco BRL). Approximately equimolar amounts (usually about 0.1-0.5 $\mu$ g DNA ) of the fragments to be ligated and the appropriately digested and purified plasmid DNA were mixed and incubated with 1 $\mu$ l of T4 ligase (1 unit/ $\mu$ l) in ligation buffer (50mM Tris HCL pH 7.6, 10mM MgCl<sub>2</sub>, 1mM ATP, 1mM DTT and 5% w/v polyethylene glycol 8000) (Gibco BRL) in a total volume of 10 $\mu$ l. Control ligations, replacing the cDNA fragments with water but retaining the plasmid DNA were also set up to calculate the degree of self ligation. Ligations were allowed to proceed either overnight at 16°C or at room temperature for 4 hours. Following ligation, the cDNA was not further purified prior to its use in bacterial transformation.

### **2.11. Transformation of bacterial strains**

Two methods were utilised to promote the uptake of plasmids into either subcloning efficiency DH5 $\alpha$  (Gibco BRL) or XL-1 blue (Stratagene) *E. coli* host cells. Initially, a heat shock method was used whereby 5 $\mu$ l (approximately 500ng of DNA) of the ligation mixture was mixed with 50 $\mu$ l competent bacterial cells and incubated on ice for 30 minutes in an Eppendorf tube. Positive control transformations were set up replacing the experimental sample with 1ng of the plasmid pUC19 to assess the efficiency of plasmid uptake. The DNA-cell mixture was then incubated at 37°C for 22 seconds before a second incubation on ice for 5 minutes. 1ml of 2xYT broth (1.6% w/v bacterial tryptone, 1% w/v yeast extract and 0.5% w/v NaCl, pH 7.5) was added to the

transformation mix and this was then incubated at 37°C with vigorous shaking for 1 hour. The bacteria were pelleted by centrifugation at 15,000xg for 10 seconds at room temperature and resuspended in 100µl of 2xYT broth. Bacteria were then plated onto 85mm petri dishes (Sterilin) containing L-agar (1% w/v bacterial tryptone, 0.5% w/v yeast extract, 1% w/v NaCl and 1.5% w/v agar, pH7.5 and 100µg/ml Ampicillin). Plates were incubated overnight at 37°C and examined for the growth of colonies of transformed bacteria the following day. The bacteria carrying the plasmid with ampicillin resistant gene will survive in the L-agar containing ampicillin.

In some experiments, and with certain plasmids, the L-agar contained 1mM isopropyl thio-β-D-galactoside (IPTG) (Gibco BRL) and 50µg/ml 5-bromo-4-chloro-3-indolyl-β-D galactoside (X-gal) (Gibco BRL). This allowed for the selection of bacteria carrying recombinant plasmids by the appearance of white colonies. Those not carrying an inserted DNA fragment retained the ability to metabolise galactose analogues and therefore produced blue colonies due to the presence of IPTG and X-gal.

An electroporation method for the high efficiency introduction of recombinant plasmids into XL-1 blue host cells was used in some experiments. A fresh XL1-blue overnight culture was inoculated into 500 ml of L broth at 1:100 dilution and the cells are grown with vigorous shaking to an OD600 of approximately 0.4. The cells were harvested by cooling on ice for 15 minutes and pelleted at 4000xg for 15 minutes at 4°C. The cells were resuspended in 250ml of ice cold distilled H<sub>2</sub>O and re-pelleted twice. This centrifugation step was repeated sequentially with 50ml of 10% glycerol. Finally the cells were resuspended in a final volume of 2ml of 10% glycerol. The cell concentration should be approximately  $3 \times 10^{10}$  cells/ml and samples were stored frozen at -80°C in 40µl aliquots.

An aliquot of the cells prepared for electroporation was thawed on ice. Plasmid DNA or ligation reaction in 1-3 µl of distilled H<sub>2</sub>O was added and the mixture of cells and DNA was then transferred to a cold 0.2 cm electroporation cuvette and placed on ice. The Gene Pulser apparatus (Biorad) was set to 25µF and 2.5 KV, the pulse controller was set

to 200W . The cells were pulsed once and the cuvette is immediately removed from the chamber and 1 ml of 2xYT was added to the cells. The cells were allowed to recover by growing at 37°C for 1 hour before plating on ampicillin plates.

### **2.1.2. Isolation of plasmid DNA**

Plasmid DNA was isolated using a modification of a previously published method (Jones and Schofield,1990). Colonies carrying a putative plasmid of interest was inoculated into 3ml of 2xYT broth containing 100µg/ml ampicillin (Sigma) and grown for 18 hours at 37°C with vigorous shaking. At the end of the growth period, 2ml of the bacterial culture were pipetted into an eppendorf tube and centrifuged at 15,000xg for 2 minutes at room temperature. The pellet was resuspended in 200µl of GTE buffer (50mM glucose, 25mM tris.HCl pH8.0, 1mM EDTA) and to this was added 400µl of freshly prepared 0.2N NaOH containing 1% SDS. This was then incubated on ice for 5 minutes before the addition of 300µl of 3M potassium acetate pH 4.8. After a further 5 minutes incubation on ice, samples were centrifuged at 15,000xg for 10 minutes at room temperature. The supernatant was transferred to a fresh eppendorf tube, mixed with 900ul of ethanol and centrifuged immediately at 15,000xg for 5 minutes at room temperature. The pellet was washed once in 1ml of 75% ethanol by centrifugation at 15,000xg for 2 minutes at room temperature. The pellet was allowed to dry at room temperature and then resuspended in 50ul of TE buffer containing 10 unites of RNase (DNase free). Following incubation for 5 minutes at 37°C, the samples were stored frozen at -20°C. This so-called 'mini-prep' generated DNA that was suitable for both restriction enzyme digestion and DNA sequencing.

For the ES cell electroporation, large scale production of high purity plasmid DNA was performed using a commercially available 'maxi-prep, kit (QIAGEN). A 50ml culture of bacteria containing the required plasmid was grown overnight to stationary phase in 2xYT broth containing ampicillin (50µg/ml). Cells were pelleted by centrifugation at 8000xg for 20 minutes at 4°C. The pellet was resuspended in 10ml of Tris·HCl pH 8.0 containing 10mM EDTA and 100µg/ml RNase A and mixed immediately with 10ml of

0.2N NaOH containing 1% SDS and incubated at room temperature for 5 minutes. 10ml of ice-cold 3M potassium acetate pH 4.8 was then added and the incubation continued for a further 20 minutes on ice, mixing by inversion every 5 minutes. The lysate was transferred equally to two 20ml centrifuge tubes, centrifuged at 15,000rpm for 30 minutes at 4°C and the pellet discarded. The supernatant was pooled and passed through a 'QIAGEN-500' column, pre-equilibrated with 10ml of QBT buffer (0.75M NaCl, 50mM 3-[N morpholino] propane sulphonic acid (MOPS), 15% ethanol, 0.15% triton X-100, pH 7.0). The eluate was discarded and the column washed with 60ml of QC buffer (1M NaCl, 50mM MOPS, 15% ethanol, pH 7.0). The bound plasmid was eluted from the column with 15ml of QF buffer (1.25M NaCl, 50mM Tri.HCl, 15% ethanol, pH 8.5), mixed with 10.5ml of isopropanol at room temperature and centrifuged at 15,000rpm for 60 minutes at 4°C. Following careful aspiration of the supernatant, the pellet was washed once in 10ml of ice-cold 70% ethanol by centrifugation at 15,000rpm for 10 minutes at 4°C. The pellet was air dried for 5-10 minutes at room temperature, resuspended in 200µl of distilled water and stored at -20°C. The concentration of DNA in the sample was estimated by absorbency at 260nm in a quartz cuvette.

### **2.13. DNA sequencing**

Nucleotide sequence of cDNA clones in a variety of plasmid vectors was analysed by a modification of the di-deoxy chain termination method (Sanger et al. 1983) using a commercially available kit (United States Biochemicals) from which all reagents were taken unless otherwise stated. 10ng of plasmid DNA was denatured in the presence of 0.2N NaOH for 15 minutes at 37°C in a total volume of 10µl. 10pg of a 17 base pair (bp) oligonucleotide sequencing primer (either supplied in the kit or made in house by Mr. H. Spence, Department of Cell Biology, Wellcome Research laboratories), in a volume of 1µl, is mixed with the denatured DNA and allowed to anneal for 5 minutes at room temperature. The DNA-primer complexes were then precipitated by the addition of 3µl of 3M KOAc pH 4.8 and 75µl of 100% ethanol and incubated at -70°C for 20 minutes, followed by centrifugation at 15,000xg for 15 minutes at room temperature. The ethanol

was aspirated and the pellet washed once in 100 $\mu$ l of 75% ethanol followed by centrifugation at 15,000xg for 5 minutes at room temperature. Following aspiration of the ethanol, the pellet was air-dried at room temperature for 10 minutes and resuspended in 8 $\mu$ l of distilled water. To this was added 2 $\mu$ l of 5x concentrated reaction buffer (0.2M Tris HCl, pH 7.5, 0.1M MgCl<sub>2</sub> and 0.25M NaCl), 1 $\mu$ l of 0.1M DTT, 2 $\mu$ l of labelling mix (7.5 $\mu$ M dCTP, 7.5 $\mu$ M dGTP and 7.5 $\mu$ M dTTP) 2 $\mu$ l of 'Sequenase' recombinant phage T7 DNA polymerase (13 units/ $\mu$ l) (pre-diluted 1 in 8 in 10mM Tris HCl, pH7.5, 5mM DTT and 0.5mg/ml BSA), 0.5 $\mu$ l (5 $\mu$ Ci) of  $\alpha$ -<sup>35</sup>S dATP (specific activity: 1000Ci/mmol, Amersham). The reaction was allowed to proceed at room temperature for 5 minutes and aliquoted into 4 Eppendorf tubes (3.3 $\mu$ l/tube). To each tube was added 2.5 $\mu$ l of one of the following termination mixes: 1).**ddA**: 80 $\mu$ M dATP, dCTP dGTP, 8 $\mu$ M dideoxy ATP (ddATP). 2).**ddC**: as above but with ddCTP replacing ddATP. 3).**ddG**: as above but with ddGTP. 4).**ddT**: as above but with ddTTP. Each tube was incubated at 37°C for 5 minutes prior to the addition into each tube of 4 $\mu$ l of stop solution (95% formamide 20mM EDTA, 0.05% bromophenol blue and 0.05% xylene cyanol). All tubes were heated to 80°C for 5 minutes and stored on ice prior to electrophoresis. In some experiments, termination mixes contained 80 $\mu$ M 7-deaza-nucleotides to help to resolve regions of sequence with strong secondary structures or high G/C contents.

Electrophoresis was performed through 6% PAGE gels containing 8M urea (Gibco BRL) in 1 x TBE buffer. Samples were run at 50W constant power for 2-3 hours at room temperature or until the bromophenol blue marker reached the bottom of the gel. In some experiments, the xylene cyanol marker was run to the end of the gel to allow reading of the sequence further from the primer binding site. After electrophoresis, gels were fixed in 20% methanol, 10% glacial acetic acid for 30 minutes, transferred to 3MM filter paper and dried under vacuum at 80°C for 1-2 hours. Dried gels were exposed to X-omat AR autoradiography film (Kodak) for at least 18 hours at -70°C in cassettes (Kodak).

## 2.14. Introduction of a synthetic oligonucleotide pair into a plasmid vector

Synthetic oligonucleotides were supplied freeze-dried and reconstituted by the addition of 500 $\mu$ l of distilled water. A 1 in 100 dilution was prepared in distilled water and the U.V. absorbance measured at 260nm against a water blank. For single stranded DNA, an absorbance of 1=approximately 37 $\mu$ g/ml. The values obtained were converted to molarity on the assumption that the average molecular weight of 1 DNA base is equal to 324 Dd using the formula:

$$\frac{1}{\text{Total oligo Mr in Da}} \times \text{oligo concentration in } \mu\text{g}/\mu\text{l} \times 10^{-6} = \text{moles oligo}/\mu\text{l}$$

Phosphate residues were added to the 5' end of each oligonucleotide in a reaction volume of 40 $\mu$ l containing 50mM Tris HCl, pH 7.5, 5mM DTT, 10mM MgCl<sub>2</sub>, 1mM ribosomal ATP and 10 units of phage T4 polynucleotide kinase (10units/ $\mu$ l) (Gibco BRL). This reaction was allowed to proceed for 30 minutes at 37°C after which time complementary pairs of oligonucleotides were pooled and 2 $\mu$ l of 5M NaCl added. The pooled oligonucleotide mix was then heated to 100°C for 5 minutes and allowed to cool slowly to room temperature over a period of 2-3 hours. Oligonucleotides were designed with the required restriction sites 'pre-cut' to obviate the necessity of restriction digestion and were not further purified prior to ligation with plasmid vector. 1 $\mu$ g of a range of dilutions of annealed oligonucleotides (from neat to 1 in 1000) were ligated with 100ng of appropriately digested plasmid as described previously for plasmid vector ligations and transformed into competent *E. coli*. Recombinant plasmid from transformed bacteria was analysed by restriction digestion and nucleotide sequence analysis.

### **2.15. Southern blot analysis of Lambda phage DNA and genomic DNA**

Analysis of genomic and lambda DNA by restriction enzyme digestion, gel electrophoresis and radioactively-labelled probe hybridisation were performed in this study. About 10µg of genomic DNA or 1µg of Lambda DNA was digested with the appropriate restriction enzymes and subjected to agarose gel electrophoresis as previously described. Following electrophoresis, the gel was photographed alongside a fluorescent ruler under U.V. light and then incubated in 10 volumes of denaturing buffer ( 0.5M NaOH, 1.5M NaCl) with gentle shaking for 45 minutes at room temperature. The denaturing solution was decanted and the gel washed briefly in several changes of distilled water prior to the addition of 10 volumes of neutralisation buffer (1M Tris HCl, pH 7.4, 1.5M NaCl). The gel was incubated in neutralisation solution for 30 minutes with gentle shaking after which time the buffer was decanted and washed again with several changes of distilled water. 4 sheets of Whatman 3MM filter paper and 1 sheet of nylon filter were cut to the same size as the gel. The nylon filter was soaked in 2 x SSC (0.3M NaCl, 42mM Sodium citrate, pH 7.2) for 20 minutes. The longer filter paper was cut and placed on a perspex block, (approximately the same size as the gel), in a bath containing 1 litre of transfer buffer (20xSSC) with the 'tails' in contact with the buffer. The gel was removed from the neutralisation buffer and placed 'well-side' down on the filter papers and surrounded with 'parafilm' (Sigma) to prevent transfer buffer flowing around the outside of the gel. The nylon filter was placed on the top of the gel and the remaining 2 sheets of filter paper (which were wetted in 2xSSC) were placed on top of the nylon filter. The entire blot assembly was rolled lightly with a glass rod to remove air bubbles from between the layers which would otherwise interfere with the transfer and another 2 sheets of filter papers placed on top. A stack of paper towels approximately the same size as the gel is placed on top of the blot assembly followed by a glass plate and a 500g weight. Capillary transfer is allowed to proceed overnight at room temperature. The next day, the gel was removed and discarded. The nylon filter was washed briefly with 2xSSC and dried between 2 sheets of 3MM filter paper at room temperature. The DNA was then baked onto the nylon at 120°C for about 20 minutes.

For blots using restriction endonuclease digested  $\lambda$  DNA, the nylon filter was prehybridised in the prehybridisation buffer [6xSSC, 0.02M  $\text{NaH}_2\text{PO}_4$ , 100 $\mu\text{g}/\text{ml}$  denatured salmon sperm DNA (Sigma) and 0.1% SDS] for 2-3 hours. At the end of the prehybridisation, a specific  $\alpha$ - $^{32}\text{P}$  dATP labelled DNA probe, prepared as described previously, was added directly to the solution and incubation was allowed to proceed at 65°C for a further 18 hours in a hybridisation oven (Scot-lab). Following the hybridisation, the blot was washed with 2xSSC, 0.1% SDS twice and 0.2 x SSC, 0.1% SDS for another two times at 65°C.

For the genomic DNA blots, the Church-Gilbert buffer (7% SDS, 40mM  $\text{NaH}_2\text{PO}_4$ , 1mM EDTA 100 $\mu\text{g}/\text{ml}$  ssDNA) was used. The blots were washed with wash buffer 1 (5% SDS, 40mM  $\text{NaH}_2\text{PO}_4$ , 1mM EDTA) at 65°C for 30 minute and wash buffer 2 (0.1% SDS, 40mM  $\text{NaH}_2\text{PO}_4$ , 1mM EDTA) at 65°C for another 30 minutes twice. The blots were removed from the last wash, dried between 2 sheets of 3MM paper for 30 minutes at room temperature and exposed to X-ray film for times between 1-3 days depending on the signal.

### **2.16. Isolation of total cellular RNA**

Total RNA was isolated using 'RNAzol™ B' a commercially available guanidinium thiocyanate-phenol method (Biogenesis Ltd.). Distilled water, treated for 18 hours with 0.2% diethyl pyrocabonate (DEPC; Sigma) and then autoclaved, was used to make all solutions not supplied with the kit. Cells growing as suspension cultures were pelleted by centrifugation at 2000xg and lysed in 400 $\mu\text{l}$  of RNAzol™B. Effective lysis was facilitated by vigorous pipetting. Following disruption, lysates were vortexed for 15 seconds in the presence of 40 $\mu\text{l}$  chloroform. Samples were then centrifuged at 15,000xg for 15 minutes at 4°C and the colourless 200 $\mu\text{l}$  upper phase (containing exclusively RNA) was removed to a fresh Eppendorf tube. RNA was precipitated by the addition 200 $\mu\text{l}$  of isopropanol and pelleted by centrifugation at 15,000xg for 15 minutes at 4°C. The RNA pellet was washed once in 75% ethanol by centrifugation at 15,000xg for 5 minutes

before being resuspended in 20 $\mu$ l TE buffer. The concentration of RNA in samples was estimated using ultra-violet spectroscopy. A 1 in 500 dilution of the sample was made in DEPC-treated distilled water and the absorbance at 260nm and 280nm was measured using quartz cuvettes and a water blank. An absorbance of 1.0 at 260nm was equal to approximately 40 $\mu$ g/ml RNA. The RNA was judged to be free from protein contaminants if the absorbance ratio 260nm/280nm was greater than 1.8.

### **2.17. Isolation of polyadenylated messenger RNA (polyA<sup>+</sup>mRNA)**

Isolation of poly A<sup>+</sup> mRNA is based upon oligo (dT) cellulose affinity binding and performed using a commercially available 'Fast-Track' kit (Invitrogen). Up to 1 x 10<sup>7</sup> cells from either suspension or monolayer culture were pelleted by centrifugation at 2000xg for 5 minutes at room temperature and washed twice in PBS by repeat centrifugation. Cells were transferred to Eppendorf tubes, centrifuged at 2000xg for 5 minutes at room temperature and the pellet lysed in 1ml of lysis buffer (PBS containing 0.1% SDS and RNase degrader as supplied with the kit) at 45°C for 20 minutes. 5M sodium chloride (NaCl) was added to a final concentration of 0.31M and the DNA that precipitated was sheared by passage several times through a 21 guage needle. One oligo (dT) cellulose tablet was added to the lysate and allowed to disperse. The mixture was then incubated with gentle shaking for 20 minutes at room temperature. The oligo (dT) cellulose was then sequentially washed by centrifugation at 5000xg 3 times each in 200 $\mu$ l of high and then low salt buffer to remove contaminating cell debris, proteins, DNA, tRNA and rRNA. Poly A<sup>+</sup> mRNA were eluted from the cellulose in 200 $\mu$ l of buffer without salt and precipitated by the addition of 10 $\mu$ l of glycogen carrier, 30 $\mu$ l of 2M sodium acetate and 600 $\mu$ l of ice cold ethanol. The precipitate was collected by centrifugation at 13,000xg for 20 minutes at 4°C, washed once with 1ml of 75% ethanol, re-centrifuged, air-dried and resuspended in 20 $\mu$ l of DEPC treated distilled water. RNA yields were quantified by ultra-violet spectroscopy as previously described.

## 2.18. Reverse transcribed polymerase chain reaction (RT-PCR)

Reverse transcribed polymerase chain reaction (RT-PCR) was performed using a commercially available 'GeneAmp RNA-PCR' kit (Perkin Elmer Cetus). Reverse transcription of RNA to cDNA was performed on 50ng of poly A<sup>+</sup> mRNA or 2µg of total RNA, isolated as described above. RNA was mixed with the following reagents supplied with the kit: 4µl 25mM MgCl<sub>2</sub>, 2µl each of 10mM dATP, dCTP, dGTP, dTTP, 1µl RNase inhibitor (20units/µl), 1µl recombinant reverse transcriptase from moloney murine leukaemia virus (50 units/µl), 1µl 50µM random sequence hexanucleotides and 2µl of DEPC treated distilled water. This mix was incubated at room temperature for 10 minutes, 42°C for 15 minutes, 99°C for 5 minutes and finally chilled on ice. This protocol allowed annealing of the random hexamers and conversion of the RNA sequence (via reverse transcriptase) into cDNA. In some experiments, a mixture of random hexamers and oligo (dT) (1µl of a 50µM stock) were used to prime poly A<sup>+</sup> mRNA for reverse transcription.

Following reverse transcription, 4µl 25mM MgCl<sub>2</sub>, and 8µl 10x concentrated PCR buffer were added to each sample. Target sequence-specific oligonucleotide primer pairs were then added to a final concentration of 20ng/ml (usually 5µl of a 40µg/ml solution) and distilled water added to take the final volume to 99.5µl. 0.5µl (5units/µl) of recombinant DNA polymerase from *Thermus aquaticus* ('Amplitaq') was added and the mixture is overlaid with 100µl of mineral oil (Sigma). The entire reaction mixture was subjected to thermal cycling under the following standard conditions: Denaturation at 95°C for 1 minutes, primer binding at 56°C for 2 minutes and sequence extension at 72°C for 3 minutes for 35 cycles.

PCR was also performed on cDNA and genomic DNA samples without the requirement for reverse transcription. In these experiments, 0.1ng -50ng of target cDNA or genomic DNA were mixed with 4µl 25mM MgCl<sub>2</sub>, 10µl 10x concentrated PCR buffer, 2µl each of 10mM dATP, dCTP, dGTP, dTTP, 20ng/ml each specific primer, 0.5µl (5units/µl) *Amplitaq* and distilled water to 100µl. Cycling was as described previously.

### **2.19. ES cell culture**

CGR8 ES cells were cultured in gelatine-coated tissue culture flasks in Glasgow modified Eagle's medium (GMEM) supplemented with 10% fetal calf serum (FCS), 1x non-essential amino acids, 0.1mM  $\beta$ -mercaptoethanol, 1mM sodium pyruvate and 100U/ml DIA/LIF

### **2.20. Purification and linearisation of the Gene targeting vector**

In this study, the gene targeting vector was purified using a QIAGEN kit and linearised with the restriction enzymes *SacI*. The linearised vector was repurified either by phenol/chloroform extraction or by elution from an agarose gel to remove the plasmid vector. 150 $\mu$ g purified DNA was used for electroporation.

### **2.21. Electroporation of ES cells**

The CGR8 ES cells were trypsinised to generate single cells, washed with cold PBS twice and counted. Cell concentration was adjusted to  $10^8$  in 0.8ml PBS. The cells were mixed with 150 $\mu$ g purified and linearised DNA and transferred to an electroporation cuvette. An electric pulse (800V, 3 $\mu$ F and time constant) was applied. The cells were transferred into 200ml of ES cell medium containing LIF (Leukaemia Inhibition Factor). 20ml of the cell suspension was aliquoted into ten 100mm gelatinised dishes and the medium containing LIF changed 24 hours after transfection.

### **2.22. Neomycin (G418) resistance colony selection**

24 hours after transfection, cells were selected in medium containing 175mg/ml of G418 for about 10 days. Single G418 resistant colonies were picked into 24-microwell plates coated with gelatin. Cells were expanded and each clone was split into 2 plates. Half of these cells was frozen *in situ*, while the other half was used for Southern blot analysis.

### **2.23. Preparation of low temperature agarose ES cell plugs**

Confluent cells grown in the duplicate 24-microwell plates were trypsinised, transferred into Eppendorf tubes and washed once with PBS, cell pellets were resuspended in 50µl of PBS and 70µl of 1% low melting agarose (prewarmed at 60°C) and left to set as a plug on ice. Agarose plugs were then transferred into Eppendorf tubes and were incubated at 55°C overnight in NDS buffer (1% lauroyl Sarcosine, 0.5M EDTA pH 9.5) in the presence of 1mg/ml of proteinase K.

### **2.24. Restriction digestion of DNA in plugs**

Plugs were washed twice with TE containing 0.1mM PMSF followed by one washing with distilled water for at least 1 hour for each wash. After washing, plugs were equilibrated with 1x restriction buffer for 1 hr at 4°C. Restriction digests were performed in 60µl of 1x restriction buffer containing 40 units of restriction endonuclease enzyme at 37°C for 4 hrs or overnight. Half or one third of a plug was used for each digest and the rest of the plugs were kept at 4°C in TE buffer.

### **2.25. Screening G418 resistant clones**

Homologous recombinant ES clones were identified by Southern hybridisation of *Hind* III and *Eco*R I respectively digested DNA prepared from agarose plugs with both 5' and 3' external probes.

### **2.26. Freezing, storage, and thawing of ES cell line**

Short-term freezing of ES cell clones in 24 well plates: The cells were grown to confluency in 24 well gelatine coated plates in the GMEM medium containing LIF. The supernatant was aspirated and 250µl/well of freshly made freezing medium (20% FCS, 10% DMSO in ES cell culture medium) was added. The plates were place in a pre-cooled box at -20°C overnight before transferred to the -70°C freezer.

Long-term freezing of ES cell stocks: The ES cells were trypsinised from 80mm flasks (Costar) to make a single cell suspension and pelleted by centrifugation at 450xg for 5 minutes. Cells were resuspended in 1.5 ml ES cell medium (the cells density was about  $5 \times 10^6$ /ml) and 0.5ml aliquots of the cell suspension were placed into freezing vials on ice. Another 0.5ml of 2x freezing medium was added to each tube. The samples were mixed gently and transferred to a pre-cooled rack in the  $-70^{\circ}\text{C}$  freezer overnight before transferring to liquid nitrogen.

Thawing of ES lines frozen on 24 well plates: The plate containing the cells was removed from the  $-70^{\circ}\text{C}$  freezer and 1 ml of pre-warmed GMEM medium was added. The plate was incubated on a pre-warmed metal block in an incubator for 5-10 minutes. The medium was aspirated and the freshly pre-warmed GMEM medium was added immediately. For the cells frozen in the vials, the tube was taken out of the liquid nitrogen and transferred to a  $37^{\circ}\text{C}$  water bath immediately. The thawed cell suspension was transferred to 10ml GMEM medium and the cells were pelleted by centrifugation and resuspended in 10ml GMEM medium containing LIF. The cells were cultured for 24 hours and the old medium is removed. The fresh GMEM medium was added to get rid of the DMSO.

### **2.27. Blastocyst injection and the production of chimeras**

Recombinant ES cell clones were microinjected into C57BL/6 blastocysts. Blastocysts were usually cultured for 1-3 hours in PB-1 medium before injection to allow the blastocoel cavities to fully expand. ES cells were trypsinised and washed once with injection medium. 15-20 ES cells were injected into each blastocyst and 6-10 injected blastocysts were transferred to the uterine horn of a pseudopregnant F1(CBA/J x C57BL/6J) recipient mouse. Chimeric pups were identified by chimeric coat colour. Because the ES cells were derived from a mouse homozygous for the agouti coat colour (129/sv) allele and the recipient blastocyst was derived from black coat colour mouse (C57 Black6). The fur of the resulting chimeras has patches of both colours because the mouse contains cells of both genotypes.

### **2.28. Germline transmission and the generation of mice heterozygous**

Chimeric males were initially test bred with MF1 females and germline transmission of the mutant iNOS allele was detected by Southern blot analysis of tail DNA from F1 offspring with grey coat colour. Germline transmitting male chimeras were bred to MF1 and 129 females to obtain the mutation on hybrid or a pure in-bred background.

### **2.29. DNA isolation from mice tails and yolk sac**

The tails of neonates, the tail tip of 3 week-old mice and the yolk sac of 10.5, 13.5, 15.5 g.d. (gestation days) onwards embryos were placed in 0.5ml of lysis buffer (10mM Tris pH8.0, 50mM EDTA, 100mM NaCl, 0.5% SDS and 500µg/ml proteinase K). Digestion was done at 55°C overnight. The next day, the lysate was extracted once with phenol and chloroform, DNA was ethanol precipitated, washed with 70% ethanol, and resuspended in 100µl of TE at 4°C overnight. 10µl of DNA was used for the restriction enzyme digestion.

### **2.30. Elicitation and culture of peritoneal macrophages**

Mice were injected intraperitoneally with 2ml of sterile 3% Brewer's thioglycollate (Difco) in PBS. 3-4 days later the mice were killed by cervical dislocation while under terminal anaesthesia and swabbed with ethanol. 5ml of DMEM was injected into the peritoneal cavity through a 28 gauge needle attached to a 5ml syringe. The carcass was gently massaged and the fluid withdrawn. The number of macrophages in the exudate was estimated using a Neubauer haemocytometer by differential microscopy. Following centrifugation at 1500xg, the cell pellet was resuspended at a cell density of  $1 \times 10^6$  macrophages/ml in DMEM medium supplemented with 10% FBS, 2mM L-glutamine, 100IU/ml penicillin and 100µg/ml streptomycin (Gibco BRL).

### **2.31. Griess reaction for NO<sub>2</sub> measurement**

Nitrite concentration in the culture supernatants was determined by a microplate assay described by Ding *et al.* (Ding, *et al.*, 1988). Briefly, 50µl samples were harvested from the conditioned medium and treated with an equal volume of Griess reagent (1% sulfanilamide / 0.1% naphthylethylene diamine dihydrochloride / 2.5% H<sub>3</sub>PO<sub>4</sub>) at room temperature for 10 minutes. The absorbance at 570nm was monitored with a microplate reader. Nitrite concentration was determined by using sodium nitrite as a standard. The results were displayed as: NO<sub>2</sub>µM.

### **2.32. Northern blot**

The RNA was separated by electrophoresis in 1.5% agarose with 7.5% formaldehyde. Briefly, 3g of agarose was melted in 175ml DEPC treated distilled water and was cooled to 60°C before adding 10ml of 20xMOPS buffer (400mM MOPS, 122mM NaOAc, 20mM EDTA pH 7.0 in DEPC water), 15ml formaldehyde, mixed and poured into the gel tray. Gels were run in 1xMOPS buffer at 100V. RNA markers for gels were purchased from Promega.

Agarose-formaldehyde gels were rinsed twice in distilled water after electrophoresis. The RNA was then transferred onto a nylon membrane (Pharmacia) by capillary blot as for DNA. After transfer, membranes were rinsed in 2xSSC, air dried and oven baked at 120°C for 20 minutes.

### **2.33. iNOS Western blotting**

Stimulated cells were washed with ice cold TBS (Tris-buffered saline) before being lysed in buffer containing 25mM Tris.Cl PH7.4, 150mM NaCl, 1% NP-40, 1mM vanadate, 1mM EDTA, 2mM EGTA, 10mM NaF, 1mM D.T.T., 50µg/ml Leupeptin, 50µg/ml Aprotinin, and 50µg/ml PMSF. Clarified lysates (30µg) were resolved on 7.5% SDS-polyacrylamide (Bio-Rad) gels and transferred to nitrocellulose membrane (Bio-Rad).

For immunoblotting with iNOS antibody, membranes were blocked in Tris-buffered saline containing 0.1% Tween-20, and 2% BSA and incubated sequentially with monoclonal anti-iNOS (Affiniti) and horseradish peroxidase-conjugated donkey anti-mouse IgG (SAPU), and visualised protein bands by using enhanced chemiluminescence (ECL: Amersham Life Science).

#### **2.34. Growth and maintenance of *Leishmania major***

*Leishmania major* strain MRHO/SU/59P, also known as LV39, was used in this study. The isolate was maintained in the laboratory by continuous passage in BALB/c mice to maintain virulence. Non-ulcerated lesions of mice, infected four to five weeks previously in the right, hind footpad with  $1 \times 10^6$  parasites in 50  $\mu$ l Phosphate Buffered Saline (PBS), were removed and cut into small pieces in a petri dish (90mm) containing 10ml PBS. Parasites were further dispersed by forcing the suspension through a 5ml syringe placed against the bottom of the petri dish. The suspension was filtered into a universal using Monofilament Nylon Filter Cloth (NITEX) (Cadisch and Sons Ltd, London, U.K.) to remove remaining debris and washed twice by centrifugation at 1300g for 10 minutes at 4°C. After the final wash the pellet was resuspended in 5mls of Complete Schneiders Medium (CSDM), consisting of Schneiders Drosophila Medium (SDM) (Gibco) containing 20% FCS (Gibco) and 2.5% L-glutamine (Gibco). The parasites were then incubated for 3-4 days at 28°C in 25cm<sup>3</sup> tissue culture flasks (Corning, New York, U.S.A.) to transform amastigotes. For storage, parasites were then centrifuged at 1300g and resuspended in 2ml of CSDM containing 10% Dimethyl Sulfoxide (DMSO) (Sigma Chemical Co., Dorset, U.K.). A 10  $\mu$ l aliquot of this suspension was removed, diluted 1:100 in PBS containing 2.5% Formalin (Sigma Chemical Co.) and the number of parasites counted using an Improved Neubauer Haemocytometer (Merck Ltd, Dorset, U.K.). Parasites were diluted to  $2 \times 10^7$ /ml in CSDM containing 10% DMSO, aliquoted into 1ml freezer vials and kept at -70°C overnight before storage in liquid nitrogen.

For growing *L. major in vitro* a vial was thawed from liquid nitrogen at room temperature and the contents cultured for three days in 5ml CSDM at 28°C. Parasites are then passaged *in vitro* in CSDM in a 80cm<sup>3</sup> tissue culture flask (Corning) and culturing at 28°C. Parasites were not maintained *in vitro* for longer than 4 passages for fear of loss of virulence.

### **2.35. *Leishmania major* infection**

Parasites at passage 1-4, but preferably using passage 1-3 at day 6-8 (in the log phase) were centrifuged and washed twice with PBS. The parasites were diluted to  $2 \times 10^7$ /ml with PBS and the mice were challenged in one of the hind footpads with  $1 \times 10^6$ /50µl *L. major* promastigotes. The lesions that developed were measured as 'footpad thickness increase' with a direct reading using a Vernier calliper gauge (GMH-309-t, gallenkamp, London).

### **2.36. Preparation of parasite antigens**

*L. major* was grown *in vitro* as described above and harvested at 7-10 days after passage. In experiments where live parasites were used, these were merely washed twice with sterile PBS, counted and resuspended at the required concentration in Complete RPMI consisting of RPMI 1640 containing 10% heat-inactivated FCS, 2mM L-glutamine, 100U/ml penicillin (Gibco), 100µg/ml streptomycin (Gibco) and 50µM 2-mercaptoethanol (Sigma). formalin-fixed parasites were obtained by fixing parasites ( $2 \times 10^8$ /ml) in 0.5% formaldehyde (Sigma) in PBS for 5 minutes at room temperature followed by three washes in sterile PBS before resuspending in complete RPMI. Soluble Antigen was prepared by freezing and thawing parasites ( $2 \times 10^8$ /ml in PBS) 5 times followed by centrifugation at 13,800g for 10minutes. The resulting supernatant was filtered using a 0.45µM filter (Millipore S.A., Molsheim, France) and diluted in Complete RPMI. Parasites were also sonicated (20kHz, 1 minute) using a Branson Sonifier 250 (Branson Ultrasonics Corporation, Danbury, CT, USA.) in PBS ( $2 \times 10^8$ /ml) and resuspended in Complete RPMI.

### **2.37. Parasite quantitation in footpads**

The number of parasites present in infected footpads was quantified using one of two methods as previously described. At the time points after infection, footpads were removed from mice by cutting the foot above the ankle. Footpads were cut into small pieces in CSDM in a petri dish (90mm) and then filtered through NITEX. The resulting suspension was serially diluted in triplicate in 96 well tissue culture plates containing complete CSDM. Plates were incubated at 28°C and examined every two days for parasite growth. Data were presented as the log<sub>10</sub> of the reciprocal of the last dilution showing parasite growth.

### **2.38. ELISA for IL-4 and IFN-γ**

In this study, the levels of cytokines in culture supernatants were measured by ELISA, using paired antibodies from PharMingen (A,M,S, Biotechnology Ltd., Witey, Oxon, UK). The cytokine levels (pg/ml) were determined according to the standard curve. Briefly, anti-cytokine monoclonal antibodies were diluted to 2µg/ml for IL-4 ELISA and to 10µg/ml for IFN-γ in the coating buffer (0.1M NaHCO<sub>3</sub>, pH 8.2) and 50µl/well applied to enhanced protein binding ELISA plates (Dynatech Immunlon 4) overnight at 4°C. The plates were washed twice with PBS/Tween 20 (0.05%) as washing buffer, and blocked with 100µl/well of 10% FCS in PBS for 1 hour at 37°C, then washed twice with the washing buffer. 50µl of the supernatant from the cell culture and diluted cytokine were added to the plate at 37°C for 3 hours. After washing four times with washing buffer, 50µl of biotinylated anti-cytokine detecting antibody (1µg/ml) was added and incubated for 1-2 hours at 37°C. The plates were washed six times with washing buffer before adding 100µl of the extravidin-peroxidase (2µg/ml) and incubated for 1 hour at 37°C. The plates were washed six times and the colour was developed by adding 100µl/well of TMB substrate for 10-30 minutes. The OD was read at 630nm with a reference filter at 490nm.

### **2.39. Measurement of specific antibody responses**

Blood was harvested from the heart of *L. major* infected mice and serum obtained by centrifugation at 350xg. Soluble *L. major* antigen as above described was coated onto Immulon-4 96-well plates (Dynatech Laboratories Ltd., Billingshurst, West Sussex, U.K.) in a volume of 50µl/well and incubated overnight at 4°C. Plates were washed twice using PBS containing 0.05% Tween-20 and blocked with 100µl/well of 20% FCS in PBS and incubated at 37°C for 1 hour. Plates were again washed twice using PBS/Tw, and serial dilutions of serum samples added to wells in a volume of 50µl, before plates were incubated for 2-3 hours at 37°C. Serum from infected mice and monoclonal antibody against gp63 (Dr. W.R. McMaster) were used as control serum against gp63. Plates were washed 6-8 times in PBS/Tw and then conjugated antibodies added to detect IgG, IgG2a or IgG1 in a volume of 100µl and incubated at 37°C for 2 hours. ELISA's detecting IgG1 were washed a further 6-8 times and 100ul of Extravidin-Peroxidase (Sigma Chemical Co.) added at a concentration of 3µg/ml. All ELISA's were then washed 8 times in PBS/Tw before developing using TMB Microwell Peroxidase Substrate (Kirkegaard and Perry Laboratories, Gaithersburg, Maryland, U.S.A.). The colour change on the plates was measured using a MR5000 Microplate reader (Dynatech) at 630nm.

### **2.40. Antigen specific proliferation *in vitro***

Antigen was prepared as described above and diluted in Complete RPMI to the required concentration before adding 100µl/well to 96-well tissue culture plates (Costar). Spleen and MLN cells were removed from mice and single cell suspensions obtained by gentle homogenisation using a 15ml glass homogeniser. Cells were filtered to remove debris using NITEX and washed 3 times in RPMI. Cells were resuspended in 2mls of Complete RPMI and again filtered before counting using an Improved Neubauer Haemocytometer under phase-contrast microscope. The cell concentration were adjusted 4x10<sup>6</sup>/ml and 100µl added to each well in quadruplicate cultures. Cells were cultured at

37°C in 5% CO<sub>2</sub>, pulsed with <sup>3</sup>H-Thymidine (1μCi per well), harvested on an automatic cell harvester and radioactivity counted in a β-counter (LKB).

#### **2.41. Carageenan inflammation mouse model**

The mice were injected in the right hind footpad with 300μg of lambda carrageenin (Sigma) in 50μl PBS. The control left hind footpad was injected with 50μl PBS alone. Footpad swelling was measured with a dial calliper as footpad thickness increase (right footpad - left footpad ±SEM).

#### **2.42. LPS mouse shock model**

The mice were injected intraperitoneally with 10mg/kg or 12.5mg/kg of LPS in 0.2ml PBS. The body weights were measured everyday up to 4 days after injection. The body weight loss was calculated for the individual mice.

#### **2.43. T-cell proliferation assays**

Spleens were removed from mice and single cell suspensions made by gentle homogenisation. The cells were washed twice with PBS and resuspended at 2x10<sup>6</sup> cells/ml in culture medium ( RPMI 1640, or DEMAM, GIBCO BRL) supplemented with 10% FCS, 200μm glutamine, 100unit/ml penicillin, 100μg/ml streptomycin and 50μm 2-mercaptoethanol. The cells were cultured in 96 well microtiter plates (Costar) at 2 x 10<sup>5</sup> cells/well. The indicated concentrations of Con A or the antigen or live promastigotes of *L. major* were added into the cell culture. The cultures were set up in triplicate and incubated for 3-5 days at 37°C in 5% CO<sub>2</sub>, pulsed for 6 hours with a high specificity <sup>3</sup>H-thymidine, harvested with an automatic cell-harvester (WALLAC Pharmacia) and radioactivity counted in a β-counter (LKB, Betaplate, Turku, Finland). The supernatants were harvested for cytokines assays from the parallel cultures or the same cultures before the <sup>3</sup>H-thymidine was supplied.

#### **2.44. T-cell phenotyping**

Expression of functional T-cell markers CD4, CD8 and CD3 were analysed by using antibodies to these markers. The antibodies used in analysis were: PE-conjugated rat anti-mouse CD4 (4µl/test, Becton & Dickinson), FITC-conjugated or biotinylated rat anti-mouse CD8 (4µl/test, Becton & Dickinson), and the pan-T cell marker hamster anti-mouse CD3 FITC-conjugated (Clone 145-211, 0.5µg/test, Boehringer Mannheim, Germany). Mouse spleen cells were dual-labelled as follows: Spleen cells were washed 2 times with ice-cold PBS containing 0.1% sodium azide. For each sample, cells were prepared in 3 separate tubes, about one million cells per tube. Cells in each of the 3 tubes were incubated for 30 minutes at 4°C, with 2 of the above antibody conjugates at different combinations: anti-CD4 (PE) + anti-CD8 (FITC), anti-CD4 (PE) + anti-CD3 (FITC), anti-CD8 (Biotin) + anti-CD3 (FITC). Cells labelled with antibodies of the third combination were further incubated with PE-conjugated avidin (Vector Laboratory). The cells were then washed twice with cold PBS and resuspended in 1ml of PBS containing 0.5% BSA for FACS analysis.

**Table 2.1. Buffer composition used in restriction enzyme digests.**  
 (All concentrations are mM and are final in the reaction mixture)

Component	Buffer A	Buffer B	Buffer L	Buffer M	Buffer H
Tris acetate	33	-	-	-	-
Tris.HCl	-	10	10	10	10
Mg-acetate	10	-	-	-	-
MgCl <sub>2</sub>	-	5	10	10	10
K-acetate	66	-	-	-	-
NaCl	-	100	-	50	100
DTE*	-	-	1	1	1
DTT*	0.5	-	-	-	-
2-Me*	-	1	-	-	-
pH at 37°C	7.9	8.0	7.5	7.5	7.5

\*DTE=Dithioerythritol. DTT=Dithiothreitol. 2-Me=2-mercaptoethanol

**Table 2.2. Restriction endonucleases used and their recognition sites**

Restriction Endonuclease	Buffer	Recognition Sequence
<i>Apa</i> I	A	5'-GGGCC / C-3'
<i>Ava</i> II	A	5'-G / G(A/T)CC-3'
<i>Bam</i> HI	B	5'-G / GATCC-3'
<i>Bgl</i> II	M	5'-A / GATCT-3'
<i>Cla</i> I	H	5'-AT / CGAT-3'
<i>Eco</i> R I	H	5'-G / AATTC-3'
<i>Eco</i> R V	B	5'-G / ATATC-3'
<i>Eco</i> 47 I	H	5'-AGC / GCT-3'
<i>Hind</i> III	B	5'-A / AGCTT-3'
<i>Kpn</i> I	L	5'GGTAC / C-3'
<i>Not</i> I	H	5'-GC / GGCCGC-3'
<i>Pst</i> I	H	5'-CTGCA / G-3'
<i>Pvu</i> I	H	5'-CGAT / CG-3'
<i>Pvu</i> II	M	5'-CAG / CTG-3'
<i>Sac</i> I	A	5'-G / TCGAC-3'
<i>Sal</i> I	H	5'-G / TCGAC-3'
<i>Sma</i> I	A	5'-CCC /GGG-3'
<i>Spe</i> I	H	5'-A / CTAGT-3'
<i>Xba</i> I	H	5'-T / CTAGA-3'
<i>Xho</i> I	H	5'-C / TCGAG-3'

## **Chapter 3**

### **Inducible Nitric Oxide Synthase cDNA Clone**

### 3.1. Introduction

The first step of a gene targeting experiment is typically cDNA cloning and sequencing in order to make a cDNA probe to screen the genomic library. This also gives an understanding of the gene structure, which is helpful for the gene targeting construct design. A cDNA library was constructed in the vector  $\lambda$ ZAPII (Stratagene) using mRNA isolated from J774 macrophages activated with 10ng/ml LPS and 100units/ml IFN- $\gamma$  by Dr. Ian G. Charles (Cell Biology Department of The Wellcome Research Laboratories). Six independent positive colonies were found in the screen with both 5' and 3' specific probes and were subcloned in pBluescript. After the restriction enzymes mapping and terminal sequencing, two overlapping clones were used to make a full-length J774 iNOS cDNA. Double strand sequence was generated by universal primer sequencing of a nested set of deletions of the cDNA. Additional sequence was generated using specific primers designed from the sequence of the nested set. Apart from a four base pair deletion in one of the cDNA clones, the whole sequence was virtually identical to the published RAW 264.7 cell iNOS cDNA sequence (Lyons *et al.*, 1992). The detail is described below.

### 3.2. $\lambda$ Phage cDNA library Screening

XL1-Blue was infected with a high density ( $10^5$ ) of  $\lambda$  phage from the J774 cDNA library and plated on to 100mm plastic disposable petri disks with LB medium. The phage were transferred to nylon membranes in duplicate. The hybridisation was performed after the phage DNA was denatured and fixed on the membranes. 5' and 3' specific probes were purified from an agarose gel and labelled with  $\alpha$ -[ $^{32}$ P] dATP by the random primer method. The 5'-probe was generated by PCR using sequences around the ATG start codon from the published iNOS sequence.

5'-GGAGAAGCTTGGATTTGGAGCAGAAGTGCAAAGT-3' (sense from bases -48 to 14) (According to the published sequence of RAW 265.7 iNOS cDNA, Lyons *et al.*, 1992) and 5'-CACTGGATCCTGCCGATGCAGCGAGGGGCATTCC-3' (antisense from bases 565 to 599). The 3' probe was generated by PCR using sequences

corresponding to the NADPH binding domains of the enzyme. 5'-CCAAGAATTCACCTACTTCCTGGACATTACGACCCC-3' (sense from bases 2456 to 2492) and 5'-GAAAGGATCCAAGGGAGCAATGCCCGTACCAGGCC-3' (antisense from bases 2922 to 2958). Following hybridisation, positive phage plaques were picked in addition to negative plaques as controls and infected with the host cells (XL1-Blue) again and plated at low density. The screening was done twice in the same way with the same probes. Three independent phage were obtained from the 5'-probe screening, while another three were isolated from the 3'-probe screening.

### **3.3. cDNA subclones**

To avoid the long procedure of cDNA subcloning involving phage DNA isolation, the  $\lambda$  ZAP II vector was used to construct the J774 library. The phage vector contains a plasmid (pBluescript) component. The two separate domains (Initiator and Terminator) within the lambda ZAP II vector arms are recognised in the host bacteria by trans-acting proteins from the helper phage which can be co-infected. pBluescript plasmids with cDNA insert can be recovered by infecting an F' *E.coli* strain with helper phage and growing in the presence of ampicillin. In this study, six overlapping cDNAs were subcloned in the *Not* I site of the pBluescript (pBSSK-phagemid). The sizes of iNOS cDNAs insert are 2.7kb; 3.3kb; 1.3kb; 1.9kb; 2.6kb; and 1.5kb respectively for Clones 2; 4; 5; 6; 7; 10 which are showed in Fig.3.1.

### **3.4. Sequencing of subclones.**

The T7 and T3 oligonucleotide primers were used for all terminal sequencing of subclones. The sequences were compared and identified with the published iNOS cDNA sequence using the GCG computer programs. The cloning map of J774 iNOS cDNA is shown in Fig 3.1.

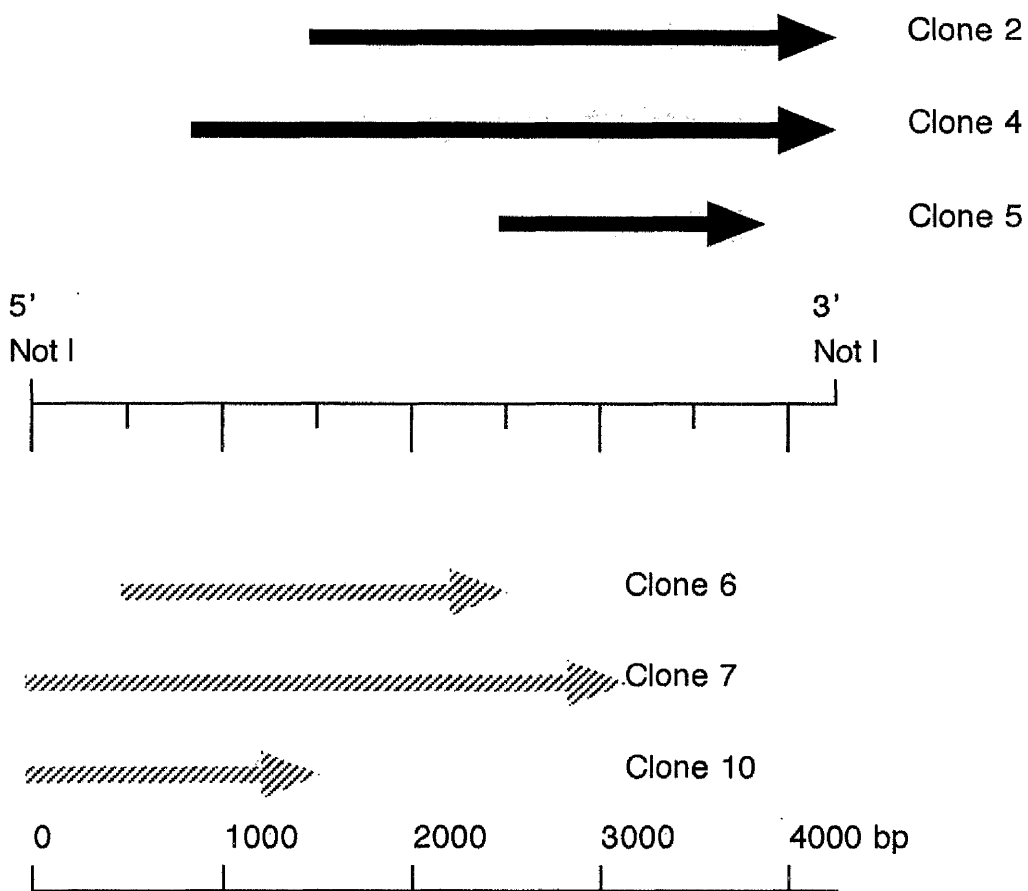


Fig.3.1. Cloning map of J774 iNOS cDNAs. Positions of clones isolated from the J774 cDNA library are indicated as arrows. Solid arrows represent clones isolated using a 3' iNOS PCR probe while striped arrows represent those isolated using a 5' probe.

### 3.5. Making a full-length murine iNOS cDNA clone

For the creation of the full-length J774 cDNA, clone 10 was digested with *Avr* II and *Xba* I while clone 4 was digested with *Avr* II, *Hind* III and *Pvu* I. The additional digestion with *Pvu* I is necessary as the insert of clone 4 is 3.0kb which is quite close in size to the vector (2.9kb for pBSSKII<sup>+</sup>), This digest effectively cuts the vector in half. Fragments of 1.0kb and 3.0kb corresponding to iNOS cDNA were recovered from the gel, ligated and inserted into *Xba* I and *Hind* III sites of pBSSKII<sup>+</sup> vector to construct the full-length J774 iNOS cDNA (pFLJ7) (Fig.3.2).

### 3.6. Double strand cDNA Sequencing for the J774 iNOS cDNA clone

7.5µg of pFLJ7 was digested with *Kpn* I (as the 3' over hang end) and *Hind* III (as the 5' overhang). The exonuclease, Exo III, is an external nuclease which will only degrade double stranded DNA from 5' overhang ends, so pFLJ7 was deleted from the *hind* III end of the iNOS cDNA. After the nested set of deletions was made, the blunt ends (which were generated by S1 nuclease) were religated and the time course of differentially deleted cDNAs were transformed into *E.coli*. DNA from representative subclones from different time points were purified by alkaline SDS mini-prep for sequencing with the T3 primer. The sequences were checked with the published iNOS cDNA sequence. The list of deleted cDNA clones and location are shown in Table 3.1 and the map of sequences covered on the full-length cDNA is shown in Fig.3.3. 3387bp of J774 iNOS cDNA sequence was obtained. The sequences corresponding to positions 1271-1823 and 3557-3727 were not obtained by the nested deletions. In order to complete the cDNA antisense sequence, three sequence oligonucleotide sequence primers (**BB78**, **BB79**, **BB80**) were made and were used to determine the rest of J774 iNOS cDNA sequence.

**BB78:** GTGGCCAACATGCTACT

**BB79:** GACCTTTCGCATTAGCA

**BB80:** TCCAGCTCAAGAGCCAG

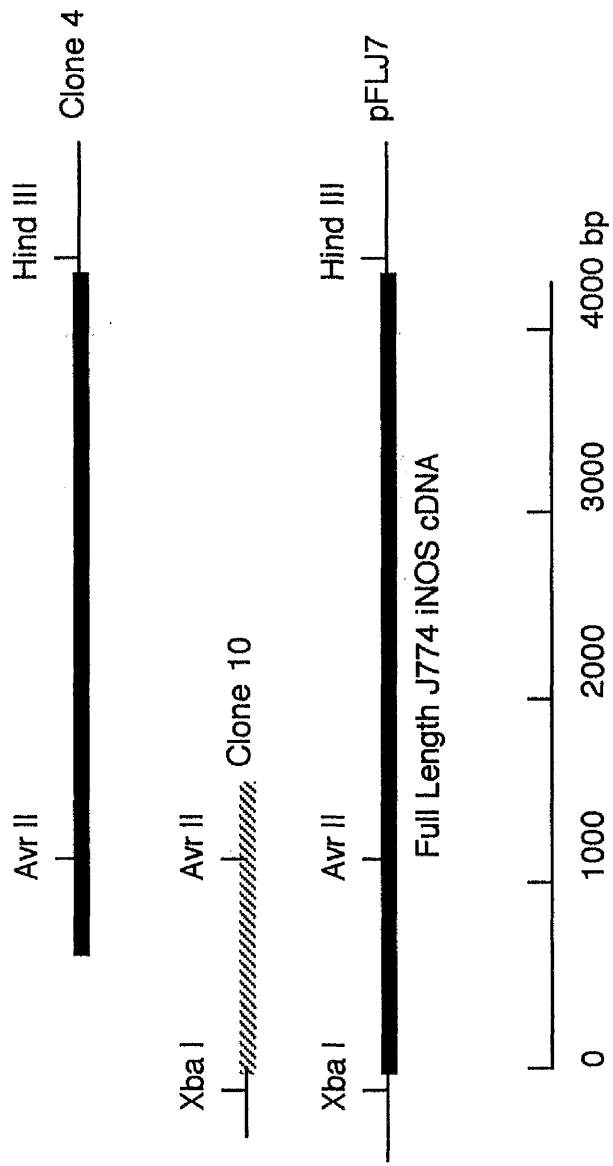


Fig 3.2. Full-length J774 iNOS cDNA construct (pFLJ7). The solid line represents clone 4 which was ligated with clone 10 (indicated as a striped line) at the Avr II site. The full-length cDNA (pFLJ7) is about 4.1kb.

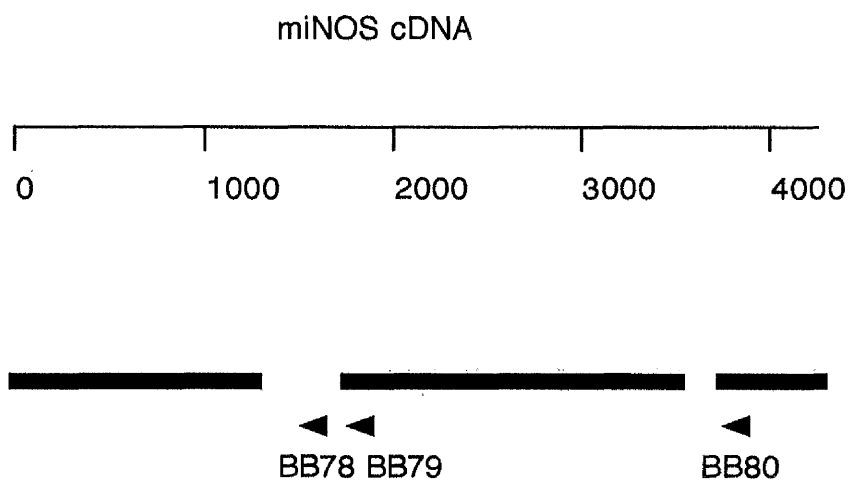


Fig 3.3. The map of J774 iNOS cDNA antisense sequencing. The solid lines represent obtained sequence with the cDNA nest-set deletion system. The small triangles show the position of the sequence specific oligonucleotides used as primers.

Table 3.1. The list of deleted cDNA clones and locations

No.	The file names	The location of iNOS cDNA sequence
1	WEI17D.DNA	-14--242
2	WEI1B.DNA	174--424
3	WEI1C.DNA	157--401
4	WEI13B.DNA	265--486
5	WEIK7.1DNA	3--256
6	WEIK13.3DNA	32--242
7	WEIK5.5DNA	-90--151
8	WEIK5.3DNA	-14--191
9	WEIK7.11DNA	140--430
10	WEIK7.2DNA	94--339
11	WEIK7.2DNA	157--396
12	WEIK11.7DNA	248--384
13	WEIK5.7DNA	458--663
14	WEIK5.9DNA	538--816
15	WEI13A.DNA	623--833
16	WEI19B.DNA	833--1010
17	WEI17A.DNA	737--970
18	WEIK9.6DNA	822--1015
19	WEIK11.12DNA	1083--1271
20	WEIK9.12DNA	1823--2036
21	WEIK17.2DNA	1908--2141
22	WEI13B.DNA	1999--2238
23	WEI17C.DNA	2033--2255
24	WEIS12.1DNA	2124--2312
25	WEIK15.6DNA	2277--2442
26	WEIS2.1DNA	2380--2556

27	WEIK15.7DNA	2317--2567
28	WEIK15.10DNA	2312--2522
29	WEIK11.5DNA	2542--2761
30	WEIK9.2DNA	2755--3017
31	WEIK13.12DNA	2573--2755
32	WEI18.3DNA	2755--2920
33	WEIK13.7DNA	2727--2897
34	WEI13.10DNA	2801--2988
35	WEIS18.6DNA	2920--3187
36	WEIK7.6DNA	2954--3204
37	WEI9C.DNA	2988--3261
38	WEIK9.10DNA	3068--3255
39	WEIS16.4DNA	3130--3295
40	WEIS16.7DNA	3073--3352
41	WEIK9.5DNA	3090--3267
42	WEI7A.DNA	3318--3569
43	WEIS12.2DNA	3346--3557
44	WEI9D.DNA	3727--3875
45	WEIS8.1DNA	3727--3875

In order to generate the sense DNA strand of the J774 iNOS cDNA, 20 sequencing oligo nucleotides were synthesised by Mr. Hugh Spence in the Cell Biology Department of the Wellcome Research Laboratories. The sequences of the 17 mers are:

<b>BB125:</b> TCAACTGCAAGAGAACG	<b>BB126:</b> GCAGCTCCTCACTGGGA
<b>BB127:</b> CAGAGACAAGCCTACCC	<b>BB128:</b> CATCGGCAGGATCCAGT
<b>BB129:</b> AGATGCCCGATGGCACC	<b>BB130:</b> AGCTCGGGTTGAAGTGG
<b>BB131:</b> AAGACCGGGCTGTCACG	<b>BB132:</b> TGA ACTATGTCCTATCT
<b>BB133:</b> TTGCTACTGAGACAGGG	<b>BB134:</b> CTCAACCACACCTTCAG
<b>BB135:</b> GTCCGAAGCAAACATCA	<b>BB136:</b> GTTCAGCTCACCTTCGA
<b>BB137:</b> TGCTCACTCAGCCAAGC	<b>BB138:</b> CATGTGCCCGCTGCCTT
<b>BB139:</b> CCCTGCTTTGTGCGAAG	<b>BB140:</b> CAGGAAGAAATGCAGGA
<b>BB141:</b> GCTACCACATTGAAGAA	<b>BB142:</b> TCTGACAGCCCAGAGTT
<b>BB143:</b> GTGGACTACTAAATCTC	<b>BB144:</b> TTTGGGTGACCACCAGG

Complete nucleotide sequence analysis of the coding region found that a four base pair deletion, from position 2595-2598 (GCAG) had arisen in clone 4. This deletion disrupted the iNOS ORF (Open Reading Frame) such that a stop codon was placed just downstream from the deleted region resulting in premature termination of any protein translation. The oligonucleotide sequence primer (BB137: TGCTCACTCAGCCAAGC) was used to sequence the remaining 3' iNOS cDNA clones (clones 2 and 5). The four base pair deletion was not found in either of them and the resulting sequence was found to be exactly same with the published sequence. The full-length iNOS cDNA (with the 4bp deletion) was used initially to construct an *E. coli* expression vector, which not surprisingly failed to express iNOS. Theoretically, any recombinant protein being produced from this construct could only have had a maximum Mr of 115kDa. The theoretical proteins translated from the cDNA with and without deletion are showed in Fig.3.4. The 5' region of the detective iNOS cDNA was digested out of pBSSKII<sup>+</sup> with *Not* I and *Stu* I and replaced with a corresponding region of clone 7 to create a full-length iNOS cDNA without the deletion. Enzymatically active recombinant iNOS was obtained

in a Baculovirus expression system (this study has done by Dr. David W. Moss, Cell Biology Department, Wellcom Research Laboratories, see attached paper). Apart from the four base pair deletion found in clone 4 mentioned above, the full-length J774 iNOS cDNA is 100% identical with the published RAW 264.7 sequence in the coding region (Lyons et al., 1992). Analysis of the 5' and 3' untranslated flanking regions of the isolated cDNA showed only one nucleotide substitution (T for C at position 3473). The map of iNOS and the whole J774 iNOS cDNA sequence are showed in Fig.3.5 and Fig.3.6.

### **3.7. Summary**

The results described above detail the iNOS cDNA cloning and sequencing. A full-length iNOS cDNA was constructed using clones isolated from a library made from mRNA isolated from activated J774 macrophages. Double-strand cDNA sequence analysis showed that the J774 iNOS clone was virtually identical to that of the RAW 264.7 macrophages iNOS cDNA sequence (Lyons, et al., 1992). Analysis of the 5' and 3' untranslated flanking regions of the isolated cDNA showed a single nucleotide substitution (T for C at position 3473). Ligation of a *Not* I fragment of pBlueScript J7iNOS containing the full-length cDNA for iNOS into the baculovirus transfer vector pVL1393 resulted in iNOS expression. The expression and enzyme kinetic studies for recombinant iNOS were performed by Dr. David W. Moss in the Cell Biology Department of the Wellcome Research Laboratories. This work has been published in the European Journal of Pharmacology 289(1995) 41-48.

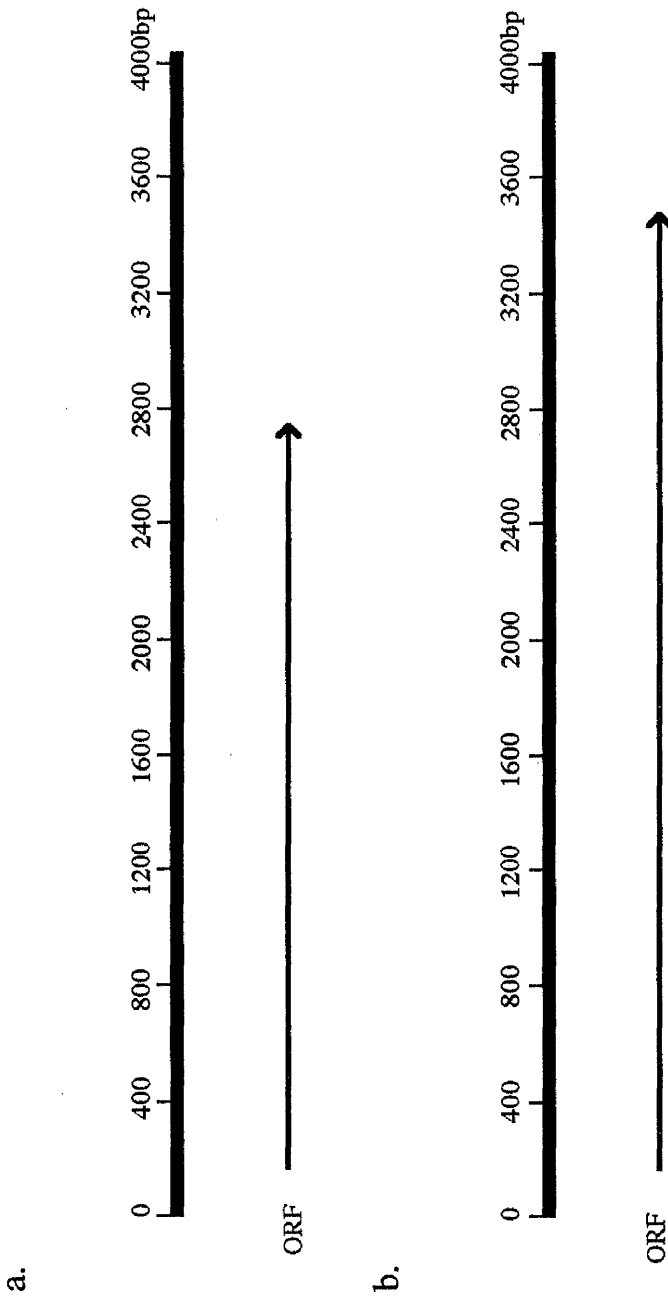


Fig.3.4. The solid lines and the arrow lines represent the iNOS cDNAs and theoretical size of recombinant proteins respectively. (a.) J774 iNOS cDNA without deletion and (b.) with deletion.

## J774 Inducible Nitric Oxide Synthase

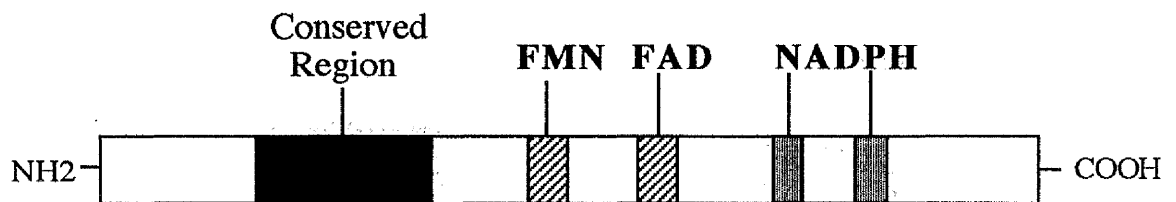


Fig 3.5. Schematic representation of the iNOS protein encoded by the J774 iNOS cDNA. The solid box represents the highly conserved region shared between all NOS isoforms. The striped boxes represent FMN and FAD binding domains. The shaded regions denote the NADPH binding domains.

Fig.3.6. The sequence of J774 iNOS cDNA

4117 bp

1 GGGACACAGT GTCACCTGGTT TGAAACTTCT CAGCCACCTT GGTGAAGGGA CTGAGCTGTT  
61 AGAGACACTT CTGAGGCTCC TCACGCTTGG GTCTTGTTCA CTCCACGGAG TAGCCTAGTC  
121 AACTGCAAGA GAACGGAGAA CGTTGGATTI GGAGCAGAAG TGCAAAGTCT CAGACATGGC  
181 TTGCCCTGG AAGTTTCTCT TCAAAGTCAA ATCCTACCAA AGTGACCTGA AAGAGGAAAA  
241 GGACATTAAC AACAACTGA AGAAAACCCC TTGTGCTGTT CTCAGCCCAA CAATACAAGA  
301 TGACCCTAAG AGTCACCAA ATGGCTCCCC GCAGCTCCTC ACTGGGACAG CACAGAATGT  
361 TCCAGAATCC CTGGACAAGC TGCATGTGAC ATCGACCCGT CCACAGTATG TGAGGATCAA  
421 AAAC TGGGGC AGTGGAGAGA TTTTGCATGA CACTCTTAC CACAAGGCCA CATCGGATTT  
481 CACTTGCAAG TCCAAGTCTT GCTTGGGGTC CATCATGAAC CCCAAGAGTT TGACCAGAGG  
541 ACCCAGAGAC AAGCCTACCC CTCTGGAGGA GTCCTGCCT CATGCCATTG AGTTCATCAA  
601 CCAGTATTAT GGCTCCTTTA AAGAGGCAAA AATAGAGGAA CATCTGGCCA GGCTGGAAGC  
661 TGTAACAAAG GAAATAGAAA CAACAGGAAC CTACCAGCTC ACTCTGGATG AGCTCATCTT  
721 TGCCACCAAG ATGGCCTGGA GGAATGCCCC TCGCTGCATC GGCAGGATCC AGTGGTCCAA  
781 CCTGCAGGTC TTTGACGCTC GAAACTGTAG CACAGCACAG GAAATGTTTC AGCACATCTG  
841 CAGACACATA CTTTATGCCA CCAACAATGG CAACATCAGG TCGGCCATCA CTGTGTTCCC  
901 CCAGCGGAGT GACGGCAAAC ATGACTTCAG GCTCTGGAAT TCACAGCTCA TCCGGTACGC  
961 TGGCTACCAG ATGCCCGATG GCACCATCAG AGGGGATGCT GCCACCTTGG AGTTCACCCA  
1021 GTTGTGCATC GACCTAGGCT GGAAGCCCCG CTATGGCCGC TTTGATGTGC TGCCCTCTGGT  
1081 CTTGCAAGCT GATGGTCAAG ATCCAGAGGT CTTTAAAATC CCTCCTGATC TTGTGTTGGA  
1141 GGTGACCATG GAGCATCCCA AGTACGAGTG GTTCCAGGAG CTCGGGTTGA AGTGGTATGC  
1201 ACTGCCTGCC GTGGCCAACA TGCTACTGGA GGTGGGTGGC CTCGAATFCC CAGCCTGCCC  
1261 CTTCAATGGT TGGTACATGG GCACCGAGAT TGAAGITCGA GACTTCTGTG ACACACAGCG  
1321 CTACAACATC CTGGAGGAAG TGGGCCGAAG GATGGGCCTG GAGACCCACA CACTGGCCTC  
1381 CCTCTGAAA GACCGGGCTG TCACGGAGAT CAATGTGGCT GTGCTCCATA GTTCCAGAA  
1441 GCAGAATGTG ACCATCATGG ACCACCACAC AGCCTCAGAG TCCTTCATGA AGCACATGCA  
1501 GAATGAGTAC CGGGCCCCGT GAGGCTGCCC GGCAGACTGG ATTTGGCTGG TCCCTCCAGT  
1561 GTCTGGGAGC ATCACCCCTG TGTTCACCA GGAGATGTTG AACTATGTCC TATCTCCATT  
1621 CTACTIONAC CAGATCGAGC CCTGGAAGAC CCACATCTGG CAGAATGAGA AGCTGAGGCC

1681 CAGGAGGAGA GAGATCCGAT TTAGAGTCTT GGTGAAAGTG GTGTTCTTTG CTTCCATGCT  
1741 AATGCGAAAAG GTCATGGCIT CACGGGTCAG AGCCACAGTC CTCTTTGCTA CTGAGACAGG  
1801 GAAGTCTGAA GCACTAGCCA GGGACCTGGC CACCTTGTTT AGCTACGCCT TCAACACCAA  
1861 GGTTGTCTGC ATGGACCAGT ATAAGGCAAG CACCTTGGAA GAGGAGCAAC TACTGCTGGT  
1921 GGTGACAAGC ACATTTGGGA ATGGAGACTG TCCCAGCAAT GGCCAGACTC TGAAGAAATC  
1981 TCTGTTTATG CTTAGAGAAC TCAACCACAC CTTCAGGTAT GCTGTGTTTG GCCTTGGCTC  
2041 CAGCATGTAC CCTCAGTTCT GCGCCTTTGC TCATGACATC GACCAGAAGC TGTCCCACCT  
2101 GGGAGCCTCT CAGCTTGCCC CAACAGGAGA AGGGGACGAA CTCAGTGGGC AGGAGGATGC  
2161 CTTCCGCAGC TGGGCTGTAC AAACCTTCCG GGCAGCCTGT GAGACCTTTG ATGTCCGAAG  
2221 CAAACATCAC ATTCAGATCC CGAAACGCTT CACTTCCAAT GCAACATGGG AGCCACAGCA  
2281 ATATAGGCTC ATCCAGAGCC CGGAGCCTTT AGACCTCAAC AGAGCCCTCA GCAGCATCCA  
2341 TGCAAAGAAC GTGTTTACCA TGAGGCTGAA ATCCCAGCAG AATCTGCAGA GTGAAAAGTC  
2401 CAGCCGCACC ACCCTCCTCG TTCAGCTCAC CTTGAGGGC AGCCGAGGGC CCAGCTACCT  
2461 GCCTGGGGAA CACCTGGGGA TCTTCCCAGG CAACCAGACC GCCCTGGTGC AGGGAATCTT  
2521 GGAGCGAGTT GTGGATTGTC CTACACCACA CCAAAGTGTG TGCCCTGGAGG TTTCTGGATGA  
2581 GAGCGTACT GGGTCAAAGA CAAGAGGCTG CCCCCCTGCT CACTCAGCCA AGCCCTCACC  
2641 TACTTCCTGG ACATTACGAC CCCTCCCACC CAGCTGCAGC TCCACAAGCT GGCTCGCTTT  
2701 GCCACGGACG AGACGGATAG GCAGAGATTG GAGGCCTTGT GTCAGCCCTC AGAGTACAAT  
2761 GACTGGAAGT TCAGCAACAA CCCCACGTTT CTGCATGTGC CCGCTGCCTT CCTGCTGTGC  
2821 CAGCTCCCTA TCTTGAAGCC CCGCTACTAC TCCATCAGCT CCTCCCAGGA CCACACCCCC  
2881 TCGGAGGTTT ACCTCACTGT GGCCGTGGTC ACCTACCGCA CCGGAGATGG TCAGGGTCCC  
2941 CTGCACCATG GTGTCTGCAG CACTTGGATC AGGAACCTGA AGCCCCAGGA CCCAGTGCCC  
3001 TGCTTTGTGC GAAGTGTGAG TGGCTTCCAG CTCCCTGAGG ACCCCTCCA GCCTTGCATC  
3061 CTCATTGGGC CTGGTACGGG CATTGCTCCC TCCGAAAGTT TCTGGCAGCA GCGGCTCCAT  
3121 GACTCCCAGC ACAAAGGGCT CAAAGGAGGC CGCATGAGCT TGGTGTFTTG GTGCCGGCAC  
3181 CCGGAGGAGG ACCACCTCTA TCAGGAAGAA ATGCAGGAGA TGGTCCGCAA GAGAGTGCTG  
3241 TTCCAGGTGC ACACAGGCTA CTCCCGGCTG CCCGGCAAAC CCAAGGTCTA CGTTCAGGAC  
3301 ATCCTGCAAA AGCAGCTGGC CAATGAGGTA CTCAGCGTGC TCCACGGGGA GCAGGGCCAC  
3361 CTCTACATTT GCGGAGATGT GCGCATGGCT CGGGATGTGG CTACCACATT GAAGAAGCTG

3421 GTGGCCACCA AGCTGAACTT GAGCGAGGAG CAGGTGGAAG ACTATTTCTT CCAGCTCAAG  
3481 AGCCAGAAAC GTTATCATGA AGATATCTTC GGTGCAGTCT TTTCTATGG GGCAAAAAG  
3541 GGCAGCGCCT TGGAGGAGCC CAAAGCCACG AGGCTCTGAC AGCCCAGAGT TCCAGCTTCT  
3601 GGCAGTGAAT AAAGATAATG GTGAGGGGCT TGGGGAGACA GCGAAATGCA ATCCCCCCA  
3661 AGCCCCCAT GTCATTCCCC CCTCCTCCAC CCTACCAAGT AGTATTGTAC TATTGTGGAC  
3721 TACTAAATCT CTCTCCTCTC CTCCCTCCCC TCTCTCCCTT TCCTCCCTTC TTCTCCACTC  
3781 CCCAGCTCCC TCCTTCTCCT TCTCCTCCTT TGCCTCTCAC TCTTCCTTGG AGCTGAGAGC  
3841 AGAGAAAAAC TCAACCTCCT GACTGAAGCA CTTTGGGTGA CCACCAGGAG GCACCATGCC  
3901 GCCGCTCTAA TACTTAGCTG CACTATGTAC AGATATTTAT ACTTCATATT TAAGAAAACA  
3961 GATACTTTTG TCTACTCCCA ATGATGGCTT GGGCTTTCCT GTATAATTTT CCTTGATGAA  
4021 AAATATTTAT ATAAAATACA TTTTATTTTA AAAAAAAAAA AAAAAAAAAA AAAAAAAAAA  
4081 AAAAAAAAAA AAAAAAAAAA AAAAAAAAAA AAAAAA

## **Chapter 4**

### **Inducible Nitric Oxide Synthase Gene Targeting**

#### 4.1. Introduction

The targeting of the iNOS gene in ES cells is a mechanism to introduce specific mutations into the murine genome. Analysis of the phenotype of mice carrying such a targeted mutation can provide an insight into the biological role of iNOS, the functions of which had previously been largely a matter of speculation. Along with iNOS cDNA cloning, genomic cloning and restriction mapping are crucial factors in the construction of a gene targeting construct for homologous recombination in ES cells. In this study, genomic DNAs from two mouse strains (B6 and 129/sv mice) were used for cloning of iNOS-specific fragments and were mapped by restriction enzymes. The most commonly used targeting vector is a replacement vector, and this type of vector was used in the iNOS targeting work. Both 5' and 3' external probes were used to screen for the gene replacement event after recombination in an ES cell line. The mutated ES cells were injected into blastocysts to generate chimeric mice, which were then mated with test breeding mice (MF1) to test for germ line transmission. This was conveniently analysed by examination of offspring coat colour. Heterozygous mice were subsequently mated to generate homozygous mice. In the iNOS gene targeting described in this chapter, an unpredicted gene-rearrangement event occurred, which made it difficult to analyse the iNOS-deletion genotype. The detail is described below.

#### 4.2. Mouse iNOS genomic DNA cloning and gene mapping

Two libraries were analysed, a B6  $\lambda$  EMBL 4 genomic library (a gift of Dr. W. Mullar, Genetic Research Institute, University of Cologne) and a 129/sv  $\lambda$  DASH genomic library (obtained from Dr. Austin Smith, AFRC, CGR, University of Edinburgh). Both libraries were screened with a J774 cDNA 5' *EcoRI* fragment (937bp) (Fig. 4.1).

One positive colony was obtained from the B6 mouse library, while another three positive colonies were obtained from the 129/sv library. The  $\lambda$  DNAs were purified and restriction enzyme mapping was carried out with *Bam* H I, *Bgl* II, *EcoR* I, *EcoR* V, *Hind* III, *Kpn* I, *Pst* I, *Sac* I, *Sma* I, *Spe* I, *Xba* I. The four genomic lambda clones

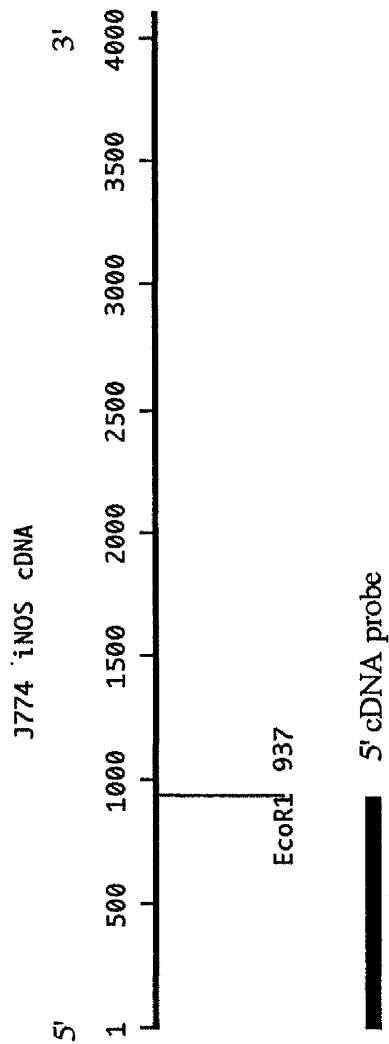


Fig.4.1. The 937bp *EcoRI* fragment was cut out from the full-length J774 iNOScDNA clone, purified from an agarose gel and labeled with  $\alpha$ - $P^{32}$ -dATP.

from B6 and 129/sv libraries overlap and cover about 21kb of iNOS genomic DNA. The above restriction enzymes sites are identical for the two different mouse strains examined. The sizes of genomic DNA fragments and restriction enzyme map are shown in Fig.4.2.

To locate iNOS introns and exons, a number of Southern blot experiments were carried out. In addition, genomic subcloning and partial DNA sequencing was carried out in this study. 6.0kb, 2.8kb, 2.2kb, 1.4kb *BamH* I fragments; 7.5kb, 4.5kb, 4.2kb, 2.2kb *EcoR* I fragments and 3.8kb, 1.6kb, 0.8kb *Pst* I genomic fragments were subcloned in *BamH* I, *EcoR* I and *Pst* I sites of pBlueScript respectively. The whole sequence was completed for a 4.2kb *EcoR* I subclone which covered the iNOS promoter and exon 1 and 2 (Fig 4.3.). The exons 3, 4, and 5 were obtained from a 6.0kb *BamH* I subclone and located by Southern blot analysis and DNA sequencing. The exon-intron junctions for exons 1-5 and 7 are shown in table 4.1. Most of these 6 intron-exon boundaries conformed to the known GT/AG donor/acceptor site rule, essentially maintaining the consensus sequence described by Mount (Mount, 1982) Exons 6 and 7 were found in 2.8kb and 1.4 kb *BamH* I subclones, but the exon 6 junction was not sequenced. Half of exon 8 was identified by the terminal sequence of 7.5kb *EcoR* I fragment subclone. In total, eight iNOS exons (from exon 1 to 8) and the promoter were found spanning some ~21kb of genomic DNA. These eight exons are quite small (from 70bp to 156bp in the first seven exons), and they only contribute 937bp of iNOS cDNA (Fig 4.4). The start codon for iNOS translation is located in exon 2. From exon 2 to exon 3, there is a large intron in between, which is about 5.5kb.

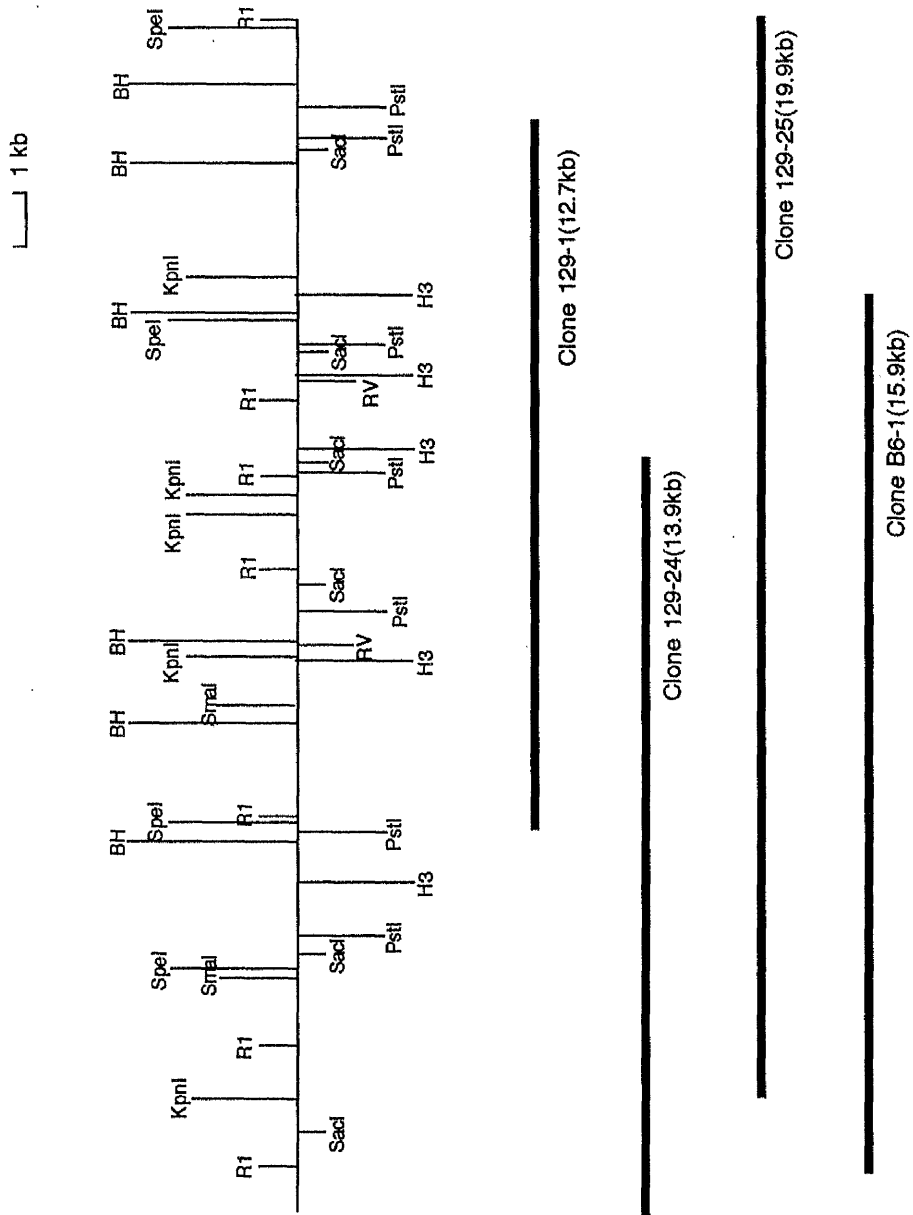


Fig.4.2. Four overlapping murine iNOS genomic DNA clones and the restriction enzymes used for the gene mapping. The clones span approximately 21kb. RI=*EcoRI*, BH=*BamHI*, H3=*HindIII*, RV=*EcoRV*,

1 kb

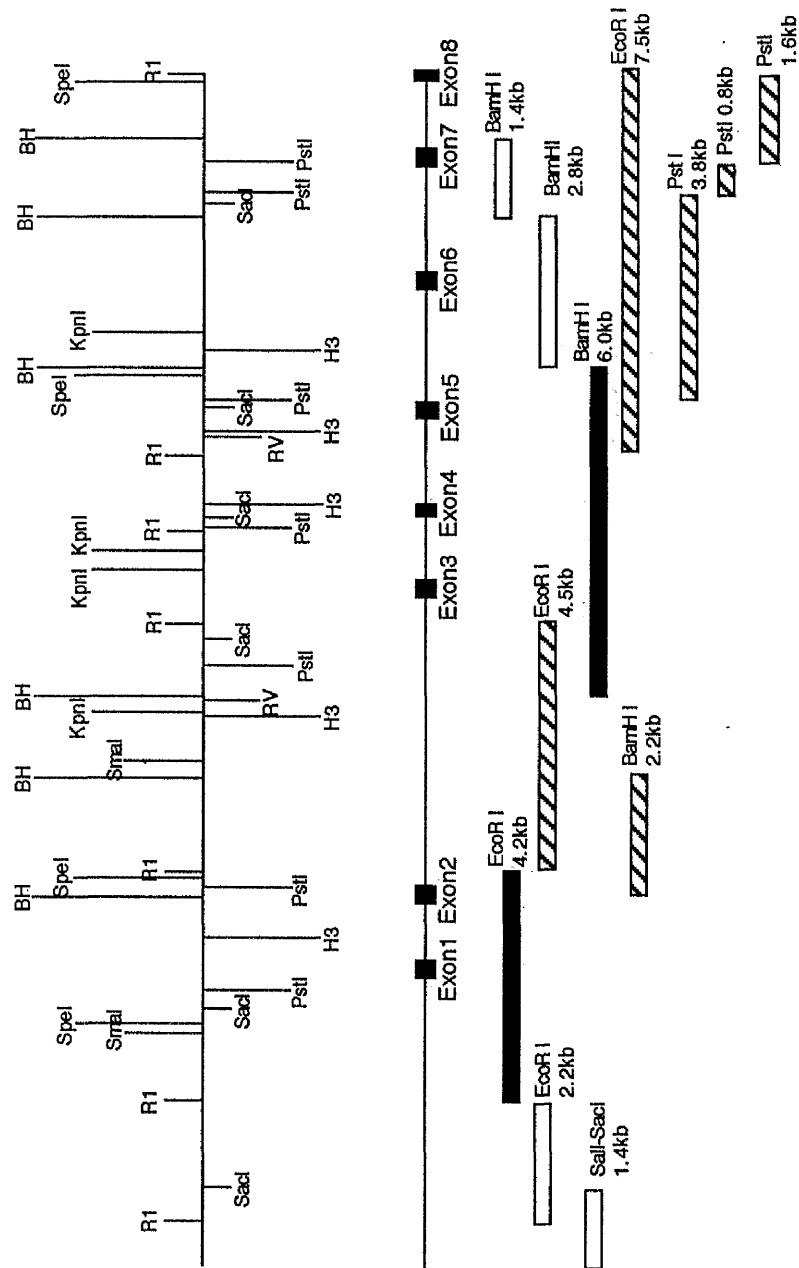


Fig.4.3. Exon 1-8 were located by Southern blotting and some subclones were sequenced. The iNOS genomic subclones are shown as bars, the solid bars are the completed DNA sequenced, the striped bars have only been partially sequenced and the empty bars are subclones that have not yet been sequenced.

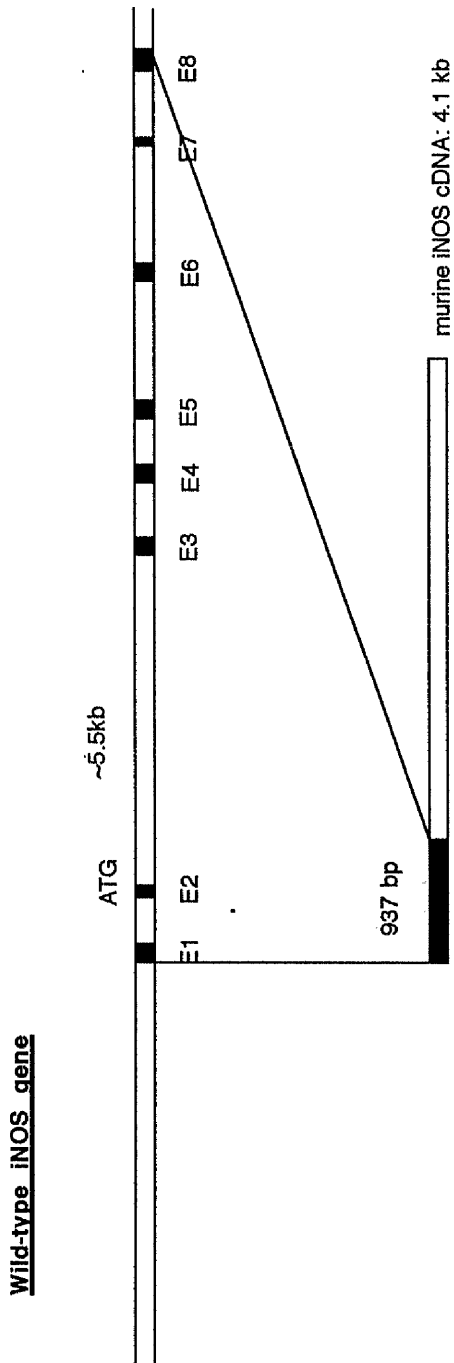


Fig. 4.4. 937bp of murine iNOS cDNA is contributed by first eight exons (E1-8). The Start codon (ATG) is located in the exon 2. A large (>5kb) intron is located between exon2 and exon 3..

Table 4.1. The intron-exon junctions of murine iNOS genome.

3' Intron	Exon size	5' Intron
tggccccaCG GGACACAGT	128bp (Exon1)	TCAACTGCAAG GTGAGTctt
cccttcctcAG AGAACGGAG	156bp (Exon2)	GCTGTTCTCAG CCCAACaat
tcctttcgcAG CCCAACAAT	70bp (Exon3)	GGACAGCACAG GTCAGTggt
accattttAG AATGTTCCA	121bp (Exon4)	CGGCCACATCG GTAAGAagtc
ccttttccAG GATTTCACT	149bp (Exon5)	CCTTTAAAGAG GCAAAAata
gtgccctgTG CAGGTCTTT	97bp (Exon7)	GTCAACATCAG GTGAGGcacc
(Y) <sub>n</sub> NYAG		GTRAGT
3' Acceptor		5' Donor

#### 4.3. Positive-negative selection constructs for iNOS gene targeting

A variety of strategies have been used to increase the number of positive clones arising from homologous recombination above the background of clones surviving selection. The most widely used of these, developed by Mansour (Mansour *et al.*, 1988) uses a second, negative selection step, in addition to the positive selection afforded by the neomycin resistance encoding gene (*neo* gene) insertion. The transcriptionally active Herpes simplex virus thymidine kinase (HSV-tk) gene when present in eukaryotic cells is not in itself, toxic to the cells. However, in the presence of the synthetic guanine analogue, ganciclovir (9-(1,3-dihydroxy-2-propoxymethyl) guanine) or the uracil derivative FIAU [1-(2-deoxy,2-fluoro- $\beta$ -d-arabinofuranosyl)-5-iodouracil], toxic metabolites are produced by the viral enzyme, which interfere with cellular DNA metabolism and ultimately, kill the cell. The idea is that an HSV-tk gene cassette is engineered to one or both sides of the DNA sequence (consisting of a *neo* gene, the targeted gene and flanking sequences) expected to be inserted following homologous recombination. In the event of homologous recombination, the HSV-tk cassette is excised. Thus, addition of ganciclovir or FIAU has no effect and the cell survives. If the targeting vector is inserted randomly, the HSV-tk gene is likely also to be included.

Addition of selection drugs will kill the cell. However the selection on the basis of G418 resistance alone would not have distinguished between the random and homologous events. The homologous recombination should be identified by Southern blot hybridisation using the external probes. Because the external probes could not hybridise with targeting construct, the band should the size would be expected due to gene targeting event. Using a PCR screening strategy, it is theoretically possible to screen more colonies in a relatively short space of time.

In this study, two constructs were made based on the positive-negative selection strategy and PCR screening. The two constructs are exactly same except for the length of 5' homologous region. One of the constructs has an 850bp 5' homologous region and is used as a positive control for PCR screening. This can be transfected into an ES cell line to generate one copy of construct B integrated into a chromosome. One of the PCR primers is located in the *neo* gene (reverse primer) of both constructs A and B, while the other primer is in the 5' homologous region of construct B and cannot hybridise with construct A (Fig. 4.4). In this way, if homologous recombination occurred, an 800bp PCR fragment should be generated by PCR from the ES cell clone that had undergone homologous recombination. This homologous recombination can be confirmed by Southern blot experiments with either an external or internal probe. In this gene targeting construct (construct A) most of exon 3 and a small fragment of the intron was replaced with the 1.1kb *neo* gene (Fig.4.5).

In the event, this iNOS gene targeting strategy was not used in this study, because the 3.9kb 3' homologous region of the construct was too short to give a high enough degree of the homologous recombination. In addition the small fragment of exon 3 deleted may not be large enough to disrupt completely iNOS function. To avoid these disadvantages, another construct was designed with genomic DNA derived from 129/sv mice.

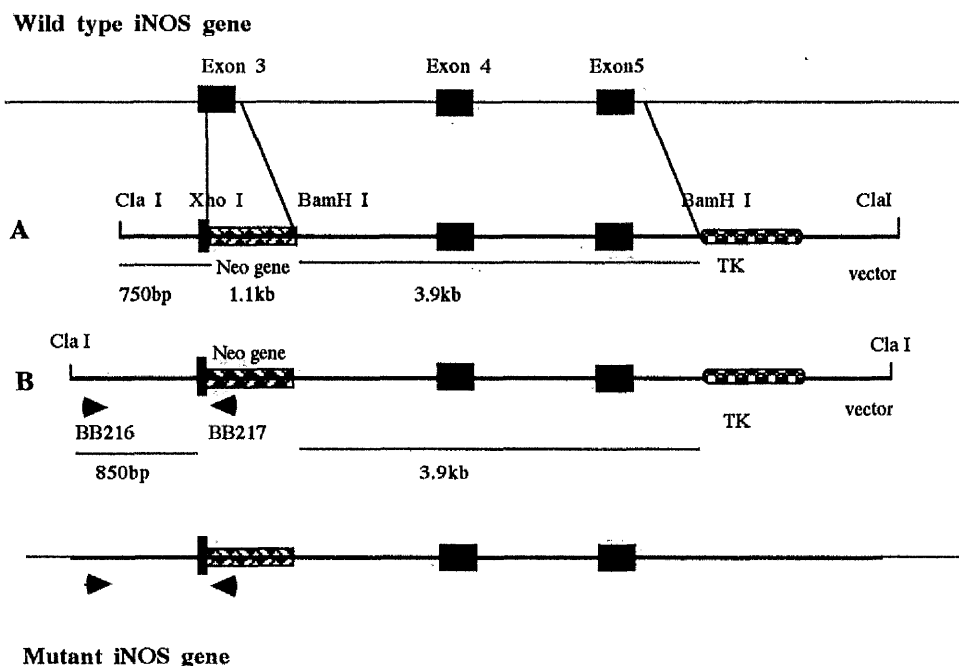


Fig.4.5. iNOS gene targeting strategy for B6 mice. In construct A, the 5' homologous region was constructed using a PCR fragment generated with primers BB214 and BB179, the *Cla*I and *Xho*I sites were created in the primers. In construct B, the 5' homologous region was generated by PCR with primers BB215 and BB179, with *Cla*I and *Xho*I sites in the PCR primers. The 3' homologous region for construct A and B were same and was generated from a 250bp PCR fragment (from primers BB180 and BB181) and a 3.75kb *Kpn*I-*Bam*HI genomic DNA fragment. Both construct A and B were linearised with *Cla*I. The arrows in the map show the PCR primers (BB216 and BB217) used for the for detection of homologous recombination. The sequence of the PCR primers used for the constructs and homologous recombination PCR screening are shown below:

BB179: AGGGTCCTCGAGTATTGTTGGGCTGCGAAAAGG  
 BB214: TGGAATCGATGCACTCAAGAAGCCCTGGCAAG  
 BB215: GAGTATCGATGACCTTGAACCTCCTGATCCCCC  
 BB180: TGGTTTGGATCCACAGTATGGAAGCCCTTCAT  
 BB181: TACTTAGGTACCAGCGCACCT  
 BB216: CCTGCCTTTGTTCCCTTTCACCTCTTTA  
 BB217: TCGCCTTCTATCGCCTTCTTGACGAG

#### 4.4. No detectable inducible nitric oxide synthase in ES cell

The absolute frequency of homologous recombination per electroporation per cell is quite low, commonly of the order of  $<10^{-6}$ , so that selection and rapid screening are necessary in order to discriminate between homologous recombination and the more commonly occurring non-homologous integration. "The promoter trap" is one of selective methods developed to enrich the ratio of homologous recombination in screening resistant colonies. The selection marker gene (the *neo* gene is commonly used as a selection marker), lacking its own promoter, can be expressed either as a fusion protein containing target gene sequences which nevertheless can retain the ability to confer geneticin-resistance (Schwartzberg, *et al.* 1989; Charron *et al.* 1990; Stanton *et al.* 1990), or as a result of reinitiation of translation of a polycistronic mRNA transcribed from the target gene promoter (Doetschman, *et al.* 1988). By this method, between one and three out of ten resistance colonies could carry homologous recombination events rather than the 1 in 100-1000 normally expected. Using picornaviral internal ribosome-entry site (IRES) to provide cap-independent translation of a selectable marker from fusion transcripts generated following homologous recombination, up to 86% of screened colonies has undergone homologous recombination (Mountford *et al.*, 1994). The design of the targeting vector for promoter trap experiments is dependent on the targeting gene being expressed in ES cells. So detection of iNOS expression in ES cells with or without stimulation became necessary.

$2 \times 10^5$  129 ES cells (CGR8) were stimulated with or without 100 units IFN- $\gamma$ , 10ng LPS or IFN- $\gamma$ /LPS respectively. The supernatants from the cultures of ES cells were used for NO<sub>2</sub> measurement by the Greiss reaction as described in Chapter 2 (2.32.). No NO<sub>2</sub> was detectable in any of the supernatants.

Both pairs of PCR primers corresponding to the iNOS cDNA 5' and 3' ends (described in Chapter 3-2) were used to amplify the mRNA from ES cell. iNOS mRNA could not be detected in the CGR-8 ES cells with or without cytokine stimulation. So, unfortunately the promoter-trap strategy could not be used for iNOS gene targeting.

#### 4.5. A large deletion positive-selection construct

To avoid the disadvantages of the initial gene targeting construct, another construct, with a larger deletion of the iNOS gene and longer homologous arms was made. Because the presence of base sequence divergencies between donor and recipient target DNA can reduce the efficiency of gene targeting (Riele, *et al.*, 1992), this construct was made with 129-derived iNOS genomic DNA. The 5' and the 3' homologous arms of the construct were 3.0kb and 3.6kb respectively. 11.5kb of iNOS genomic DNA, including exons 1-5 and part of the promotor, were replaced with 1.7kb of  $\beta$ -actin promotor and *neo* gene. To avoid the possibility of iNOS repressor sequences which may have suppressed *neo* gene expression, the  $\beta$ -actin-*neo* gene was reversed with respect to the iNOS gene in the gene target construct (Fig.4.6). To generate an efficient, economic and convenient Southern blot screening protocol for the gene replacement event, a *Hind* III site was created by insertion of a double stranded oligonucleotide into the *Bam*H I site between the 5' arm and the  $\beta$ -actin-*neo* gene as described in Chapter 2 (2.14). The oligonucleotide sequences were BB60: CTATAGTTCGAACTAG, BB61: TTCGAACTATAGCTAG. The construct was linearised with *Sac*I sites in both homologous region (Fig.4.6).

#### 4.6. The design of 5' and 3' specific external probes

The 1.4kb *Sal*I-*Sac*I DNA from a 5' genomic subclone was used as **Table 4.4** e a 7.0kb single band for the *Hind* III digestion and an approximately 12kb single band for the *Bam*H I digestion of normal ES cell chromosomal DNA in Southern blots (Fig.4.7). Because the external probe cannot hybridise with the targeting construct, only an homologous recombination event should show an additional hybridising band which should be reduced in size from 7.0kb to 5.4kb. Any random integration event will not give this band. The single signal from this 5' external probe also indicated that the 5' region of the iNOS gene is unique in the 129 genome.

Both 0.8kb and 1.2kb *Pst*I fragments from 3' specific genomic subclones were initially tested as the probes to detect the targeting event. However, both probes gave a

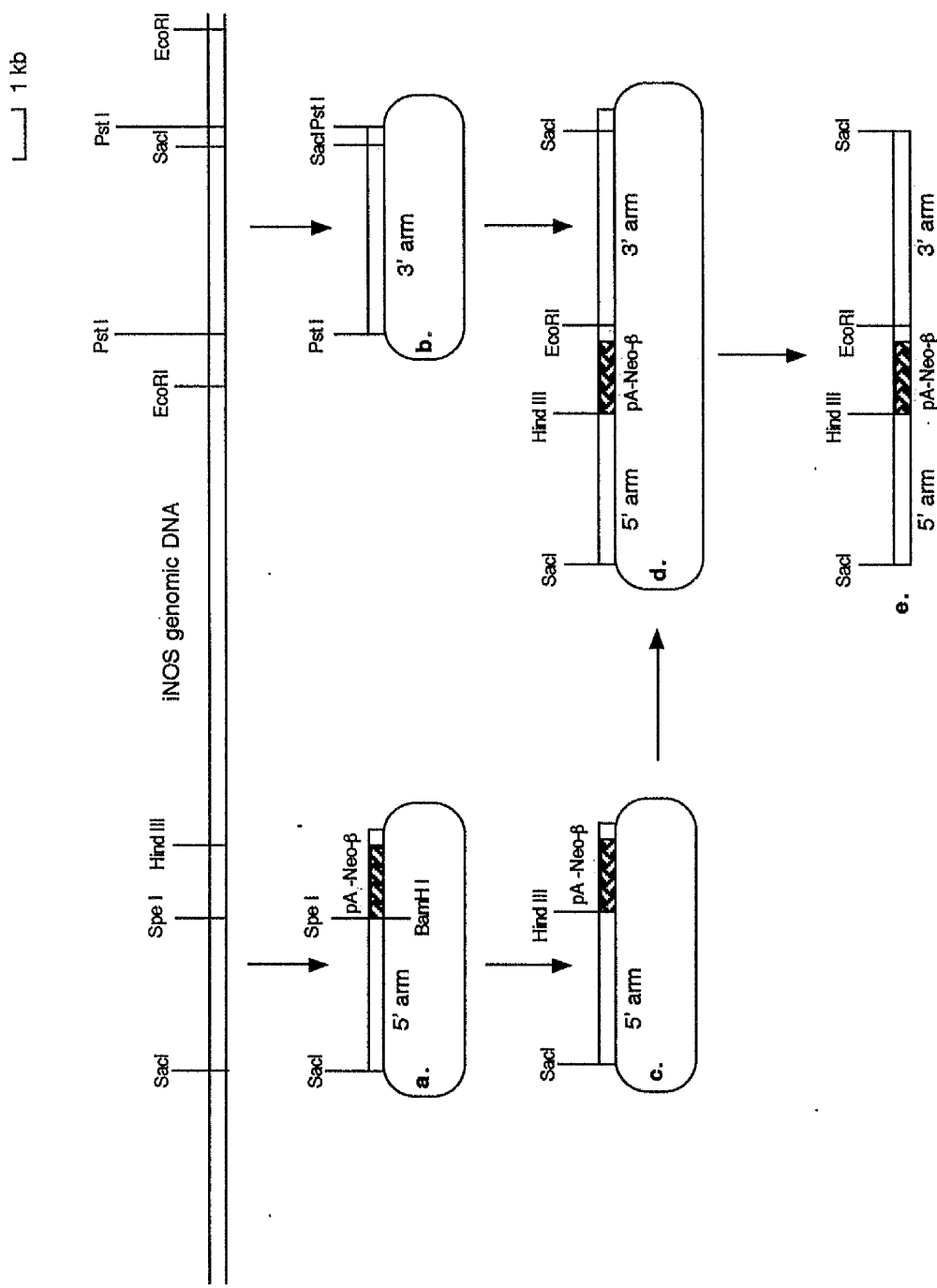


Fig.4.6. The iNOS gene replacement targeting construct. (a) the 5' homologous region arm was subcloned into *SacI* and *SpeI* sites of the  $\beta$ -actin promoter neomycin resistance gene cassette ( $\beta$ -actin promoter, Neo= neomycin resistance gene; pA: polyA tail). (b) the 3' homologous arm was subcloned into the *PstI* site of pBlueScript. (c) a *HindIII* site was introduced into the *BamHI* site of the *neo* gene cassette with synthetic oligonucleotides. (d) the *SmaI-SalI* fragment of the 3' homologous arm was inserted into the *EcoRV* and *SalI* sites of construct C. (e) the replacement construct was linearised with *SacI* for ES cell electroporation.

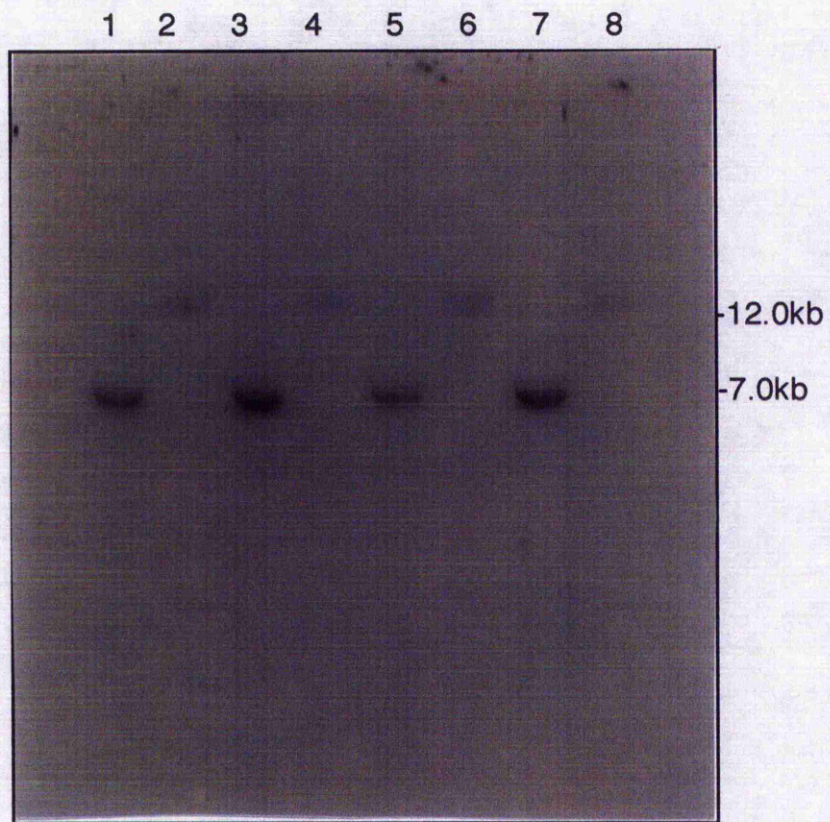


Fig 4.7. Southern blot analyses to select functional external probes. ES cell genomic DNAs were digested with either *Hind* III (lane 1,3,5,7,) or *Bam*H I (lane 2,4,6,8,) and hybridised with a 1.4kb *Sal* I-*Sac* I genomic fragment as a 5'-specific external probe.

smear hybridisation pattern in both *EcoRI* digestion and *EcoRV* genomic Southern blots, indicating non-specific hybridisation (Fig.4.8). Terminal DNA sequence analysis was carried out with T7 and T3 universal primers for the 0.8kb and 1.6kb *Pst I* subclones (Fig.4.3), and exon 7 of iNOS was identified. Two PCR primers (BB321 and BB322) were designed according to the sequence of the introns flanking exon 7 to generate a 300bp product.

BB321: TGACCTGTAGAAGAAATGCCCTCTGTCC

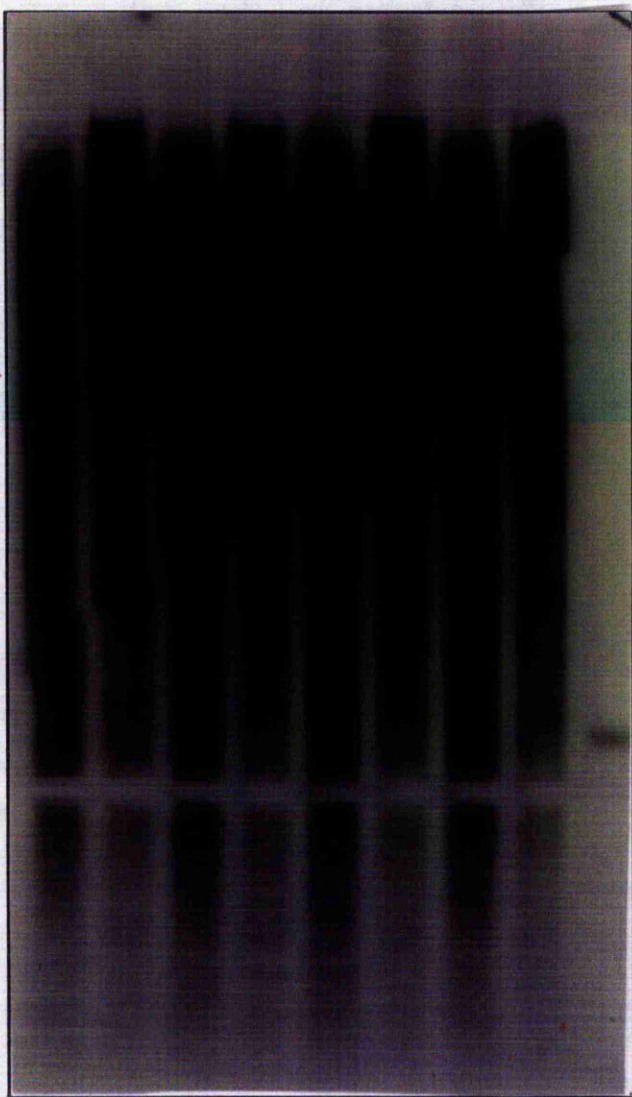
BB322: CCTCTCCTGTGCTCTCCAGCATCTTCTTCC

This 300bp PCR fragment was purified from an agarose gel to make the 3' external probe, which gave a single 7.5kb band with *EcoR I* digested DNA or 6.5kb band with *EcoR V* digested ES cell chromosomal DNA (Fig.4.9). Following a targeting event an additional hybridising fragment of 6.0kb should be obtained with *EcoR I* digested DNA (but not in DNA with a random integration event). The expected Southern blot bands given by both 5' and 3' end probes would indicate whether or not the correct gene replacement event occurred. If only one of them gave the expected recombinant band, then the double cross-over event would not have occurred. However, the gene may still be targeted and it may be sufficient to cause a gene defect. The position of the 5' and 3' end probes are shown in Fig.4.10.

#### **4.7. Selection and screening of ES cell lines for iNOS gene targeting**

In this study, the CGR-8 ES cell line (Mountford. *et al.*, 1994) was electroporated with linearised targeting construct DNA. After 8 days of G418 selection, single colonies were isolated and then were divided into two, one for gene screening and another for a freeze-stock. Half of the sample was used to make chromosomal DNA plugs which were digested with *HindIII*, and the other half with *EcoRI*. The 5' specific external probe was used for the first hybridisation screening. One clone (No.133) showed the expected additional hybridisation band for a homologous recombination event. This clone also gave expected fragment with 3' external probe, apparently confirming the replacement (Fig.4.11).

a.



b.



Fig.4.8. Southern blot analyses to select a specific external probe for the 3'-targeting event. ES cell genomic DNAs were digested with either *EcoR* I (a. lane 1,3,5,7, and b. lane 1') or *EcoR* V (a. lane 2,4,6,8, and b. lane 2') and hybridised with either a 1.2kb *Pst* I fragment (a.) or a 0.8kb *Pst* I fragment 3' end probe (b.).

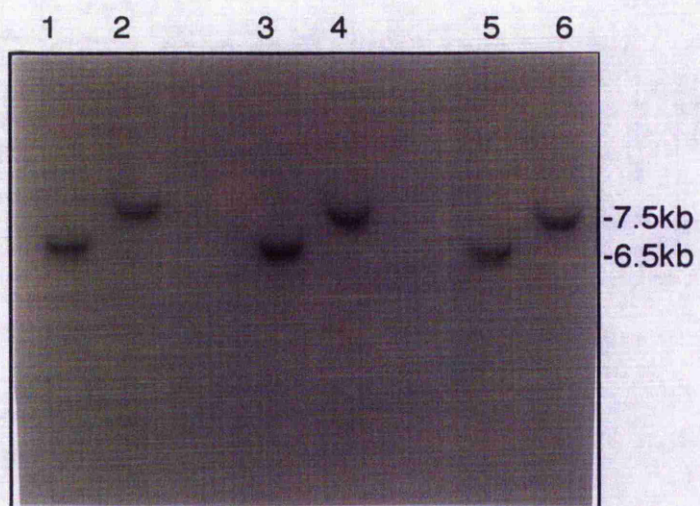


Fig.4.9. Southern blot by using a 300bp PCR fragment as a 3' end external probe to hybridise with ES cells DNAs digested with either *EcoR* V (lane 1,3,5,) or *EcoR* I (lane 2,4,6,)

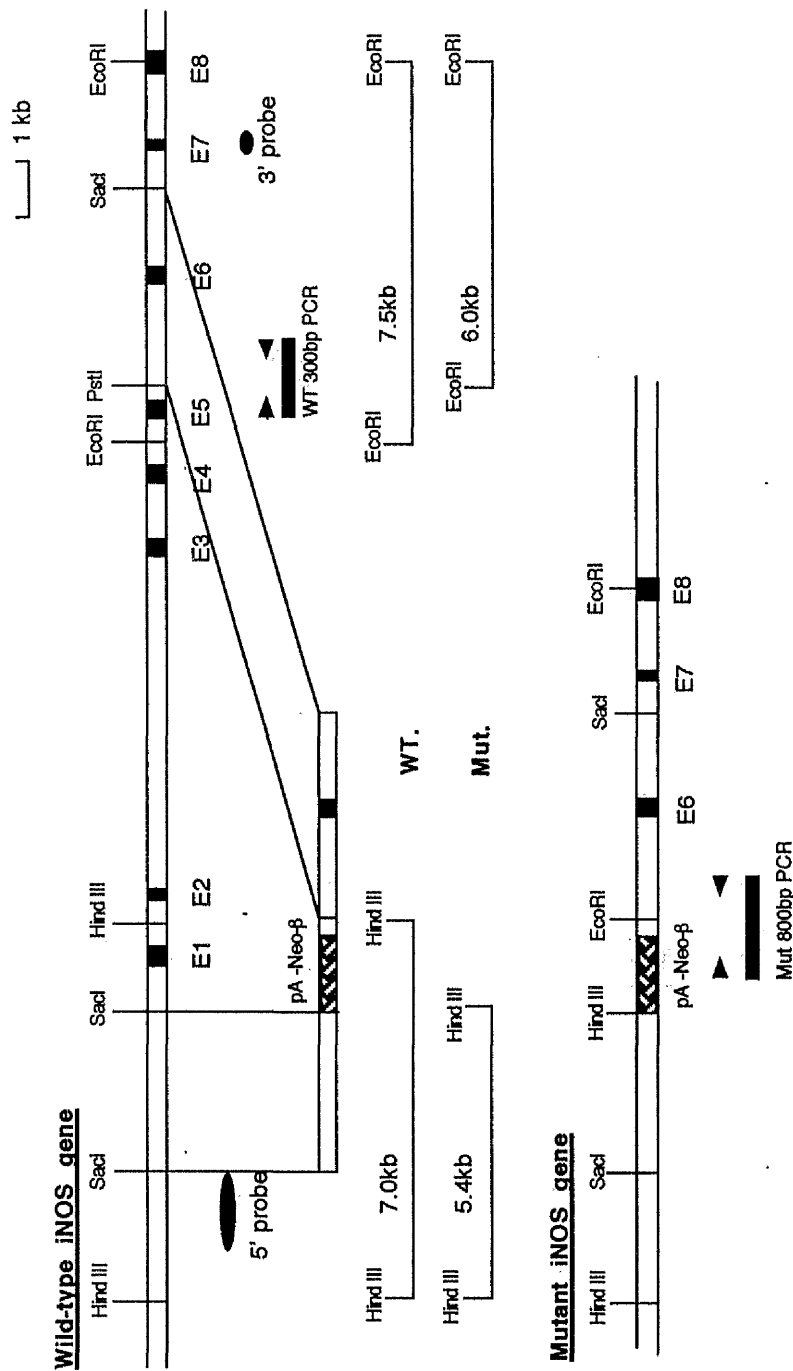


Fig.4.10. The linearised gene replacement construct with the  $\beta$ -actin neo gene replacing the wild-type gene causes a reduction of the hybridisation band size for *Hind*III digestion or *Eco*RI digestion with 5' or 3' specific external probes. The expected 1.1.5kb deletion caused by the replacement of the wild type gene is shown in the bottom bar. The solid triangles show the PCR primers for mutant and wild type genotype detection.

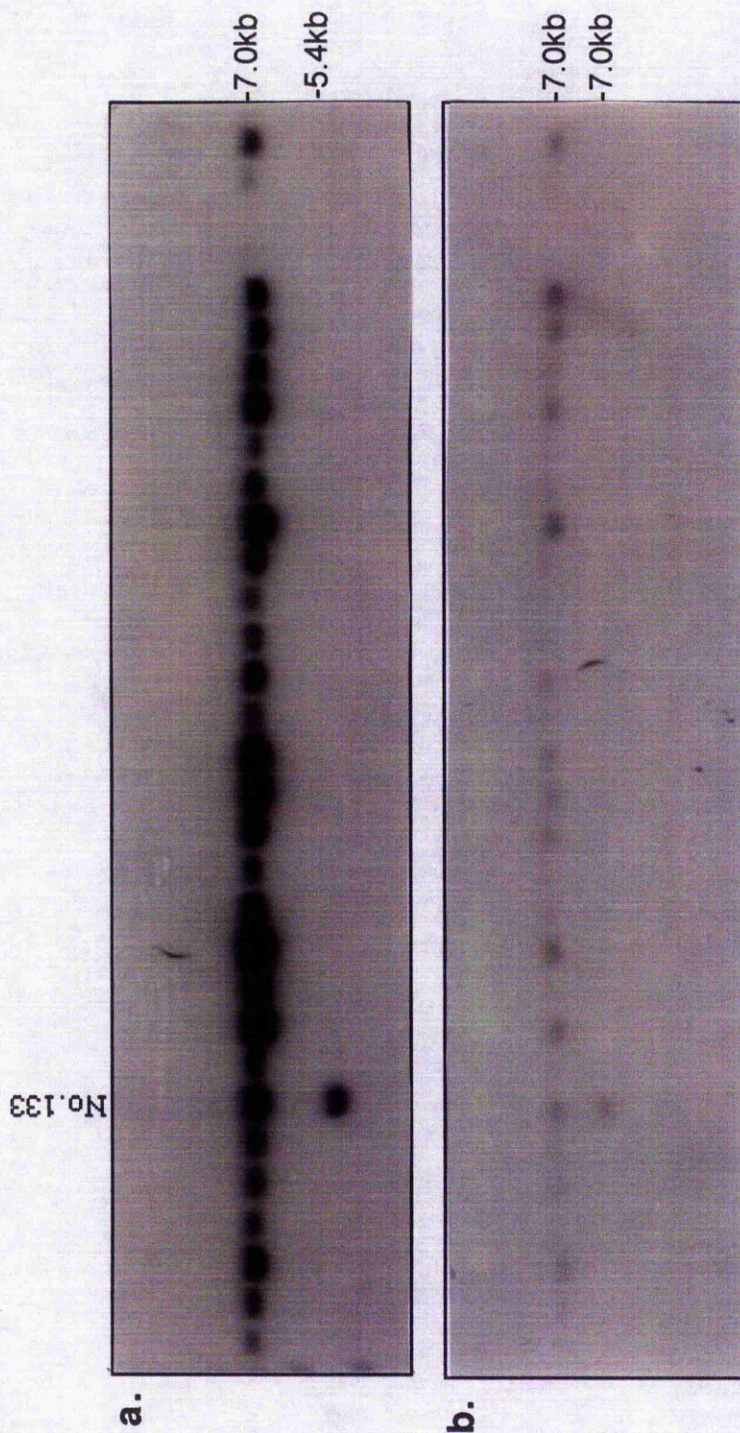


Fig 4.11. Southern blot analysis for gene targeting event screening. ES cell genomic DNAs from G418 resistant colonies were digested with either *Hind* III or *Eco*RI and hybridised with either a 1.4kb 5'-end external probe for *Hind* III digestions (a) or a 300bp PCR 3' end external probe for *Eco*RI digestions (b). The expected size reduced bands appeared in clone No.133 for both 5' and 3' specific external probes.

Re-hybridisation of the *Hind*III digestion Southern blot with a *neo* gene probe, showed one copy of the *neo* gene was present. In this iNOS gene targeting experiment, only a single targeted clone was identified from 636 screened samples after two independent electroporations.

Before the blastocyst injection, the chromosomes were stained and the number was counted under the microscope. 80% of ES cells had 40 chromosomes which indicated that the line was normal and should contribute to generate chimeras and give germ line transmission.

#### **4.8. Production of chimeras and germ line transmission to offspring**

Mammalian embryos are extremely resilient in the early stages of their development and can not only tolerate abuse or loss of tissue, but can also functionally incorporate cells from other embryos. This property of mammalian embryos, the ability to incorporate foreign cells during development, has been exploited for several purposes including the elucidation of cell lineages, the investigation of cell potential, and the perpetuation of mutations produced in ES cells by gene targeting. The cells from two embryos which contribute to one body is called a chimera. The foreign cell, with specific gene mutation, can go through the chimera's germ line to the offspring and this is known as germ line transmission.

The identified iNOS gene targeted 129/sv ES cells (No.133), were injected into C57 Black 6 blastocysts. These blastocysts were then transplanted into the uterus of C57xCBA F1 pseudopregnant mice (This was done by Jan Ure in Gene Targeting Laboratory, Centre for Genome Research, University of Edinburgh). The coat colour is the indicator for the quantification of chimeras. Good chimeras have more agouti coat colour (which was contributed by 129 ES cells) than the black coat colour from C57black6 embryos, but germ line transmission need not necessarily arise from good chimeras. The 129 ES cells were from the inner cell mass of male blastocysts, so the majority of good chimeric mice were males rather than females. Germ line transmission is

a crucial step in the generation of gene targeting mice. Test breeding the chimeras with MF1 female mice is the easiest way to detect the germ line transmission and can be analysed by the coat colours of the offspring. 129xMF1 offspring give a grey coat colour that means germ line transmission has occurred. However a black colour from C57 Black 6 x MF1 means transmission has not occurred. In this study, 10 chimeras were generated from two injections and 5 of these gave germ line transmission. In ES cells, there are two pair sets of chromosomes (from both parents) and both can form the germ cells to give grey coat colour of the offspring. However, the gene mutation is introduced into only one of pair sets, so 50% of grey mice should carry the gene mutation which was made in the ES cells. To find out the number of grey mice with the iNOS gene mutation, their tails were tipped, DNAs were purified and digested with *HindIII* for Southern blot analysis with the 5' specific external probe. Of the 59 mice analysed, 30 offspring were heterozygous.

#### **4.9. Segregating genotypes**

The heterozygous mice identified in the above procedure can normally be mated together to produce litters with, wild type normal, heterozygous and homozygous mutant mice. Five matings were set up with one male and two females heterozygous offspring (F1) in each group. All 97 offspring (F2) were genotyped with the 5' specific external probe. The number of wild type : heterozygous : homozygous was 25:72:0. It was considered at this stage that perhaps the mice with the homozygous mutation genotype were lost during the embryo development.

#### **4.10. Investigation of the homozygous embryos during development**

To find what was happening to the homozygous mice, heterozygous mice (F2) were used in a time mating experiment. After mating, the vaginal plugs were checked. If vaginal plugs were found, the mice had mated and the gestation time was taken as 0.5 day. By 10.5, 13.5 and 14.5 gestation days, the murine embryos were removed. Most of the 70 embryos analysed developed normally except for 2 absorption embryos. In

addition some embryos showed excessive blood. The litter sizes were quite normal, suggesting that a quarter of the homozygous mutant mice were not lost in the early development. The yolk sacs were isolated and DNA was purified for hybridisation with the 5' specific external probe to genotype the animals. None of the homozygous genotype was found in all 70 embryos analysed from 6 litters. Strangely, the mice with heterozygous genotype were found in numbers much greater than 50%. In some litters, 100% of mice had the heterozygous genotype (Table 4.2). This finding indicated that either the iNOS gene mutation caused enhanced activity of germ cells or alternatively some of the heterozygous genotype mice were in fact homozygous for the presumed replacement event, but also that the wild type allele was still detectable for some reason (All the heterozygous genotypes discussed above are based on the 5' and 3' specific Southern blots experiments). This strange observation could be explained if, for some reason, the iNOS gene had duplicated. The mice (F2) used for the time mating were all the offspring from F1 heterozygous genotype intercross, so some of F2 mice could have been homozygous for the mutant genotype which could not be detected with the external probe. This idea was confirmed later by a back-cross study.

Table 4.2. The genotype of embryos from F2 heterozygous mice mating.

The Pairs	Gestation Days	Litter Size	W.T.	Het.	Homo.
1-1AX13-2A	10.5	9	0	9	0
11-AX33-2A	10.5	12	5	7	0
4BX34-1A	10.5	9	3	6	0
1CX41-1A	10.5	15	0	15	0
11CX40-1A	12.5	13	0	13	0
4-1AX30-1A	13.5	12	0	12	0

#### 4.11. Identification of the homozygous mice by back-crossing

Why were so many mice embryos with a heterozygous genotype generated from F2 heterozygous mice? To answer this question, some of the F2 males and females with heterozygous genotypes were mated with the females and males with a wild type MF1 background mice respectively (this was called a "back cross"). The offspring of the "back cross" were genotyped with the 5' specific external probe in Southern blot experiments. One male (EM: 11C) and two females (EM: 14C and 31C) with an apparent heterozygous genotype gave 100% heterozygous genotype offspring (F3) while the rest of them gave about 50% heterozygous (Table 4.3). The result indicated that the mice that gave 100% transmission were in effect homozygous which meant that both of the chromosomes had an iNOS gene replacement mutation. This result ruled out the suggestion of the super ability of sperm. The conclusion from the results obtained above was that iNOS mutant mice were not lethal in homozygous mice during embryogenesis.

Table 4.3. The genotype of offsprings from F2 back-cross.

The ear Mark No.	Sex	Litter Size	WT.	Heter	( % )
11C	male	15	0	15	<b>100</b>
10C	male	8	5	3	37.5
1C	male	9 + 8	7	10	58.8
30C	female	13	7	6	46.2
14C	female	13+12	0	25	<b>100</b>
31C	female	14	0	14	<b>100</b>

#### 4.12. iNOS gene duplication after gene targeting

Why was the wild type allele still detectable in the homozygous mice after the replacement event? (the homozygous animals discussed here are based on the "Back cross" analysis). Either there were two copies of the iNOS gene in the murine genome or the gene had been duplicated during the gene targeting event. To try to answer this

question, both 5' and 3' specific external probes were used in Southern blot experiments with DNA digested with different restriction enzymes. DNA samples from wild-type, heterozygous, and homozygous mice were analysed. The restriction enzymes were chosen in homologous recombination regions of the construct. The homologous recombination should not change the restriction enzymes sites in the homologous recombination regions and flanking sequence. If there was a duplicate gene in wild type mice, double bands should appear with some restriction enzymes. This should also appear in iNOS gene targeting mice. Unexpectedly, after certain digests, the 5' external probe gave two hybridising bands in heterozygous and homozygous, but not in the wild type mice. This result suggested that iNOS gene duplication was the result of the gene targeting. There is no evidence for the existence of the duplication copies of the iNOS gene in the mouse as there is in man and the great apes (Xu, *et al.*, 1995).

For the 5' external probe hybridisation, *Sac* I *Pst*I, *Spe* I *Bam*HI and *Kpn*I were used to digest the tail DNA from wild-type, heterozygous and homozygous mice. The *Sac*I and *Pst*I digests gave the single hybridisation band respectively. However, the *Spe*I, *Bam*HI and *Kpn*I gave two bands in heterozygous and homozygous but not in wild-type (Table 4.4). This result indicated that change of restriction enzymes sites had occurred ~2.3kb upstream of the *Sac* I site after the gene targeting event (Fig.4.12). Using the 300bp and 400bp 3' specific external PCR probes [400bp PCR fragment probe was amplified from a 1.4kb *Bam*H I subclone (Fig.4.3)] in Southern blot. The *Sac*I gave single hybridising band and the *Bgl*II gave two bands (because there is *Bgl* II site in between of two PCR probes) in all genotypes of mice. However, the *Kpn*I and *Hind*III digestion gave two hybridising bands in heterozygous and homozygous mice but not in the wild-type mice (Table 4.4.) This result indicated that the change of enzyme sites had occurred approximately 5.0kb down stream of the *Eco*R I site (Fig.4.12). All the above Southern blot results suggested that part of the iNOS gene had been duplicated after gene targeting. Either both 5' and 3' ends of targeting construct extension copied the targeting gene and integrated, or part of the iNOS gene had integrated somewhere after the gene

replacement. The two possibilities could not be distinguished by the 5' and 3' specific external probes.

Table 4.4. The restriction fragments of hybridising bands with 5' and 3' external probes.

Enzyme	5' external probe			3' external probe		
	W.T.	Hete.	Homo	W.T.	Hete.	Homo
<i>Bam</i> H I	12.0kb	12.0kb 9.5kb	12.0kb 9.5kb			
<i>Bgl</i> II				7.0kb 1.9kb	7.0kb 1.9kb	7.0kb 1.9kb
<i>Hind</i> III				12.0kb 11.0kb	12.0kb 11.0kb	12.0kb 11.0kb
<i>Kpn</i> I	6.5kb	6.5kb 13.0kb	6.5kb 13.0kb	10.0kb	10.0kb 12.0kb	10.0kb 12.0kb
<i>Pst</i> I	5.0kb	5.0kb	5.0kb			
<i>Sac</i> I	2.3kb	2.3kb	2.3kb	3.6kb	3.6kb	3.6kb
<i>Spe</i> I	6.0kb	6.0kb 5.5kb	6.0kb 5.5kb			

#### 4.13. The expected deletion had not occurred.

To find out whether or not the 11.5kb iNOS gene fragment was deleted by the gene replacement, an internal probe (1.2kb *Hind*III-*Eco*RI fragment located in the expected deletion area) was used as internal probe for Southern blot analysis with *Hind*III digested genomic DNA samples from mice with wild-type, heterozygous and homozygous genotypes. 4.0kb hybridisation bands were detectable in all these mice with three different genotypes.

Three oligonucleotides were synthesised for the PCR strategy to identify the genotypes. One primer (P2) is in the 3' end of the gene targeting construct which will bind to both the wild type gene and the replacement construct. The other two bind either

to the neomycin gene (P1) or the expected deleted area of the iNOS gene (P3) (Fig.4.10). The primers sequence are shown below.

P1: GCGGCCGGAGAACCTGCGTGCAATCC (CB843)

P2: CAGAGTAGGAGGTTGAGACCCAATG (CB844)

P3: GCTCCTGCCTCATGCCATTGAGTTCA (CB845)

P2 and P3 amplified a 300bp PCR fragment for the wild type allele, while the P2 and P1 primers give an 800bp product for the knockout allele. Unfortunately, the wild type allele was detected in all the homozygous mice. Both PCR and Southern blot results showed that the expected deletion had not occurred although the external probes showed homologous recombination had occurred.

#### **4.14. The murine iNOS gene rearrangement and mutation**

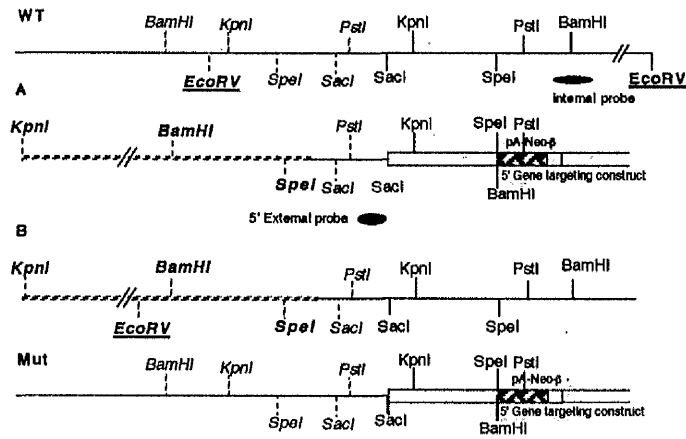
All the above evidence showed that on the one hand, a homologous recombination event had occurred, but that the expected deletion had not occurred. This can be explained it both ends of the targeting construct extension copied the flanking sequences, then integrated into the gene. To find out whether part of the wild type gene or the replacement gene targeting construct had been integrated elsewhere in the genome, the 1.2kb *HindIII*-*EcoRI* internal probe was used in Southern hybridisation experiments (Fig. 4.12). This probe does not hybridise with the replacement gene targeting construct. The Southern blot with *EcoRV* digested DNA showed that ~14kb wild type allele disappeared and was replaced by an approximately 16kb hybridisation band in the homozygous mice (Fig.4.13).

Using the 5' specific external and internal probes for Southern blot analysis, it was clear that two copies of the iNOS gene could be detected in the homozygous mice, but not in wild type mice. This result suggested two possibilities. One is that the wild type gene had not been changed but the targeting construct picked up about 2.3kb 5'-end sequence and 5.0kb 3'-end sequence which could hybridise with the 5' and 3' external probe respectively, and this was then integrated somewhere (which is shown as **WT** and **A** in the top map of the Fig.4.12). Another possibility is the targeting construct replaced

the iNOS gene, however the replaced region of the iNOS gene plus flanking sequences integrated elsewhere to generated a pseudo wild-type allele and caused the restriction enzyme sites (*KpnI*, *BamHI* and *SpeI*) change seen in the Southern blot analysis of the homozygous mice DNA (which is shown as **B** and **Mut** in the top of the map of Fig.4.12). The 5' specific external probe can not tell which event has occurred (**WT** and **A** or **B** and **Mut**). Using the 1.2kb *HindIII-EcoRI* internal probe which only hybridises with the wild type gene (gives 14kb *EcoRV* restriction fragment), *EcoRV* digested Southern blot analysis showed that an altered *EcoRV* restriction fragment (16kb) was identified in homozygous and heterozygous mice, but not in wild-type and 129 ES cells (Fig.4.13), which indicated that a strain polymorphism is unlikely. Because *EcoRV* site is between the other two enzyme sites (*KpnI* and *SpeI*) which have been changed in the homozygous mice, so the duplication events are more likely to be the **B** and **Mut** (Fig.4.12) rather than **WT** and **A**. This result suggested that wild-type sequences are now contiguous with novel 5' sequences *i.e.* either they have been transposed elsewhere in the genome or some rearrangement has occurred around the iNOS gene locus. Using the 1.2kb *HindIII-EcoRI* internal probe to detect the alteration in the iNOS gene, the wild type, heterozygous and homozygous mutation genotypes were identified in the offspring from F1 heterozygous mating. The number of the three genotypes were 25:47:21 respectively.

If a fragment of the wild type gene was transposed as a result of the homologous recombination event, it is possible that the iNOS gene expression could have been disrupted. In order to test this hypothesis, peritoneal cells were collected from homozygous and wild type mice and cultured in the presence of IFN- $\gamma$  and LPS. The cells were harvested 6h or 8h after activation, and total RNA isolated for the Northern blot analysis. Using the 937bp 5' iNOS cDNA probe, about ~4.0kb iNOS signal was detected in RNA extracted from both wild type mice and a murine macrophage cell line (J774, ATCC). A larger band of about 4.5kb was detected in RNA extracted from the homozygous mice (Fig.4.13).

5' end external probe



3' external probe

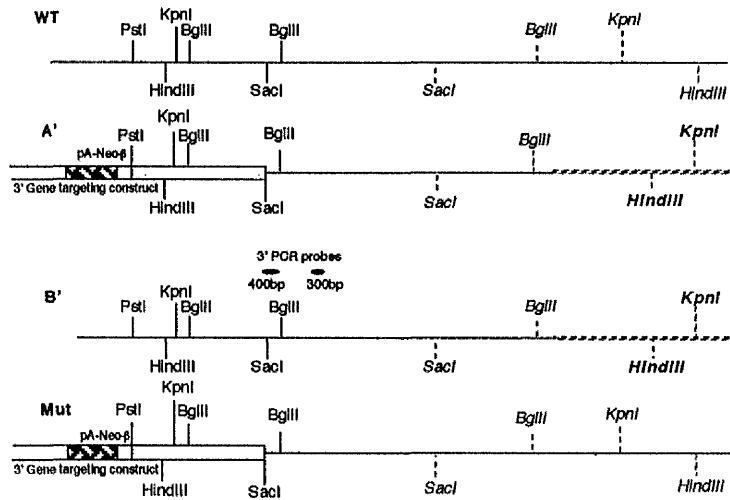


Fig.4.12. Using the both 5' and 3' specific external probes to map the flanking regions of the iNOS gene by Southern blotting for DNA from ES cells, wild type, heterozygous and homozygous mice. The top map shows the 5' end and the bottom the 3' end. The solid lines are the wild type iNOS genomic DNA, the dotted lines are unconfirmed region of the gene. The plain text enzyme sites were mapped with the cloned iNOS gene, the *Italic* enzymes-sites were mapped by Southern blot. The bold *Italic* enzyme sites show the changes after gene targeting. The empty bars show the homologous arms.

#### **4.15. The iNOS transposition and replacement events may have occurred in the same locus**

The internal and external probes were used to attempt to detect the transposition and replacement events respectively. Tail DNA isolated from the offspring of the back-crossing experiment (Chapter 4.11) was digested with *EcoR* V, *Hind*III and *Eco*RI respectively. A Southern blot with *Eco*RV digested DNA was hybridised with the internal probe, while the *Hind*III and *Eco*RI blots were probed with the 5' and 3' external probes respectively. Analysis of DNA from 92 offspring from the back-crossing, showed that the replacement and translocation events were always detected in the same mouse's tail DNA. This strongly suggests that the two events *i.e.* translocation and gene replacement are linked.

#### **4.16. No detectable iNOS protein in homozygous mice by Western blot**

Both peritoneal and spleen macrophages from wild type mice and homozygous mice were cultured and stimulated with IFN- $\gamma$  and LPS under the conditions reported earlier (Liew, *et al.*, 1991). Western blots were carried out in four separate experiments with monoclonal (Fig.4.13) and polyclonal (Fig.4.14) anti-iNOS antibodies. A distinct band at Mr 130k was seen in the samples from wild-type mice and control J774 cells, but no protein band was visible in the samples from the homozygous mice.

#### **4.17. Culture supernatant NO<sub>2</sub><sup>-</sup> measurement by the Greiss method**

Peritoneal macrophages were cultured and stimulated with IFN- $\gamma$  and LPS. High concentrations of nitrite were detected in cultures of the activated cells from wild-type and heterozygous mice, whereas no nitrite was detected in the cultures of cells from the homozygous mice at 24 hours (Fig.4.13). By 72 hours, however, a low level of nitrite was detectable in the supernatant of cells from the homozygous mice while no detectable nitrite was detectable from unstimulated control cells. They may reflect the accumulation of nitrite produced by increased calcium-dependent NOS, which has recently been shown to occur in J774 cells and can be increased markedly by LPS (Dusting, *et al.*, 1995)

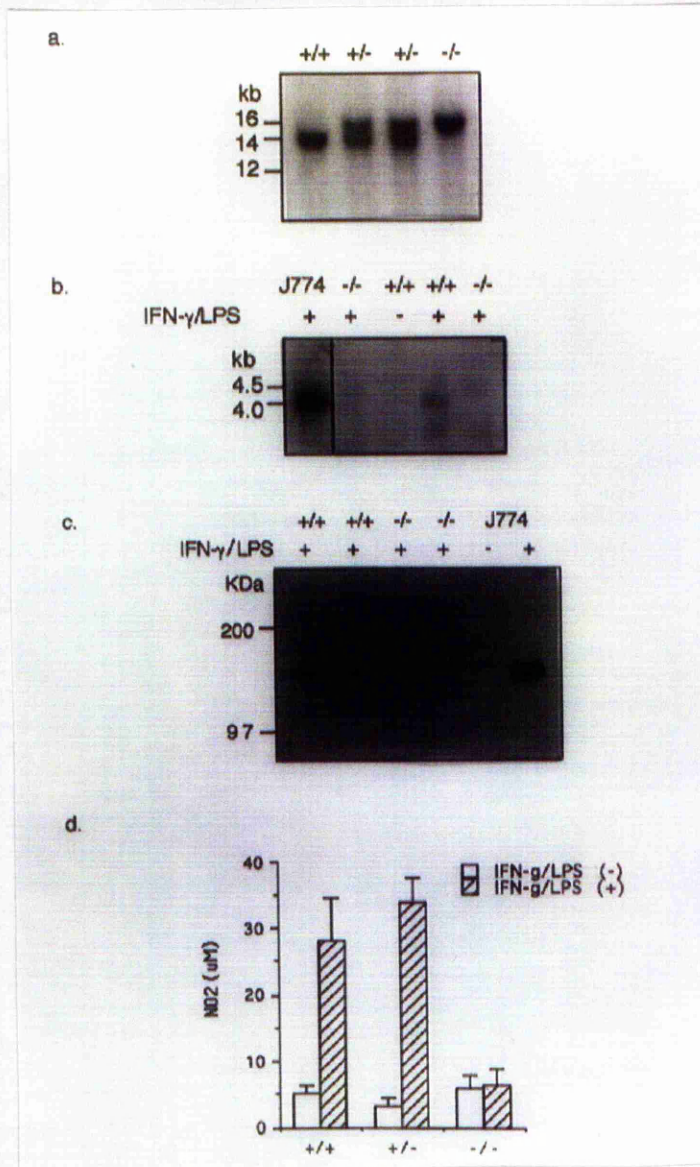


Fig 4.13. (a) Southern blot analysis. Genomic DNA isolated from the tail tips of offspring of heterozygous intercrosses were digested with *EcoRV* and hybridised with a 1.2kb *EcoRI-HindIII* fragment as an internal probe. The wild-type allele migrates as a 14kb fragment, while the mutant is 16kb. (b) Northern blot analysis. Total RNA was extracted from peritoneal macrophages after activation with IFN- $\gamma$  and LPS. The bands from wild-type and J774 cells are about 4.0kb, while the bands from mutant mice are about 4.5kb. (c) Western blot analysis. Protein extracts from the macrophages after 18hr activation with IFN- $\gamma$  and LPS and stained with monoclonal anti-murine iNOS antibody. The wild-type and J774 cells showed bands about 130kDa, while no detectable band appeared in activated macrophages from mutant mice. (d) The culture supernatants of macrophages from wild-type, heterozygous and mutant mice were collected at 24 hours after stimulation with IFN- $\gamma$  and LPS, and assayed for nitrite by the Griess method. Vertical bar=1SD, n=3.

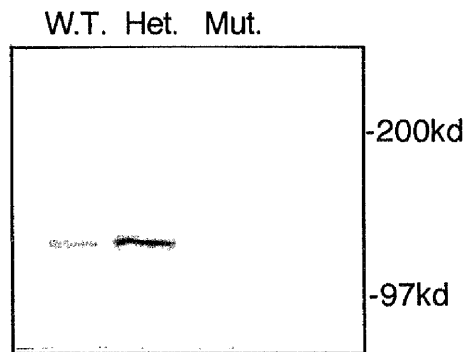


Fig.4.14. Western blot analysis. Protein extracts from the macrophages at 20 hours after stimulation with IFN- $\gamma$  and LPS and stained with polyclonal anti-murine iNOS antibody. The wild-type and heterozygous mice show strong bands about 130kd, while no detectable band appeared in activated macrophages from mutant mice.

#### 4.18. Summary

In this study, an iNOS gene mutation was introduced into the 129 ES cell line by *neo* gene replacement of the 11.5kb region of the iNOS spanning exons 1-5. The deletion also removed half of the promoter. A single targeting clone was identified from 636 screened after two independent electroporations experiments of the CGR8 embryonic stem cell line. Germline transmission was obtained for five of ten chimeras analysed. The gene replacement event was identified with both 5' and 3' specific external probes. Intercrossing the heterozygous offspring (F1) from the germ line transmitting chimeras, however demonstrated that the wild type gene specific band persisted in the offspring (F2) of the heterozygous breeding. Back cross experiments with heterozygous F2 mice and MF1 wild type mice demonstrated that some of heterozygous mice gave 100% heterozygous genotype transmission, while the others gave about 50% heterozygous and 50% wild genotypes. The back-cross results indicate that the iNOS gene or at least part of it had been duplicated. Southern blot analysis, using different restriction enzyme digests of genomic DNA from ES cells, wild type mice, heterozygous and homozygous mice tail DNA respectively, showed that the part of iNOS wild type gene had been duplicated after the gene replacement event. Using a specific internal probe which should only hybridise with the wild type gene, demonstrated that a ~14kb band found in wild type animals and 129 ES cells was replaced with a ~16kb mutant band in the homozygous mice. DNA from heterozygous animals showed two bands at about 14 and 16kb. The ratio of wild type, heterozygous and homozygous was normal (25:47:21). Southern blot experiments suggested that two separate gene rearrangement events could have occurred in the iNOS gene targeted mice. One involved the neomycin resistance gene replacing the 11.5kb of iNOS exons 1-5, the other involved part of the iNOS gene transposition. These events appeared to cause the iNOS gene deficiency resulting in no detectable iNOS protein translation. Similarly, no nitrite could be detected from the supernatant of the activated peritoneal macrophages from mutant mice within 24 hours. The conclusion from all of the above results is that iNOS mutant homozygous mice are viable and fertile. There is no evidence of histopathological abnormalities for the spleen, kidney, brain, lung, heart,

lymphnodes, intestine from three homozygous mutant mice compared with three wild type mice ( this investigation was carried out by Dr. G Lindop in the Pathology Department of Western Infirmary, University of Glasgow).

Human iNOS genomic mapping showed that the human iNOS gene has 27 exons and introns through 37kb of genomic DNA (Xu, *et al.*, 1995; Chartrain, *et al.* 1994) In the study reported above, the genomic DNA mapping for the murine iNOS gene was not carried out completely, but it showed the same pattern. Only eight exons and the promoter were located in 21kb of three overlapping genomic clones. These eight exons contributed to 937bp of the 4.0kb of iNOS mRNA. A large part of the iNOS gene was not cloned and mapped in this study, which makes it difficult to understand exactly the gene rearrangement events that have occurred in the iNOS mutant mice. According to the Southern blot results, there were two possibilities. To understand the recombination events that occurred during the generation of the iNOS mutant mice further experiments are required. A homozygous genomic library has been made and a cDNA library will be made from mutant mice. Mapping the mutant iNOS gene and DNA sequencing of iNOS clones from the cDNA library will provide detailed information on the gene rearrangement. It is important to analysis the phenotype for the targeted gene. Normally these phenotypes have been demonstrated previously with the other techniques. Some of the functions suggested for iNOS have been experimentally supported by analysis of these iNOS mutant mice. This work is described in next chapter.

## **Chapter 5**

### **Biological Phenotypes of iNOS Mutant Mice**

## 5.1. Introduction

Nitric oxide (NO) is a critical mediator of many biological functions, including endothelium-related vascular relaxation, platelet aggregation and neurotransmission, as well as in anti-microbial and tumoricidal activity of murine macrophages (reviewed in Liew F.Y. *et al.* 1991, Moncada S. *et al.* 1991, Green S.J. *et al.* 1993). Cytokine-induced synthesis of NO from L-arginine is characteristic of many mammalian cell types and was first described in murine peritoneal macrophages (Stuehr, *et al.*, 1985). Since then, inducible nitric oxide synthase (iNOS), the enzyme which catalyses the conversion of L-arginine and molecular oxygen to L-citrulline and NO, has been purified, cloned, and shown to be expressed by many other cell types, *e.g.*, fibroblasts, endothelial cells, hepatocytes, articular chondrocytes, cardiac myocytes, and keratinocytes etc. Depending on the cell types, the site of release, and also on the local NO concentration, the generation of NO by iNOS may lead to diverse consequences. There is increasing evidence that NO may play a key role in nonspecific defence mechanisms against pathogens, and may be involved in the signalling between macrophages and T cells (Liew, *et al.*, 1991). In most cases, the biological role of NO has been demonstrated by using L-arginine analogues such as L-N<sup>G</sup>monomethyl-arginine (L-NMMA) to inhibit NO synthesis *in vivo*. L-NMMA is not NOS isoform-specific (*i.e.* it can also block the activity of ncNOS, ecNOS and arginase activity). The iNOS deficient mice constructed in this study have provided a powerful tool for obtaining direct evidence for the various biological functions of iNOS which had been controversial from previous experiments using the L-arginine analogues. In this chapter, the phenotype of the iNOS deficient mice in *Leishmania* infection, local inflammation and LPS-induced shock are described.

## 5.2. Mice lacking iNOS have normal T cell functions

### 5.2.1. Spleen cell proliferation after ConA stimulation

Spleens were harvested from group of 5 wild type or mutant mice. Single-cell suspensions were pooled for each group, resuspended at  $2 \times 10^6$  cells/ml, and dispensed at

100µl/well in flat bottom 96-well plates. ConA (0.1, 0.5, 2.5, 5.0 and 10.0µg/ml) was added to each well and the cultures incubated at 37°C in an atmosphere of 5% CO<sub>2</sub>. Supernatant (100µl) was collected at 17, 24, 48 and 72 hours for cytokine measurement. [<sup>3</sup>H]thymidine (1µCi/well) was added for the final 6 hours of incubation, then harvested and counted in a β-scintillation counter. There was no significant difference at all doses and time course tested in the proliferation of the spleen cells between iNOS mutant and the wild type mice (Fig.5.1). The optimal proliferation was at 5.0µg/ml of ConA by day 2 after stimulation.

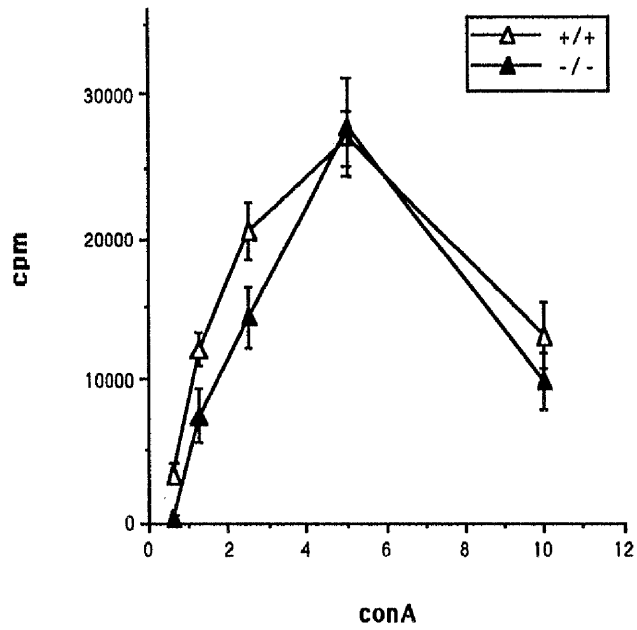
#### 5.2.2. Analysis of spleen cells from immunologically naive mice

Spleen cells from four individual mutant and wild type mice were analysed for CD3<sup>+</sup>, CD3<sup>+</sup>CD4<sup>+</sup>, CD3<sup>+</sup>CD8<sup>+</sup> subsets by flow cytometry using the appropriate antibodies. There was no significant difference in the percentage of CD3<sup>+</sup>, CD3<sup>+</sup>CD4<sup>+</sup>, or CD3<sup>+</sup>CD8<sup>+</sup> subsets of T cells in the splenic population of untreated mutant and wild type mice (Fig.5.2).

#### 5-2-3: IFN-γ and IL-4 produced by spleen cells *in vitro*

Supernatant from spleen cell culture was collected at 17, 24, 48 and 72 hours after stimulation with 5µg/ml of ConA. Concentrations of IFN-γ and IL-4 were measured by ELISA. IFN-γ and IL-4 production reached plateau concentrations at day 2 and day 3 respectively. There was no significant difference between the concentrations of IFN-γ or IL-4 produced by the spleen cells from mutant or wild-type mice at all the times points treated (Fig.5.3).

a.



b.

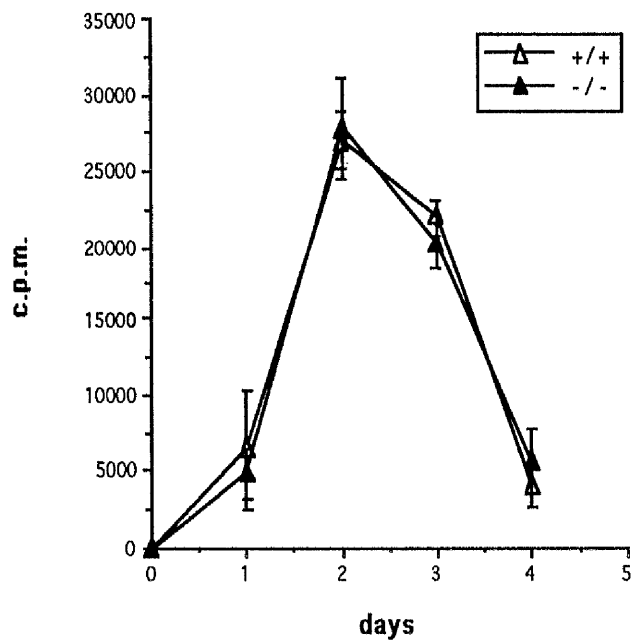


Fig. 5.1. Proliferation of spleen cells from wild type (open triangle) and mutant mice (filled triangle); (a.) cultures were incubated for 2 days; (b.) cultures were stimulated with 5.0 μg/ml of ConA. Vertical bars=1SD, n=3. Data are representative of two experiments.

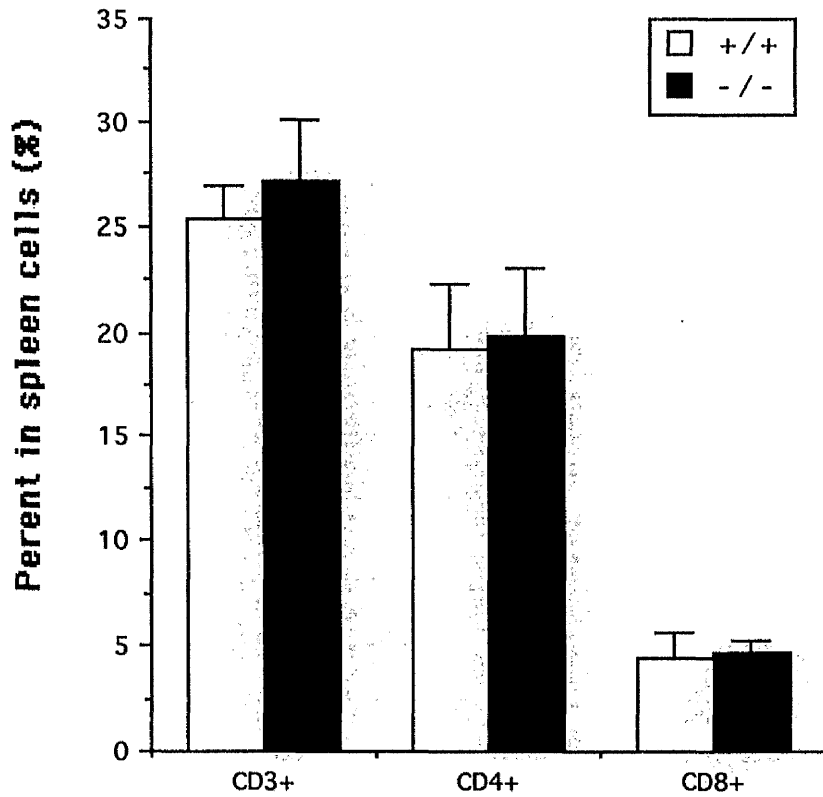
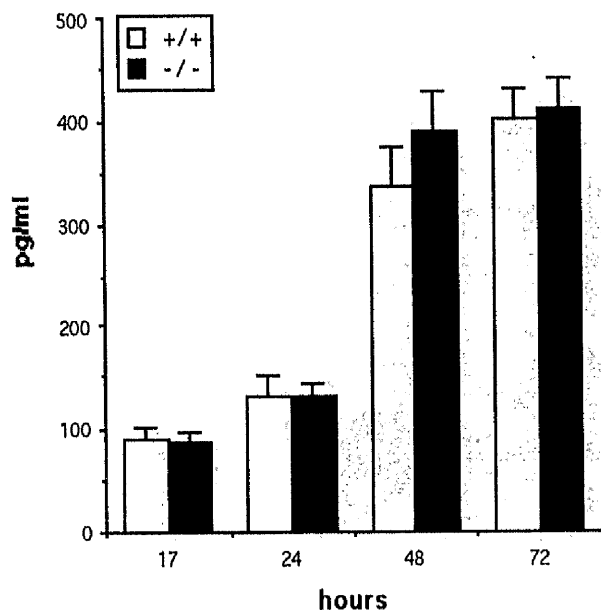


Fig.5.2. No significant difference in the percentage of CD3<sup>+</sup>, CD3<sup>+</sup>CD4<sup>+</sup>, or CD3<sup>+</sup>CD8<sup>+</sup> subsets of T cells in the splenic population of untreated mutant mice (filled columns) and wild type mice (open columns). Vertical bars=1SD, n=5. Data are representative of 2 experiments.

### IFN- $\gamma$



### IL-4

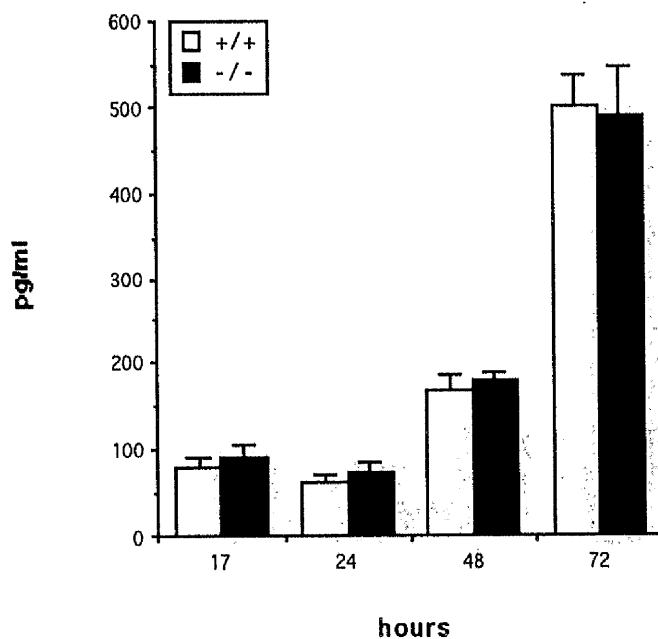


Fig 5.3. IFN- $\gamma$  and IL-4 produced by spleen cells of mutant mice (filled columns) and wild type mice (open columns). The culture was stimulated with 5 $\mu$ g/ml ConA. Vertical bars=1SD, n=5. Data are representative of 2 experiments.

### 5.3. Mice lacking iNOS fail to control a *Leishmania major* infection

#### 5.3.1. The Lesion of *L. major* infection

Anti-microbial activity of NO *in vivo* was previously suggested by reports which either documented high urinary excretion of nitrate in resistant mice infected with *L. major* (Evans, *et al.*, 1993) or progressive disease in animals treated with L-NMMA (Liew, *et al.*, 1990), an inhibitor of both the constitutive and inducible type of NOS. Furthermore, using Northern blot, PCR and immuno-histological techniques, iNOS mRNA and protein were detected in tissue after the mice were infected with *L. major* (Stenger, *et al.*, 1994), toxoplasma (Gazzinelli, *et al.*, 1993), listeria (Boockvar, *et al.*, 1994), or viruses (Korprowski, *et al.*, 1993). In this study, iNOS mutant mice were used to provide a direct evidence for the functions of iNOS in *L. major* infection. Groups of 5 wild-type, heterozygous and mutant homozygous mice were infected in the footpads with  $1 \times 10^6$  stationary-phase (day 7 culture) *L. major* (LV39) promastigotes. Lesion development was measured at regular intervals with a dial calliper and expressed as the footpad thickness increase of the infected right hind foot compared with the uninfected left hind foot. The wild type and heterozygous mice achieved spontaneous healing, but mutant homozygous mice failed to do so (Fig.5.4). The experiment was terminated (as required by the guidelines of animal experimentation of the Home Office, UK) when the lesion in the mutant mice became ulcerated. The healing wild type and heterozygous mice were in excellent health. The mutant mice had spleens and draining lymph nodes approximately 2 to 3 times larger than those from the wild-type and heterozygous mice.

#### 5.3.2. Parasite load of infected footpads

The foot pads of the mice infected with *L. major* were removed. Footpad tissue from the individual mice homogenised in 10ml PBS, and 50ul portions of suspension were sequentially diluted fivefold in Schneider medium containing 20% FCS. They were placed into flat-bottom 96-well plates and incubated at 28°C in humidified room air. Individual wells were examined daily using an inverted microscope for the presence of

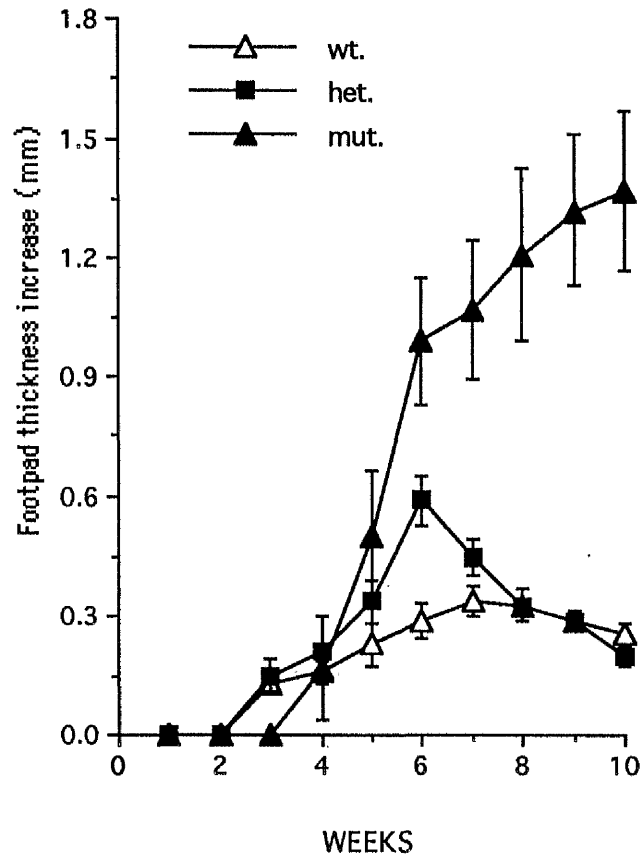


Fig.5.4. Footpads swelling differences at weeks after infection with  $10^6$  *L. major*. The mutant mice (closed triangles) had significantly larger foodpads than those of the heterozygous (closed squares) and wild-type mice (open triangles). Vertical bars = 1SE; n=5.

motile promastigotes. The geometric mean ( $\log_{10}$ ) and standard error of the last positive reciprocal dilution for each group was calculated. The result demonstrated a significantly higher parasite load in the infected footpads of homozygous mice than the wild-type and heterozygous mice (Table 5.1).

#### Tissue 5.1. Content of *L. major* in the infected footpad

Groups (n=3)	( $\text{Log}_{10} \pm \text{SEM}$ )
	Titre of viable <i>L. major</i>
Wild-type	3.82±0.8
Heterozygous	3.3 ±0.0
homozygous	6.09±0.4

#### 5.3.3. T-cell analysis of mice infected with *L. major*

Spleen cells were harvested and pooled from 3 mice per group on day 70 after infection with *L. major*. They were analysed for CD3<sup>+</sup>, CD3<sup>+</sup> CD4<sup>+</sup> and CD3<sup>+</sup> CD8<sup>+</sup> subsets of T cells by flow cytometry using the appropriate antibodies (Table 5.2). Spleen cells from mutant mice infected with *L. major* contained a significantly higher proportion of CD3<sup>+</sup> and CD3<sup>+</sup>CD4<sup>+</sup> T cells than those from the infected wild-type and heterozygous mice. Figures underlined are significantly different ( $P < 0.05$ ) from those of wild type mice.

Table 5-2: T-cell analysis of spleen cells from mice infected with *L. major*

Splenic T cells (%)	Wild-type	Heterozygous	Homozygous
CD3 <sup>+</sup>	16.9	19.1	<u>22.2</u>
CD4 <sup>+</sup>	7.7	11.9	<u>16.8</u>
CD8 <sup>+</sup>	4.0	3.9	3.1

#### 5.3.4. Spleen cell proliferation of mice infected with *L. major*

Spleen cells were also cultured at  $1 \times 10^6$  cells per ml in flat-bottom 96 well-plates. Cultures were stimulated with graded concentrations ( $10^5$ - $10^7$  organisms equivalent per ml) of soluble *L. major* antigen which was prepared by 3x freeze-thawing and high-speed centrifugation as described in Chapter 2 (2.37.), or Con A (0.5, 2.5 and 5.0 $\mu$ g/ml) for 1 to 4 days. The optimal proliferation of the cells from all three groups was on day 4 at  $10^6$  organisms equivalent per ml of antigen, and on day 3 at 5 $\mu$ g/ml Con A (Table 5.3).

Table 5.3. Spleen cell proliferation after stimulation with *L. major* antigen and ConA

	wild-type	heterozygous	mutant
<i>L. major</i> antigen	576 $\pm$ 276	<u>3,374<math>\pm</math>644</u>	<u>20,833<math>\pm</math>5,640</u>
Con A	17,676 $\pm$ 6,010	9,261 $\pm$ 1,592	<u>61,812<math>\pm</math>9,982</u>

\* The data are mean $\pm$ 1SD, n=3. Figures underlined are significantly different ( $P < 0.05$ ) from those of wild type mice.

#### 5.3.5. IFN- $\gamma$ and IL-4 production after stimulation with *L. major* antigen *in vitro*

Spleen cells were also cultured at  $1 \times 10^6$  cells per ml with  $10^6$  organisms equivalent per ml of soluble leishmanial antigen in 24-well plates. Supernatant was collected on days 1 to 4 and assayed for IFN- $\gamma$  and IL-4 by ELISA using paired monoclonal antibodies. IFN- $\gamma$  and IL-4 levels reached plateau concentrations at day 3 and day 4 after *L. major* antigen stimulation. The homozygous mice produced more IFN- $\gamma$  and less IL-4 than the wild-type and heterozygous mice (Fig.5.5).

#### 5.3.6. Serum IgG types of mice infected with *L. major*

Sera collected on post-infection day 70 were titrated against soluble *L. major* antigen-coated plates as described in Chapter 2 (2.40.). There was no significant difference in the anti-leishmania antibody among the three groups of mice. The concentrations of IgG2a were all higher than those of IgG1 in three groups (Fig.5.6)

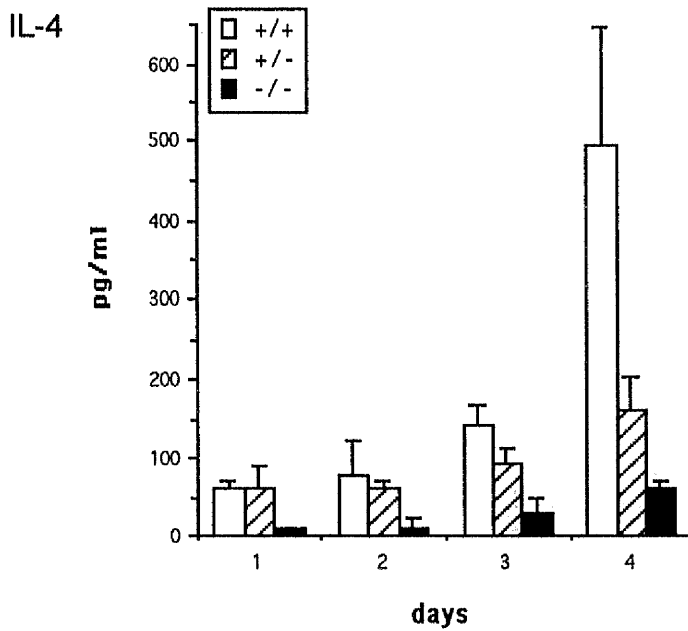
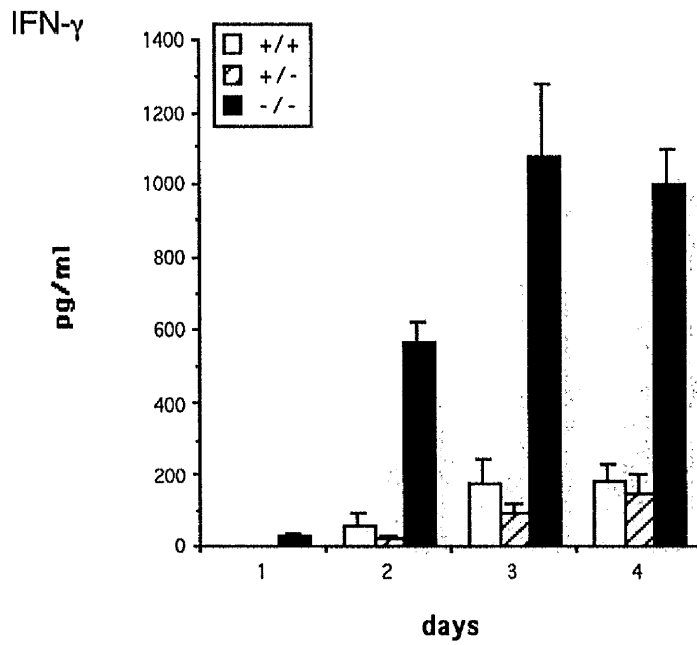


Fig.5.5. IFN- $\gamma$  and IL-4 productions by spleen cells after stimulation with  $10^6$  organisms equivalent per ml of soluble leishmanial antigen (*L. major*). The spleen cells from mutant mice (filled columns) produced more IFN- $\gamma$  and less IL-4 than those from heterozygous mice (striped columns) and wild-type mice (open columns) by day 2 and day 4 after stimulation. Vertical bars=1SD; n=3.

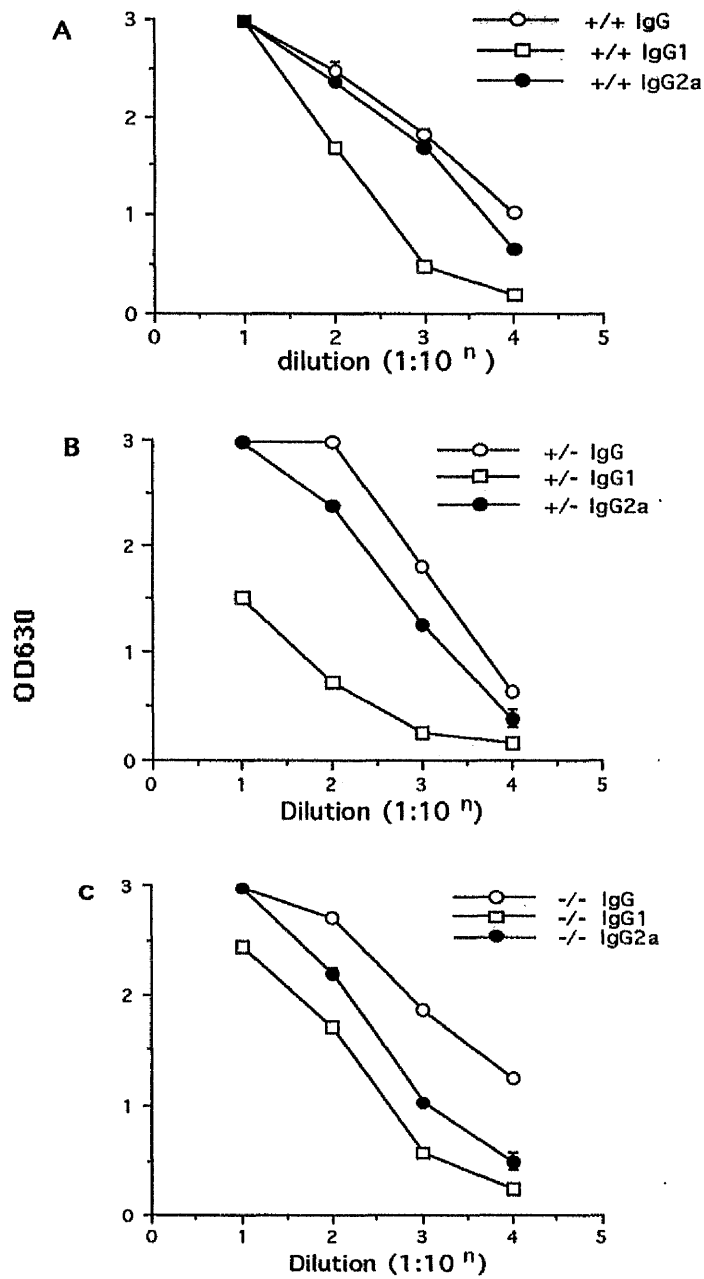


Fig.5.6. Serum IgG types of mice infected with *L. major*. There were no different pattern among the wild-type (A), heterozygous (B) and homozygous mutant mice (C). The vertical bar = 1SD, n=3.

## 5.4. Response to local inflammation

### 5.4.1. Reduced inflammation to carrageenin in mutant mice

NO is involved in the acute inflammatory response following foot pad injection of carrageenin (Ialenti, *et al.*, 1992, Ianaro *et al.*, 1994). Using the iNOS mutant mice in this study, the role of nitric oxide in acute inflammation was directly demonstrated. Groups of 5 mice were injected in the right hind footpad with 300µg of lambda carrageenin in 50µl PBS. The control left hind footpad was injected with 50µl PBS alone. Footpad swelling was measured daily with a dial calliper up to six days after injection, and the data shown represent mean footpad thickness increase (right footpad-left footpad). The mutant mice generated significantly less footpad swelling than wild type mice at day1 and 2 after injection with carrageenin. Footpad swelling had all decreased after day 3 of injection (Fig 5.7).

### 5.4.2. T cell analysis after injection with carrageenin

Spleen cells from mice injected with carrageenin were harvested at 21 days after injection and analysed for CD3<sup>+</sup>, CD3<sup>+</sup> CD4<sup>+</sup> and CD3<sup>+</sup>CD8<sup>+</sup> subsets by flow cytometry using the same antibodies as described in Chapter 2 (2.45.). Spleen cells from mutant mice had higher proportion of CD3<sup>+</sup>, CD3<sup>+</sup> CD4<sup>+</sup> and CD3<sup>+</sup>CD8<sup>+</sup> T cells than those from the wild type mice (Table 5.4).

Table 5.4. T-cell analysis of the mice at 21 days after injection with carrageenin

Splenic T cells (%)	wild type (n=5)	Homozygous (n=5)
CD3 <sup>+</sup>	19.42±1.27	<u>39.32±0.81</u>
CD3 <sup>+</sup> CD4 <sup>+</sup>	8.91±0.44	<u>14.69±0.94</u>
CD3 <sup>+</sup> CD8 <sup>+</sup>	2.83±0.61	<u>9.38±1.03</u>

\*Data are mean±1S.D. Figures underlined are significantly different (P<0.05) from those wild-type mice.

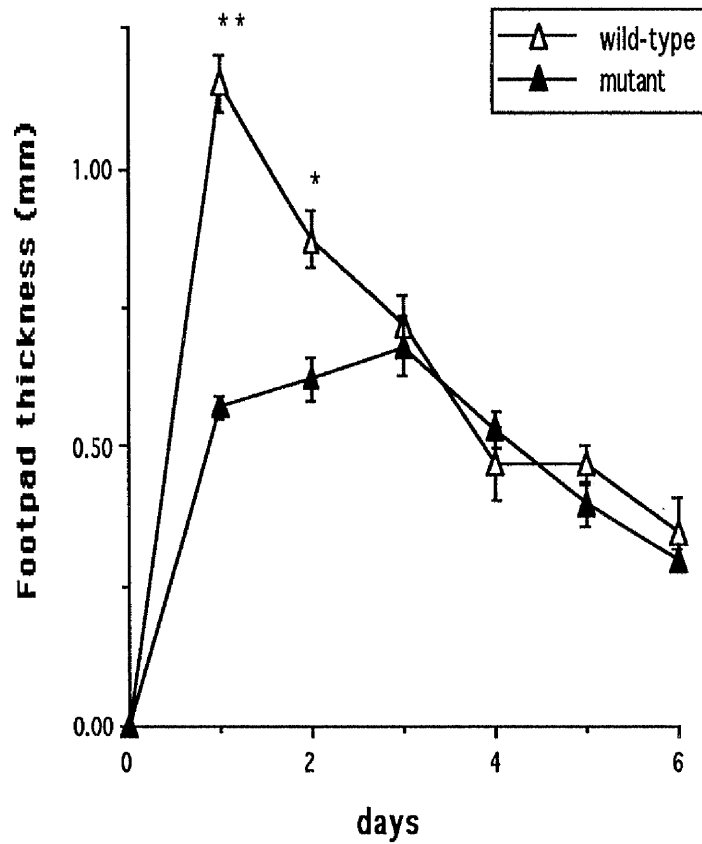


Fig.5.7. Footpad swelling was significantly reduced at day 2 and day 3 after injection with 300 $\mu$ g of carrageenin in mutant mice (solid triangles) compared with wild-type mice (empty triangles). Vertical bar=SEM, n=5. \*P=0.02; \*\*P<0.001.

#### 5.4.3. Spleen cells of mutant mice had higher proliferation

Spleen cells were also pooled from 5 mice per group and cultured at  $1 \times 10^6$  cells per ml in flat bottom 96-well plates with graded concentration of ConA (0.1, 0.5, 2.5, and  $10.0 \mu\text{g/ml}$ ). Proliferation of spleen cells were measured on day 1 to 3 after stimulation according to the method described in Chapter 2 (2.44). Spleen cells proliferation of mutant mice was significantly higher than that of the wild-type mice on day 2 and 3 at doses of 0.5 to  $10.0 \mu\text{g/ml}$  ConA. The optimal proliferation of the cells from mutant mice was on the day 3 at  $2.5 \mu\text{g/ml}$  ConA, while that of the wild-type mice on the day 2 at  $2.5 \mu\text{g/ml}$  ConA (Fig.5.8).

#### 5.4.4. IFN- $\gamma$ and IL-4 produced after ConA stimulation *in vitro*

Supernatant of cultures was also collected on day 1 to 3 after stimulation with  $2.5 \mu\text{g/ml}$  ConA *in vitro*. IFN- $\gamma$  and IL-4 levels were measured by ELISA as described in Chapter 2 (2.39.). Cells from the mutant mice produced significantly higher levels of IFN- $\gamma$  than those from wild type mice at all time points. Analysis of IL-4 production however showed no significant differences between the two groups at all time points tested (Fig.5.9).

### **5.5. Mice lacking iNOS are more resistant to LPS-induced loss of mass and mortality than wild type mice.**

#### 5.5.1. Reduced loss of mass during LPS-induced shock

Groups of 5 mice were injected intraperitoneally with  $10 \text{mg/kg}$  LPS in PBS. The wild-type mice developed severe symptoms with up to 12% loss of mass. In contrast, the mutant mice showed only minimum symptoms after transient loss of mass within 24 hours, and they all recovered by 72 hours after injection (Fig5.10.a).

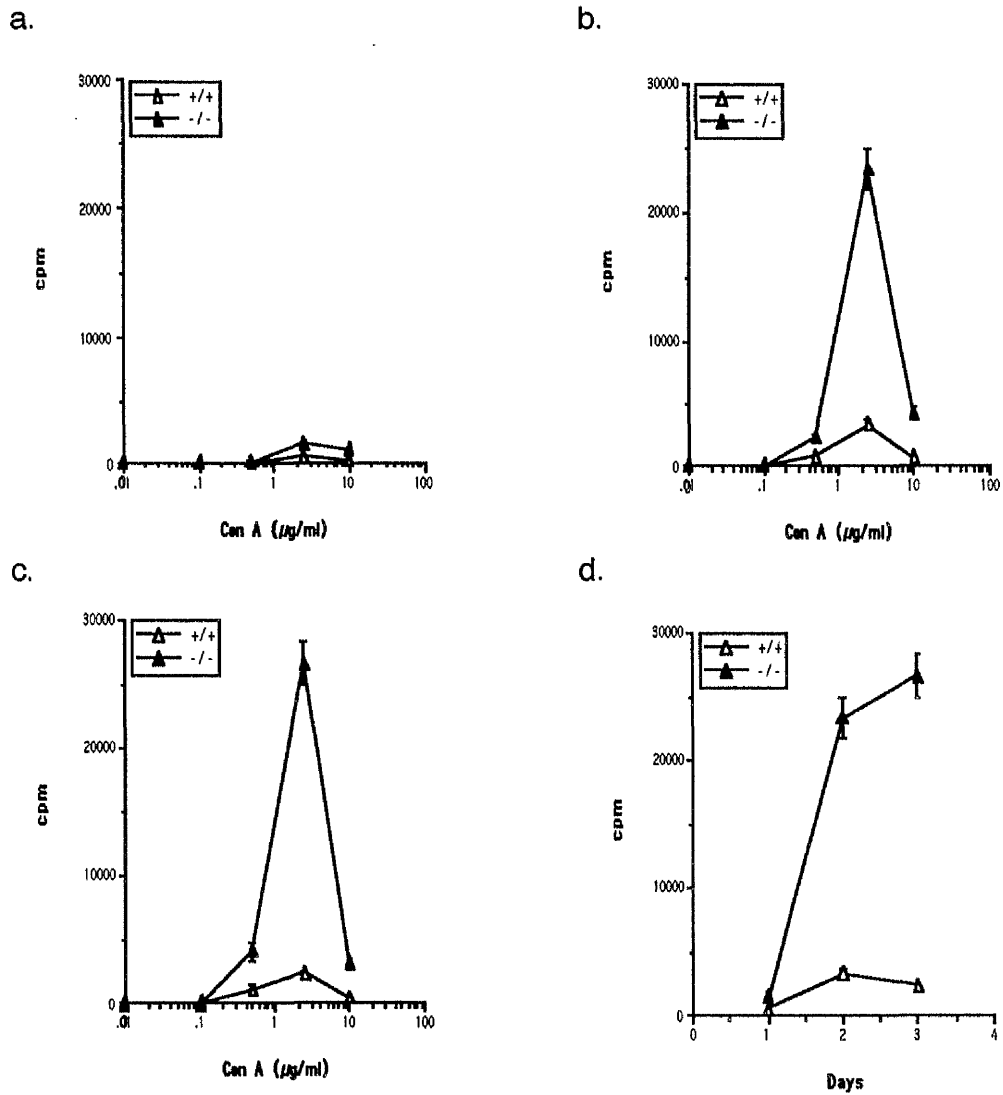


Fig.5.8. Proliferation of spleen cells from carrageenin injected mutant mice (solid triangles) and wild-type mice (empty triangles). Cultures were incubated for 1 day (a), 2 days (b) or 3 days (c) with graded concentrations of ConA. Cultures were stimulation with 2.5 $\mu\text{g/ml}$  of ConA (d). Vertical bars=1 SD, n=3.

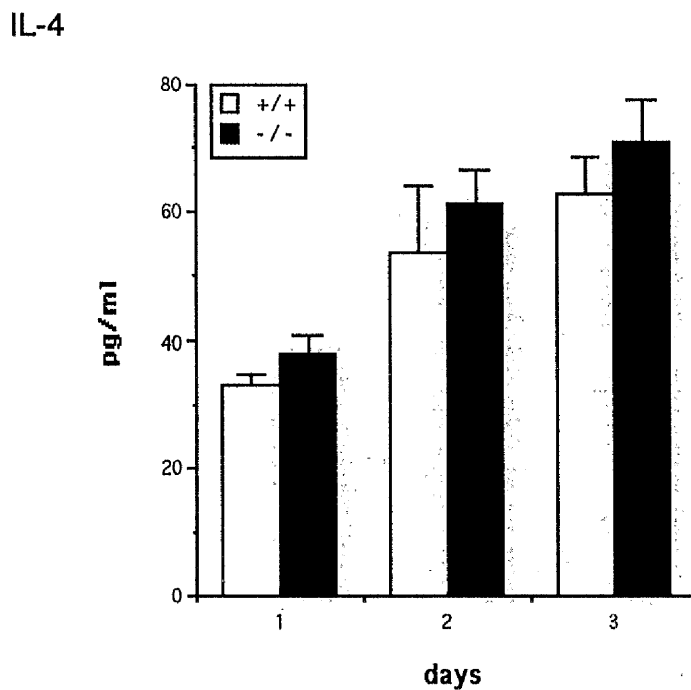
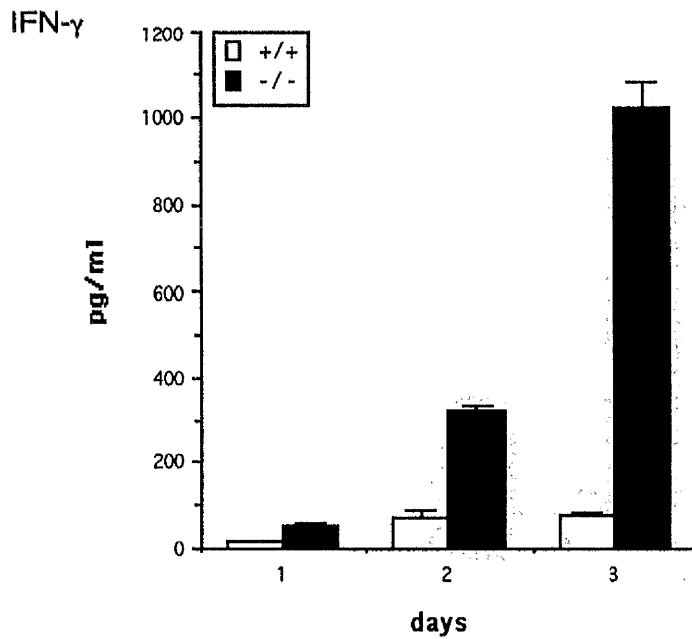


Fig.5.9. IFN- $\gamma$  and IL-4 production in carrageenin-injected mice after stimulation with 2.5 $\mu$ g/ml ConA, spleen cells from mutant mice (filled columns) produced significantly higher amount of IFN- $\gamma$  than wild-type mice (open columns), but no significant difference for IL-4 production was noted at all the time points. Vertical bars=1SD, n=3.

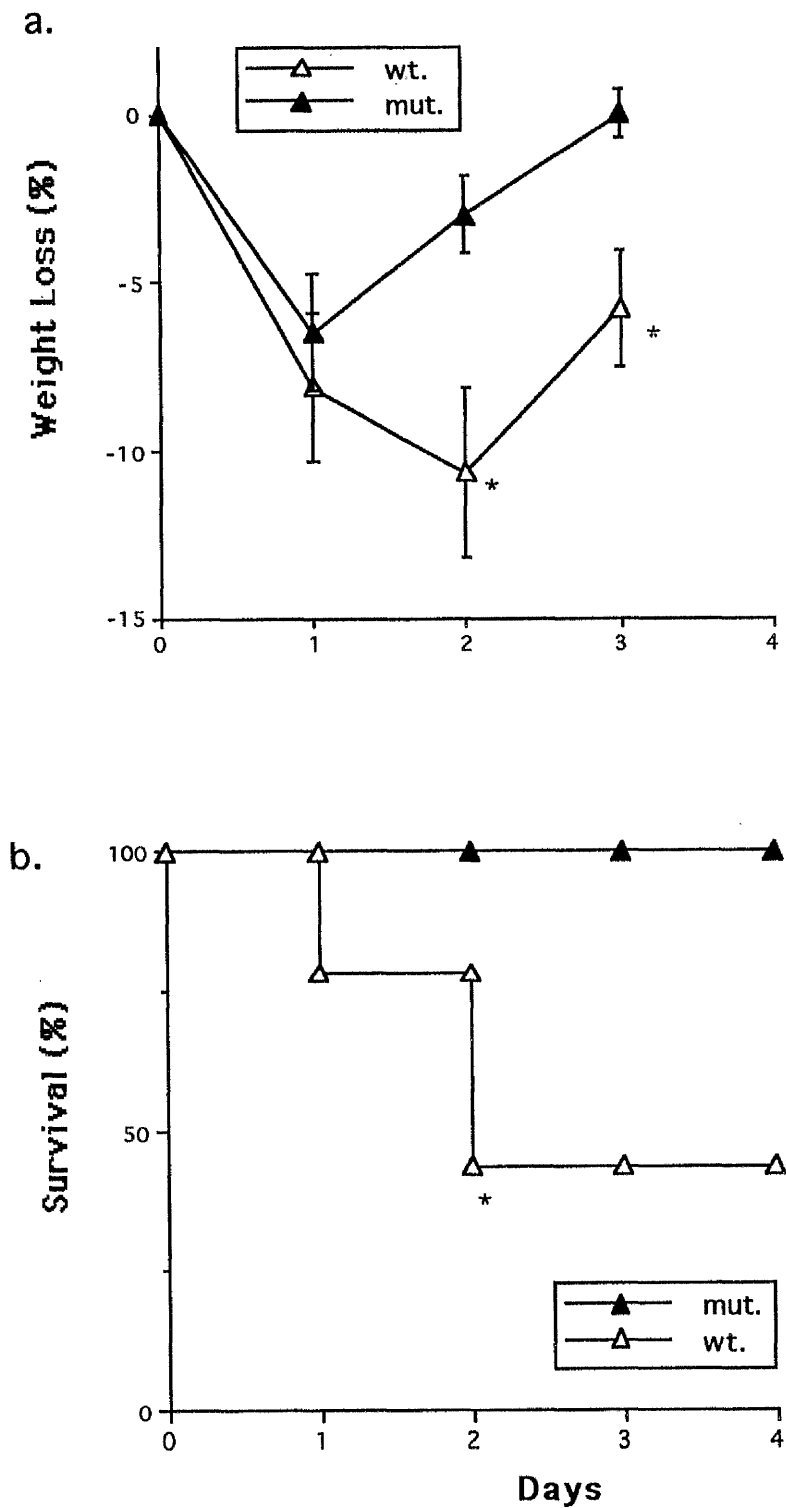


Fig 5.10. (a) Wild-type mice (open triangles) had more body mass loss after injection with 10mg/kg of LPS than mutant mice (closed triangles) \* $P < 0.05$ ;  $n = 5$ . (b) All the mutant mice survived after 12.5mg/kg of LPS, while about 45% wild-type mice (open triangles) survived. \* $P = 0.16$  (survival test);  $n = 9$ .

### 5.5.2. Mutant mice survived from endotoxin-induced shock

Groups of 9 mice were injected i.p. with 12.5mg/kg LPS, 5 of 9 wild type mice died within 72 hours with extensive subcutaneous haemorrhage. In contrast, all the mutant mice recovered from an initial transient loss of mass (Fig. 5.10.b). All the mutant mice body weight recovered earlier than survived wild-type mice.

### **5.6. Summary**

Inducible NOS gene was disrupted in embryonic stem cells which were then used to produce germline chimeras. F1 heterozygous mice for the mutation were bred to obtain homozygous mice for the disrupted iNOS gene. Loss of the wild type allele was confirmed by Southern blotting which was described in Chapter 4. Homozygous animals were viable and fertile, and there was no evidence of histopathology within the major organs examined (The histological examinations for three mice in each groups were carried out by Dr. G. Lindop, The Department of pathology, Western Infirmary, University of Glasgow). Inter-breeding of mutant mice gave rise to a stock of mice that were used for the following experiments. Some of biological phenotypes were defined by the homozygous mice, which were compared with sex- and age- matched animals of wild type mice or heterozygous mice.

Spleen cells from unimmunized mutant mice gave similar levels of IFN- $\gamma$  and IL-4 production compared with those from the wild-type mice when induced with concanavalin A and also proliferated to the same degree. There was also no difference in the proportion of T cells between the two groups.

The wild-type mice and the heterozygous mice were highly resistant to *L. major* infection, and all animals achieved spontaneous healing after footpad infection with  $10^6$  promastigotes. In contrast, the mutant mice were highly susceptible to the infection and developed visceral disease by day 70 post-infection. There was no significant difference in lesion size between the three groups of mice until 5 weeks after infection, indicating that the innate response, possibly under the influence of the Natural resistance associated

macrophage protein (*Nramp*) gene, is unlikely to be associated with the NO effector mechanism. *Nramp* is believed as one of the control gene for natural resistance to infection with intracellular parasites (it will be explained more in Chapter 6.4).

Spleen cells from mutant mice infected with *L. major* contained a significantly higher proportion of CD3<sup>+</sup> and CD3<sup>+</sup>CD4<sup>+</sup> T cells than those from the infected wild type and heterozygous mice. Spleen cells from the infected mutant mice also showed significantly higher levels of T-cell proliferation than those from the wild-type or heterozygous mice when cultured with Leishmania antigens or concanavalin A *in vitro*. They produced more IFN- $\gamma$ , but less IL-4 than those from similarly infected wild-type or heterozygous mice when stimulated with soluble Leishmania antigens *in vitro*. Anti-Leishmania antibody titres were comparable in all the three groups of mice, but the concentrations of IgG2a were greater than those of IgG1.

The capacity of these mice to develop local inflammation was also investigated. The mutant mice generated significantly less footpad swelling than wild-type mice after injection with carrageenin. Spleen cells from carrageenin-treated mutant mice also had a higher proportion of CD3<sup>+</sup>, CD3<sup>+</sup>CD4<sup>+</sup> and CD3<sup>+</sup>CD8<sup>+</sup> T cells than those from the wild-type mice, and produced more IFN- $\gamma$  than those from the wild-type mice when stimulated with concanavalin A *in vitro*. The spleen cells from the mutant mice treated with carrageenin had a higher proliferation rate than those from the wild-type mice. However, the relatively lower proliferation of the wild type spleen cells at day 21 after the carrageenin stimulation suggests that higher NO production could suppress the T-cell response to the ConA.

The mutant mice were also more resistant to LPS-induced death than wild-type mice, which developed severe loss of mass when injected intraperitoneally with LPS. The mutant mice showed an initial malaise and loss of mass, but recovered completely by 24 hours, and showed no further sign of ill health. In contrast, wild-type mice underwent substantial loss of mass with about 50% mortality by 72 hours after injection with 12.5 mg/kg body mass.

Mice deficient in iNOS provide a powerful tool that will not only facilitate formal demonstration of the effect roles of NO in microbicidal, tumoricidal, transplantation and in a range of immunopathologies, but also help to define the involvement of NO in immune regulation, immunological tolerance and antigen processing and presentation. This is highlighted by the recent demonstration that human monocyte / macrophages express iNOS (Mossalayi, *et al.*, 1994; De-Maria, *et al.*, 1994.) and generate NO in quantities sufficient to kill *Leishmania* parasites (Vouldoukis, *et al.*, in press).

# **Chapter 6**

## **General Discussion**

The development of gene targeting technology, through homologous recombination between exogenous DNA and the endogenous genomic homologue in mouse embryonic stem (ES) cells, provides a powerful tool for generating mutant mouse strains with defined genetic modifications. These animal models allow us to study the functions of the targeted genes *in vivo*. The technology is especially attractive for studying genes specific for immune responses, since the modification of these genes is unlikely to be lethal to embryo development of the mutant mice. In this study, iNOS gene mutant mice were made by using the ES cell gene targeting technology. In this chapter, a number of points will be addressed. (1). 5' iNOS gene organisation. (2). Optimum gene targeting strategy. (3). Mutation that may occur by gene rearrangement events. (4). Explanations of iNOS biological phenotype. (5). Conclusion and future works.

### **6.1. 5' murine iNOS gene structural organisation**

To design the iNOS gene target construct, 5' end of cDNA fragment was used as probe to clone the genomic DNA. Four overlapping iNOS gene clones were obtained from two mouse strain genomic libraries. The restriction enzymes (*EcoRI*, *BamHI*, *HindIII*, *BglII*, *KpnI*, *SacI*, *PstI*, *SmaI*, *SpeI*, *XbaI*) mapping for the DNA from both strain is exactly identical. Although no difference was found for the restriction enzymes mapping between 129/sv and B6 strains, Possible variations outside of the enzyme sites could largely reduce the efficient homologous recombination (Riele, *et al.*, 1992).

The first eight exons were located in these four overlapping genomic clones. They span over 21kb of cloned DNA. Intron-exon junctions were sequenced for six of the eight exons (Exons 1,2,3,4,5,7). Most of them conformed to the Mount consensus for spliced junction sequences (3' Acceptor: (Y)<sub>n</sub>NYAG; 5' Donor: GTRAGT)(Chapter 4.2). Murine iNOS exons (exons 1 to 8) were found to be structurally similar to the human iNOS gene. All the eight exons which have been identified in the present study are small. Unlike human iNOS has a large intron 5 (about 6kb), murine iNOS has a large intron 2 which is about 5.5kb. However, the start codon (ATG) is located in exon 2 which is the same as human iNOS and ncNOS gene (Chartrain, *et al.* 1994; Hall, *et al.*, 1994).

## 6.2. Optimum gene targeting strategy.

### 6.2.1. Maximising efficient homologous recombination

Homologous recombination between transferred DNA and the chromosomal gene, termed gene targeting, provides a way of making specific alterations in the genome. In mammalian cells, integration of transferred DNA into the chromosomes occurs much more frequently by nonhomologous than by homologous recombination, an effect that impedes the detection and recovery of the rare targeted cells (Capecchi, 1989; Deng, *et al.*, 1992.). The mechanism of the homologous recombination is not well known. Many experiments have been carried out to investigate the strategies which can influence the efficiency of homologous recombination. Although different gene loci may have different recombination efficiency, these investigations could help gene targeting design.

Length of homologous region. The homologous sequences in the vector, specifically their length (Thomas, *et al.*, 1987; Hasty, *et al.*, 1991) and the degree of polymorphic variation between the vector and the chromosome (Riele, *et al.*, 1992), have been shown to affect targeting frequencies. As a general rule, the greater the length of homology the higher the targeting frequency. For most vectors, the range of five to ten kilobases is recommended. In the iNOS gene targeting vector, the length of homology is about 6.5kb (left arm: 3.0kb plus right arm: 3.5kb). The asymmetry homology arm for the PCR screening strategy can also have an effect on the targeting frequency, since the length of the short arm may become suboptimal, although cross-over have been observed to occur with less than 500bp on the short arm (Hasty, *et al.*, 1991).

Isogenic gene construct. It is known from studies on extra-chromosomal and intra-chromosomal recombination, and recently, from gene targeting experiments (Riele, *et al.*, 1992), that a significant variation in sequence homology between the two elements involved in the genetic exchange can reduce homologous recombination/targeting frequency. The number and extent of polymorphic variations between two mouse strains in any given locus is unknown but may vary widely from gene to gene. In particular,

introns are likely to be more divergent than exonic sequences. To avoid gene variation between B6 and 129/sv mice, iNOS gene targeting construct was generated from 129/sv ES cells genomic DNA.

Gene transcription in ES cells. Much direct and indirect evidence has shown that transcription enhances homologous recombination in mammalian cells (Nickoloff, *et al.*, 1992; Johnson, *et al.*, 1989; Mansour, *et al.*, 1988; Nickoloff, *et al.*, 1990; Shenkar, *et al.* 1991). Before designing the iNOS gene targeting constructs, attempts were made to detect iNOS gene expression by measuring nitrite from supernatant of ES culture and by using RT-PCR. No detectable iNOS gene expression was found in the ES cells, even after stimulation with IFN- $\gamma$  and LPS which can induce iNOS gene expression in murine macrophages. The low efficient homologous recombination events in this iNOS gene targeting (one in 636 G418 resistant clones screened) may be due to the fact that iNOS gene is tightly controlled in the ES cell.

Size of deletion. The gene targeting frequencies and recombination products generated have been investigated by a series of replacement deletion vectors which target the *hprt* (hypoxanthine phosphoribosyltransferase) locus in the mouse ES cells (Zhang, *et al.*, 1994). The efficiency of homologous recombination was apparently not influenced by the size of deletion for the disrupted gene, however the different integration was demonstrated in the large deletion vector targeting. In this study, the replacement vector used was by deletion of 11.5kb from the first 5 exons and part of promoter of iNOS gene. As described in Chapter 4.5, Southern blotting with both 5' and 3' end specific external probes was consistent with a gene replacement event. But the replaced wild type gene appeared to have translocated and integrated in the gene locus identified by the *EcoRV* digested Southern blot. The precise integration pathway is at present unclear because of the limited mapping of the iNOS gene. The possibilities of the gene rearrangement will be described below.

Vector cutting out in homologous region. Enzyme cutting in both homology regions can enhance the efficiency of homologous recombination by 3-4 times compared

to a cut in one homologous region alone (personal communication with M. Li. Gene Targeting Laboratory, Centre for Genome Research, University of Edinburgh.). In this study, *SacI* was used to linearise the targeting construct to expose both the 5' and the 3' homology regions.

#### 6.2.2. Enrichment for targeted clones in culture

Gene trap strategy. Using selection markers in the targeting construct can enrich the targeted clones in culture. However, they could not influence the efficiency of homologous recombination. Promoter trap targeting vectors are designed to use the transcriptional machinery of the endogenous target gene to drive the positive selection cassette cloned in the targeting construct. Typically, promoter trap selection will yield an enrichment of about 100-fold for targeted clones. In some gene targeting experiments, 86% targeted clones has been generated from G418 resistance CGR8 ES cell clones (Mountford, *et al.*, 1994). However, good candidate genes for this selection scheme are those gene expression in the target cell. In this study, the iNOS gene expression has not been detected in the ES cells. The iNOS gene is probably too big for the polyadenylation trap targeting strategy and is therefore not suitable for this study.

Positive and negative selection. Positive and negative selection is commonly used for enrichment scheme. The idea is that a targeting construct is designed to contain the neomycin resistance gene cassette encoding for resistance to geneticin for positive selection. In addition, the construct may contain an HSV-tk gene for negative selection, which is capable of converting Ganciclovir into toxic intermediaries. Cells that undergo homologous recombination are Ganciclovir and G418-resistant. Cells which contain the randomly integrated construct will retain both the neomycin and HSV-tk genes and although G418-resistant, will be Ganciclovir sensitive (Mansour, *et al.*, 1988). In the present iNOS gene target, we exposed both homology ends to enhance targeting efficiency. A positive selection marker can not be used, because *SacI* will cut the positive selection marker (HSV-tk gene) off. Although only the positive selection marker (*Neo* gene) was used in the iNOS gene targeting strategy, the efficiency of homologous

recombination (1/636) was not as low as the positive and negative selection strategy (1/980) which was used in the same gene locus of the iNOS gene targeting (Macmicking, *et al.*, 1995). The low ratio of targeted gene may due to the characteristic of iNOS gene locus.

### **6.3. The iNOS gene mutation**

#### **6.3.1. iNOS gene is not duplicated in wild-type mice**

Using both 5' and 3' specific external probes, two hybridisation bands (7.0kb wild-type band and 5.4kb targeted band for 5' probe; 7.5kb wild-type band and 6.0kb targeted band for 3' probe) were always detected in the homozygous mice. Unlike the heterozygous mice, the band densities were equal. In heterozygous mice, wild-type bands for both external probes were more dense than the targeted bands. But the genotype was difficult to identify with Southern blot analysis using the external probes. This result suggested that there may be duplicated iNOS gene in the wild-type mice, one of them had been replaced with the targeting vector and the other persisted. To test this possibility, genomic DNA from ES cells and three genotype mice tail tipplings were digested with enzymes with restrictive sites in the targeting vector homology region. If the duplicate genes are not exactly identical, Southern blot with 5' or 3' external probe should show double band in all of them. However, the result showed that the duplicated bands were only obtained with DNA from the homozygous and heterozygous mice and not from that of the wild-type mice or ES cell. This result therefore indicated that it is unlikely that there is duplication of iNOS gene in the wild-type mice.

#### **6.3.2. End extension of the targeting construct**

To study the mechanism of targeted recombination, a wild-type gene was introduced into a mutant Chinese Hamster Ovary (CHO) cell line which is homozygous adenine phosphoribosyl transferase (APRT) deficient. The truncated end of the *aprt* gene was corrected by extending the end beyond the region of homology to the target locus (Aratani, *et al.*, 1992). In the present study, Southern blot analysis, using both the

external probes, indicated that the introduced targeting vector had entered the gene locus. Furthermore, extension from both ends which had resulted in the gene duplication (Fig.6.1).

### 6.3.3. Targeted iNOS gene

The limited map of the iNOS gene from this study makes it difficult to understand the genetic events in the gene targeted mice. So far, we know that end extension had occurred (Fig.6.1), which either caused end extension targeting vector integration or wild-type genomic DNA integration. There are four possibilities. (a) The end extension targeting vector was randomly integrated. This should not make any change for wild-type allele. (b) The end extension targeting vector had integrated into the iNOS gene. (c) The wild-type genomic DNA was randomly integrated or (d) into the iNOS gene locus. Any of these events can result in iNOS gene mutation except (a). However Southern blot analysis with *EcoRV* digested DNA using internal probe showed that the 12kb wild-type band was replaced by a 14kb band in the homozygous mice. This result indicated that it is unlikely that (a) had occurred.

Two gene altered events can be identified by using internal and external probes for Southern blot analysis. These two genotypes could not be segregated by back-crossing experiments. This may indicate that both the recombination events had occurred in the iNOS gene locus. To demonstrate the precise iNOS gene targeted events in this strain of mice, the large region of wild-type and mutant iNOS genome will have to be mapped. This will be discussed in the section on future work (6.7.1.).

### 6.3.4. The larger mutant mRNA

Using 973bp 5' iNOS cDNA probe for Northern blot analysis, the 4.0kb iNOS mRNA was also shown to be altered to 4.5kb in the mutant homozygous mice. The possibilities of gene rearrangements (b, c and d described in 6.3.3.) can lead to the transcription of larger messenger. The end extension targeting vector integrating into the iNOS gene, or the 5' iNOS genomic DNA integrating into up-stream targeted gene could

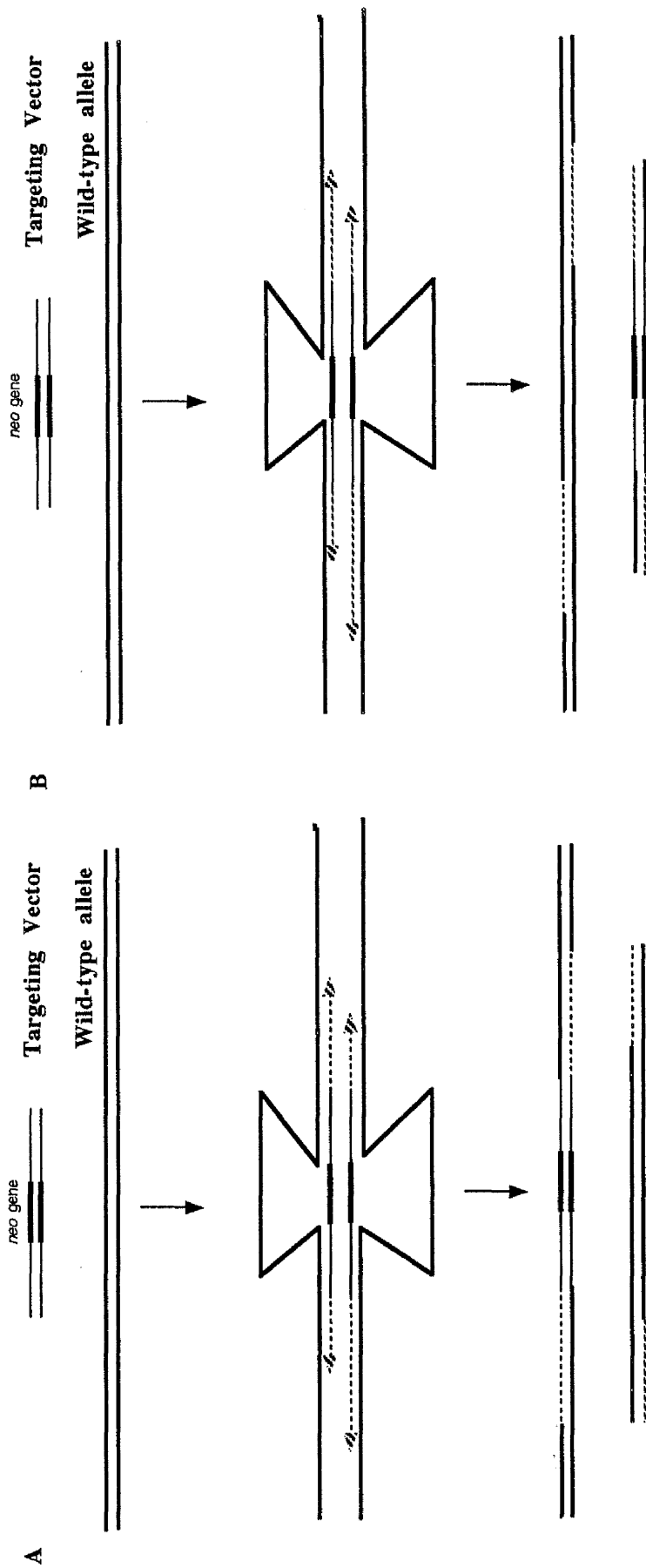


Fig.6.1. End extension model by homologous recombination. Two possible ways are shown (A and B), and the process of recombination and resulting products are depicted. Thin lines indicate the target construct homology DNA. Thick lines indicate genomic DNA. Broken lines represent a *neo* gene extension copied DNA from genomic DNA. Arrow head broken lines represent both end extension copying. The *neo* gene is shown as black bars.

cause some exons duplication. Transcription might go through the whole targeted gene resulting in a large messenger with duplicated part of sequence in the middle of the messenger (Fig. 6.2). The other possibility for the larger messenger is that part of iNOS genomic DNA had integrated into another gene (X gene) locus (fig. 6.3). This integration event might resulting in a fusion messenger, since a part of iNOS genomic DNA might still contain a functional promoter which could switch gene transcription after induction by IFN- $\gamma$  and LPS. However, this integration event detected by internal probe, and the gene replacement targeting event detected by external probe, could not be segregated in the offspring from back-crossing breedings. This result was obtained by Southern blot analysis of DNA from 92 offsprings. Two events in the same gene locus appeared to be more likely.

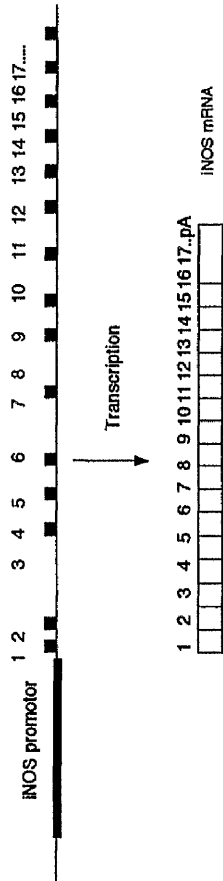
#### 6.3.5. Abrogation of iNOS protein translation

Although the larger messenger was detectable by Northern blot analysis in the peritoneal macrophages at 6 hour after IFN- $\gamma$  and LPS induction, no iNOS protein was detectable up to 20 hours after induction by Western blot analysis (ECL system) with either monoclonal or polyclonal iNOS specific antibodies. This result may indicate that the larger mutant messenger was either in incorrect reading frame or unstable for translation of iNOS protein.

#### 6.3.6. Detectable Nitrite production after longer culture

Nitrite was measured by Griess method up to 6 days for the culture supernatants from the activated peritoneal macrophages. After 24 hours activation, a large amount of nitrite was detected in cell culture of peritoneal macrophages from the wild-type and heterozygous mice. However, no detectable nitrite production was found at 24 hours from homozygous mice, in some experiments even no nitrite production till 4 days after activation. For most cases, however, nitrite could be detectable by 72 hours after stimulation, but not in control unstimulated cell culture. It is known that macrophages have two forms of NOS, one is calcium-independent (iNOS) and the other is calcium

**Wild type**



**gene targeted**

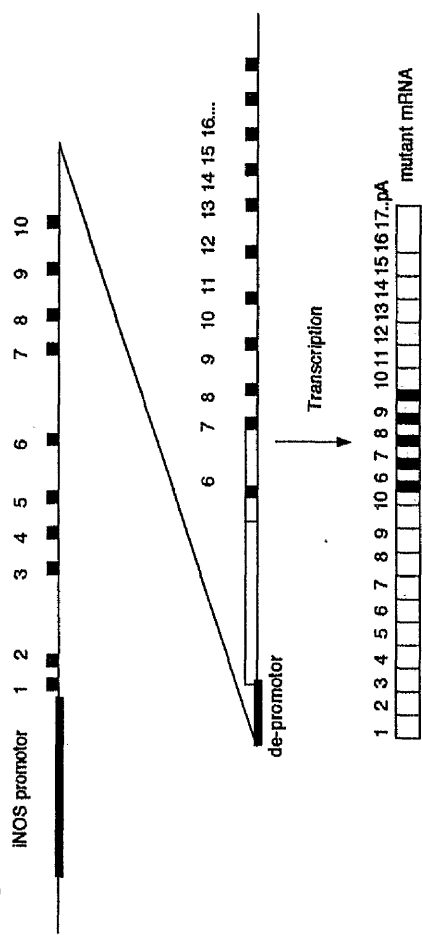


Fig.62. Duplication exons sequence in the middle of INOS mRNA may result in a larger messenger. Upper map represents wild-type gene transcription. Bottom map shows the mutation either by end extension targeting vector integration or a part of 5' INOS genomic DNA integration in front of the targeted gene. Black boxes represent the exons in the gene. Empty boxes indicate the exons sequence in the mRNA. Shaded boxes represent the duplicated exons sequence in the mutant messenger.

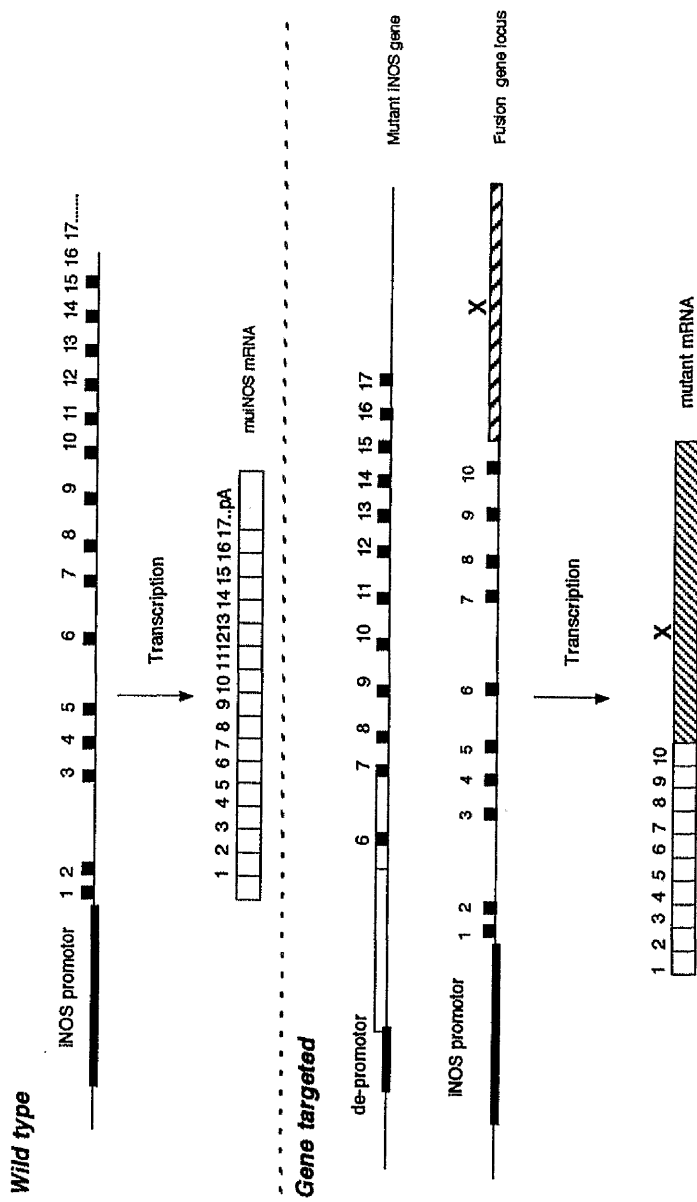


Fig.63. Fusion messenger may also result in a larger mRNA which can be detected with 5' INOS cDNA probe by Northern blot analysis. Upper map represents wild-type gene transcription. Bottom map shows the mutation by a part of wild-type INOS gene integration into another gene (X) locus. Black boxes indicate INOS gene exons. Empty boxes represent the excess sequence in the mRNA. Stripped bar represents the duplicated excess sequence in another gene (X) or in the mutant messenger.

dependent (ncNOS and ecNOS). In J774 macrophage cell line, both iNOS and cNOS activities are increased markedly by LPS stimulation (Dusting, *et al.*, 1995). The nitrite production from iNOS mutant mice may either come from up-regulation of constitutive NOS or the other form of yet unidentified NOS.

#### **6.4. The role of iNOS in immunology defence**

##### **6.4.1. iNOS is important against leishmania infection**

There is increasing evidence that NO from iNOS plays a key role in nonspecific defence mechanisms against pathogens, and may be involved in the signalling between macrophages and T cells. CD4<sup>+</sup> T helper (Th) cells which are critical in host defence have been implicated in chronic inflammatory diseases. Two types of Th cell are distinguished by the pattern of cytokines secreted upon activation. Th1 cells release IL-2 and IFN- $\gamma$ , whereas Th2 cells produce IL-4, IL-5 and IL-10 (Mosmann, *et al.*, 1989). These patterns of cytokine production largely determine the effector functions of the two subsets of murine and human T cells (Romagnani, 1991). The Th1 and Th2 subsets also modulate each other's activity in such a way that the balance between them frequently determines the outcome of infectious and autoimmune diseases. IFN- $\gamma$  produced by Th1 cells promotes the differentiation of T-cell precursors (Th0 cells) to Th1 cells, and inhibits the proliferation of Th2 cells. By contrast, IL-4 produced by Th2 cells can drive the proliferation of Th2 cells, and IL-10 can indirectly inhibit the secretion of IFN- $\gamma$  by Th1 cells (Fitch, *et al.*, 1993). NO may balance these two subsets of Th cells.

Experimental leishmania infection in the murine model has been well established, especially for cell-mediated immunity (Liew, 1990). A large amount of evidence supports the notion that Th1 dominant will be protective against *L. major* infection (Scott, *et al.*, 1988; Holaday, *et al.*, 1991; Morris, *et al.*, 1993). One of the mechanisms is that IFN- $\gamma$  produced by Th1 cell activates macrophages to produce NO, which is toxic to the parasites. Mouse peritoneal macrophages stimulated *in vitro* with IFN- $\gamma$  in the presence of LPS are efficient in killing *leishmania* and this leishmanicidal activity can be completely blocked by

L-NMMA in a dose-dependent manner, but not by its D-enantiomer (D-NMMA) (Green, *et al.*, 1990; Liew, *et al.*, 1990).

To define the iNOS functions *in vivo*, the iNOS gene mutant homozygous mice as well as the control heterozygous and wild-type mice were infected with *L. major*. The wild-type and the heterozygous mice were highly resistant to *L. major* infection, and all animals achieved spontaneous healing by contrast, the iNOS mutant mice were highly susceptible to the infection and developed visceral disease by 70 days postinfection. The parasite load was 1,000 times higher in the footpad of the homozygous mice than in that of the wild-type or heterozygous mice.

T cells were analysed for the three groups of infected mice. Spleen cells from homozygous mice had higher proliferative response to Con A and also to leishmania antigen than those from wild-type or heterozygous mice. Percent of CD4<sup>+</sup> T cells (T helper cells) was also significantly higher in infected homozygous mice than in the wild-type or heterozygous mice. In the T helper cells populations, The ratio of Th1/Th2 was higher in the mutant mice than in the wild-type or the heterozygous cells, because their spleen cells produced higher concentration of IFN- $\gamma$  and lower levels of IL-4 compared to those from the wild-type or heterozygous control. It seems that the cell-mediated immunity in the homozygous mice worked very hard to protect the host against leishmania infection, but without the weapon (NO) to do so. This result provides a direct evident that iNOS is important for the host defence leishmania infection *in vivo*.

#### 6.4.2. Possible mechanisms of the altered immune response in iNOS mutant mice

NO from activated macrophages could kill the leishmania and macrophages themselves. Substantial amounts of NO produced from iNOS kill parasites efficiently, at the same time, it can also killed activated macrophages. Activated macrophages produce cytokines such as IL-12 which can push Th0 cells to Th1 cells. The Th1 then produce more IFN- $\gamma$  to active the macrophages to produce more iNOS and NO to kill the parasites even more efficiently. When the parasite was killed, the antigen-specific T cells go down

to normal level. However, in the mutant mice, activated macrophages could not kill the parasites, and also many macrophages continued to be activated. These macrophages could produce more IL-12 to drive Th1 cell development, and the leishmania antigen could also continue to activate T cells.

NO from iNOS may directly inhibit the T cell activity. Substantial amount of NO produced from iNOS may inhibit the T cell activity, especially for Th1 cells. Hoffman *et al.* 1990, first reported that NOS activity was detected during phytohaemagglutinin (PHA)-stimulated proliferation of rat spleen cells and also in mixed lymphocyte responses, and that the addition of NOS inhibitor, L-NG<sup>G</sup> monomethyl arginine (LNMMA), to the cultures suppressed NOS activity and allowed a robust proliferation response to occur. These findings have since been extended to both *in vitro* and *in vivo* murine models, indicating that NO inhibits the proliferation of T cells. Macrophage activation in experimental murine trypanosomiasis induces the release of NO, which down regulates the proliferative response of T cells during infection (Sternberg, *et al.*, 1992; schleifer, *et al.*, 1993). Results from the present study indicated that T cell activity is enhanced by the absence of large amounts of NO production from iNOS.

NO from iNOS in endothelial cells may be involved in defence. Without iNOS production from endothelial cells, endothelial cells might not be activated during the infection. The activated T cell might not migrate to the infected tissue to help killing the parasite, Thus, antigen specific T cells continued to expand in the circulation and peripheral lymphoid organs. That may also explain the low inflammation for the carageenan and small footpad swelling in the early stage of Leishmania infection.

#### 6.4.3. iNOS may not be involved in parasite growth control of the *Nramp* gene .

The ability of a host to resist infection with a wide range of viral, bacterial, and parasitic pathogens is strongly influenced by genetic factors (reviewed by Skamene, 1985). In the mouse, infection with leishmania is biphasic, with an early non-immune phase (0-3 weeks) characterised by rapid proliferation of the pathogen of susceptible

strains and absence of parasite growth in resistant strains. The late phase (3-6 weeks) is associated with specific immune response, leading either to clearance of the pathogen load or to persistent infection in the tissue of the susceptible strains. While the late phase of infection is under control of genes linked to the major histocompatibility complex, the difference in innate susceptibility detected in the early phase is controlled by the expression of a single dominant gene in chromosome 1. One of the transcription units in this gene has been cloned as *Nramp* (Nature resistance associated macrophage protein, Vidal, *et al.*, 1993)

*Nramp* is isolated from a group of genes (*Lsh/Ity/Bcg*) controlling the priming activation of macrophages for leishmania, Salmonella and mycobacterium infection. *Nramp* encodes a polytopic integral membrane protein that has structural features common to prokaryotic and eukaryotic transporters and includes a conserved binding-protein-dependent transport motif which may be involved in interaction with peripheral ATP-binding subunits. The N-terminal sequence also carries a proline/serine rich putative SH3 binding domain, consistent with a role for tyrosine kinases in regulating *Nramp* function of  $\beta_1$  integrins, which signal via tyrosine kinases. Transfection studies with the resistant allele demonstrated that *Nramp* also plays a role, either directly or as an additional pleiotropic effect, in IFN- $\gamma$ /LPS upregulated L-arginine transport across the macrophage membrane, thus providing the substrate required to generate NO for both signal transduction and anti-microbial activity (Blackwell, *et al.* 1994). The present study showed that there was no difference in the size of the footpads till five weeks after infection. This may indicate that *Nramp* is not involved in the NO production from iNOS.

#### **6.5. The roles of iNOS in acute inflammation and LPS-induced death**

In the present study, carageenin was injected into the footpads of wild-type and homozygous mice to induce acute inflammation. The result suggested that iNOS was involved in local inflammation. This result also confirmed the result from an early study using L-NMMA to inhibit NO production (Ianaro, *et al.*, 1994). However, spleen cells

from mutant mice, stimulated with Con A, had a higher proliferative response and INF- $\gamma$  production than those from wild-type mice at the 21 days post-treatment. The result from using L-NMMA showed a decrease in INF- $\gamma$  production in the T cells of DLN (draining lymph node ) which were removed at the peak of the inflammatory response. In the present study, however, the spleen cell response was examined at 21 days after inflammation and NO may act at a different stage of inflammation and on T cells at a different location.

In the present study, the LPS-induced death was also tested for the homozygous mice and the wild-type mice. About 50% of wild-type mice died after 3 days of the injection with 12.5mg/kg of LPS, while none of the iNOS mutant mice died. The result suggested that iNOS was involved in LPS-induced death. The other reported iNOS mutant mice were also resistant to LPS-induced death under anaesthesia (MacMicking *et al.* 1995). However, unanaesthetised iNOS mutant mice suffered as much LPS-induced liver damage as wild-type mice. These authors suggested that there exist both iNOS-dependent and iNOS-independent routes to LPS induced hypotension and death. The difference between the two iNOS mutant mice in response to LPS-induced shock may be due to the different gene back ground of the two strains of mice. The outbred mice (MF1) which were used in our study may be more resistant to the liver damage of the LPS-induced shock than the inbred mice (129/sv) reported by MacMicking *et al.* (1995).

## **6.6. Conclusions**

Results from the present study show that although iNOS can be induced in nearly every cell type, the animal is viable without iNOS in the mutant mice. This may be the result of redundant functions of the other isoform of NOS. However, iNOS or NO production from iNOS is involved in the host defence against parasite infection and in regulating cell-mediated immunity *in vivo* when the immune system is activated by pathogens. iNOS is also involved in the LPS-induced death and the acute inflammation.

The iNOS mutant mice, provide a useful tool that will not only facilitate formal demonstration of the effector roles of NO in microbicidal, tumoricidal, transplantation and in a range of immunopathologies, but also help to define the involvement of NO in immune regulation, immunological tolerance and antigen processing and presentation.

## **6.7. Future work for the iNOS mutant mice**

### **6.7.1 Analysis of recombination events**

Although the iNOS expression is disrupted by the iNOS gene targeting in the present study, there appears not to be a straight forward deletion of exons 1-5 as intended, but an insertion and translocation of the disrupted iNOS gene. This could be a unique hitherto unreported recombination event which could have a fundamental influence on gene-targeting technology. The following work may be carried out:

In the construction of the iNOS-deficient mice, about 21kb iNOS genomic DNA (containing 8 exons contributing to 937 of the 4117bp iNOS mRNA) was cloned from B6 and 129/sv mice genomic libraries. Genomic libraries from both wild-type and mutant mice can be screened with the following probes: 5' and 3' end iNOS gene-specific probes (used for screening iNOS gene targeting events), iNOS cDNA probe, and *neo* gene probe. The cloning genomic DNA from the two strains could then be mapped and compared to find the exact mutation point. If the translocation occurred far away from the wild-type iNOS gene locus, pulse field gel or even fluorescence *in situ* hybridisation may be used to locate it.

### **6.7.2 Human iNOS (hiNOS) transgenic mice**

The result from this study shown that iNOS plays a crucial role as a mediator of inflammation and as a key agent in LPS-induced death. Thus, inhibitors which are highly specific and selective for human iNOS could potentially be of great therapeutic value for some of the most important immunopathologies. Introduce human iNOS gene into the

iNOS-deficient mice and the resultant human iNOS transgenic mice would be extremely valuable for the rational screening of human iNOS-specific inhibitory compounds.

Human iNOS cDNA can be driven by the murine iNOS promoter which has been cloned in our laboratory. Full length human iNOS cDNA with murine iNOS promoter can be constructed together with selection marker gene cassette,  $\beta$ -actin-*neo* gene. The construct can then be transfected into a murine cell line (J774 or Raw), and transfectants selected in medium containing G418. Expression of hiNOS can then be ascertained by stimulating the G418-resistant cells with IFN- $\gamma$  and LPS, and detected by Western blot with anti-human iNOS specific antibody or Northern blot with a human iNOS specific cDNA probe. The successful constructs can then be injected into fertilised eggs from homozygous iNOS -deficient mice. Copies of the transfected gene can be analysed by Southern blot using the *neo* gene probe or hiNOS cDNA probe to hybridise the restriction enzymes digested DNA extracted from tail clips. Western and Northern blots can then be used to identify expression of hiNOS in the peritoneal macrophages from homozygous transgenic mice. This approach, though more straight forward, may result in a strain of hiNOS transgenic mice whose iNOS expression will be significantly different from that of the wild-type mice. This is because the nature of the regulatory elements upstream of the iNOS promoter is not yet defined.

An alternative strategy would be to create a functional hiNOS gene replacement construct, using the murine iNOS promoter as the 5' homologous arm followed by hiNOS cDNA, selection marker *neo* gene cassette and the 3' homologous arm. Functional expression of the construct can be tested as above. Successful constructs can then be transfected into ES cells and recombinants detected by PCR or Southern blot. The ES cell line with hiNOS can then be injected into the blastocysts to generate chimeras as described earlier. Heterozygous from germ line transmission chimeras can then be bred to generate homozygous hiNOS transgenic mice with full of regulation area (including Promoter, repressor and enhancer) and thus may retain the level of iNOS expression akin to the murine system.

These mice can then be used to screen a panel of candidate compounds which are being prepared by a number of pharmaceutical houses. Initially, the LPS-induced death and carrageenin-induced inflammation models can be used. These two modes are well-established.

#### 6.7.3. Phenotypic analysis of iNOS deficient mice

So far, using the iNOS gene targeted mice, we have established the critical role of NO in leishmanial infection, local inflammation and endotoxin-induced death. However, the precise mechanisms mediated by NO in these diseases are unknown. The cytokine and cellular profiles induced in the iNOS-deficient mice following carageenin or LPS injection can be closely monitored with respect to dose-response and kinetics. The role of NO in the production of cytokines such as TNF- $\alpha$ , IL-1 $\beta$ , IL-6, IL-8, IL-12 and IL-15 can be determined *in vivo* and *in vitro*.

## Bibliography

Adams LB, Hibbs J.B, Taintor R.R, Krahenbuhl J.L. **Microbiostatic effect of murine macrophages for *Toxoplasma gondii* : role of synthesis of inorganic nitrogen oxides from L-arginine.** *J. Immunol.* 1990; **144**: 2725-2729.

Albina J.E, Abate J.A, Henry W.L. **Nitric oxide production is required for murine resident peritoneal macrophages to suppress mitogen-stimulated T cell proliferation: role of IFN- $\gamma$  in the induction the nitric oxide synthesizing pathway.** *J. Immunol.* 1991; **147**: 144-148

Alexander P, Evans R. **Endotoxin and double stranded RNA render macrophages cytotoxic** *Nature New Biol.* 1971; **232**: 76-78.

Aratani Y, Okazaki R, Koyama H. **End extension repair of introduced targeting vectors mediated by homologous recombination in mammalian cells** *Nucleic Acids Research* 1992; **20**: 4795-4801.

Barnes BJ, Liew FY. **Nitric oxide and asthmatic inflammation.** *Immunology Today* 1995; **16**: 128-130.

Blackwell JM, Barton CH, White JK, Roach TIA, Shaw MA, Whitehead SH, Mock BA, Searle S, Williams H, Baker AM. **Genetic regulation of leishmanial and mycobacterial infections: the *Lsh / Ity / Bcg* gene story continues** *Immunology Letters* 1994; **43**: 99-107.

Bogle RG, Baydoun AR, Pearson JD, Moncada S, Mann GE. **L-arginine transport is increased in macrophages generating nitric oxide.** *J. Biochem.* 1993; **284**: 15-18.

Boockvar KS, Granger DS, Poston RM, Maybodi M, Washington MK, Hibbs JB, Kurlader RL. **Nitric oxide produced during murine listeriosis is protective.** *Infect. Immun.* 1994; **62**: 1089.

Bradley A, Evans M, Kaufman MH, Robertson E. **Formation of germline chimeras from embryo-derived teratocarcinoma cell lines.** *Nature.* 1984; **309**: 255-256.

Bredt DS, Ferris CD, Snyder SH. **Nitric-oxide synthase regulatory sites-phosphorylation by cyclic AMP-dependent protein kinase, protein-kinase-C, and calcium calmodulin protein kinase identification of flavin and calmodulin binding sites.** *J. Biol. Chem.* 1992; **267**: 10976-10981

Bredt DS, Hwang P M, Glatt CE, Lowenstein C, Reed RR, Snyder SH. **Cloned and expressed nitric-oxide synthase structurally resembles cytochrome-P-450 reductase.** *Nature* 1991; **351**: 714-718.

Capecchi MR. **The new mouse genetics - altering the genome by gene targeting.** *Trends in Genetics.* 1989; **5**: 70-76.

Chan J, Xing Y, Magliozzo RS, Bloom BR. **Killing of virulent mycobacterium-tuberculosis by reactive nitrogen intermediates produced by activated murine macrophages.** *J. Exp. Med.* 1992; **175**:1111-1122.

Charles IG, Palmer RMJ, Hickery MS, Bayliss I, Chubb AP, Hall VS, Moss DW, Moncada S. **Cloning, characterization, and expression of a cDNA encoding an inducible nitric oxide synthase from the human chondrocyte.** *Pro. Natl. Acad. Sci. USA.* 1993; **90**: 11419-11423.

Charron J, Malynn BA, Robertson EJ, Goff SP, Alt FW. **High-frequency disruption of the N-myc gene in embryonic stem and pre-B cell lines by homologous recombination.** *Molecular and Cellular Biology.* 1990; **10**: 1799-1804.

Chartrain NA, Celler DA, Koty PP, Sitrin NF, Nussler AK, Hoffman EP, Billiar TR, Hutchinson NI, Mudgett JS. **Molecular cloning, Structure, and chromosomal localization of the human inducible nitric oxide synthase gene.** *J. Bio. Chem.* 1994; **269**: 6765-6772.

Cocks TM, Angus JA, Campbell JH, Campbell GR. **Release and properties of endothelium-driven relaxing factor (EDRF) from endothelial cells in culture.** *J. Cell. Physiol.* 1985; **123**: 310-320.

Corbett JA, Sweetland MA, Wang JL, Lancaster JR, McDaniel ML. **Nitric oxide mediate cytokine induced inhibition of insulin secretion by human islets of langerhans.** *Proc. Natl. Acad. Sci. USA.* 1993 **90**: 1731-1735.

Cunha FQ, Weiser WY, David JR, Moss DW, Moncada S, Liew FY. **Recombinant migration-inhibitory factor induces nitric oxide synthase in murine macrophages.** *J. Immunol.* 1993; **150**: 1908-1912.

Dalton DK, Pittsmeek S, Keshav S, Figari IS, Bradley A, Stewart TA. **Multiple defects of immune cell-function in mice with disrupted interferon -gamma genes.** *Science* 1993; **259**: 1793-1742.

Demaria R, Cifone MG, Trotta R, Rippo MR, Festuccia C, Santoni A, Testi R. **Triggering of human monocyte activation through CD69, a member of the natural-killer-cell gene -complex family of signal transducing receptors.** *J. Exp. Med.* 1994; **180**: 1999-2004.

Deng C, Capecchi MR. **Reexamination of Gene Targeting Frequency as a Function of the Extent of Homology between the Targeting Vector and the Target Locus** *Molecular and Cellular Biology.* 1992; **12**: 3365-3371.

Dinerman J.L, Dawson TM, Schell MJ, Snowman A, Snyder SH. **Endothelial nitric oxide synthase localized to hippocampal pyramidal cells: implications for synaptic plasticity.** *Proc. Natl. Acad. Sci. USA* 1994; **91**,4214-4218.

Ding AH, Nathan CF, Stuehr DJ. **Release of reactive nitrogen intermediates and reactive oxygen intermediates from mouse peritoneal macrophages comparison of activating cytokines and evidence for independent production.** *J. Immunol.* 1988; **141**: 2407-2412.

Doetschman T, Maeda N, Smithies O. **Targeted mutation of the Hprt gene in mouse embryonic stem cells.** *Pro. Natl. Acad. Sci. USA.* 1988; **85**: 8583-8588.

Drapier JC, Wietzerbin J, Hibbs JB. **Interferon-gamma and tumor necrosis factor induce the L-arginine-dependent cyto-toxic effector mechanism in murine macrophages.** *Eur. J. Immunol.* 1988; **18**: 1587-1592.

Dusting GJ., Hickey H, Akita K, Jachno K, Mutch D, Ng I. **Cyclosporin a Suppresses expression of Two isoforms of Nitric Oxide Synthase in Cultured Macrophages and Vascular smooth Muscle.** *Endothelium* 1995; **3**: 241 s61.

Eizirik DL, Bjorklund A, Welsh N. **Interleukin-1-induced expression of nitric oxide synthase in insulin producing cells is preceded by c-FOS induction and depends on gene transcription and protein synthesis.** *FEBS Lett.* 1993; **317**: 62-66.

Evans MJ, Kaufman MH. **Establishment in Culture of Pluripotential Cells from Mouse Embryos.** *Nature* 1981; **292**:154-156.

Evans TG, Thai L, Granger DL, Hibbs JB Jr. **Effect of in vivo inhibition of nitric oxide production in murine leishmaniasis.** *J. Immunol.* 1993; **151**: 907.

Farrell AJ, Blake DR, Palmer RMJ, Moncada S. **Increased concentrations of nitrite in synovial fluid and serum samples suggest increased nitric oxide synthesis in rheumatic disease.** *Ann Rheum Dis.* 1992; **51**: 1219-1222.

Fehleisen. **Ueber die Zuchtung der Erysipelkokken auf kunstlichen Nahrboden und ihre Uebertragbarkeit auf den Menschen.** *Dtsch Med Wochenschr* 1982; **8**: 553-554.

Fitch FW, McKisic MD, Lancki DW, Gajewski TF. **Differential regulation of murine T lymphocyte subsets.** *Annu. Rev. Immunol.* 1993; **11**: 29-48.

Fujisawa H, Ogura T, Kurashima Y, Yokoyama T, Yamashita J, Esumi H. **Expression of 2 types of nitric oxide synthase messenger RNA in human neuroblastoma cell-lines.** *J. Neurochem.* 1994; **63**: 140-145.

Furchgoot RF. **Studies on endothelium-dependent vasodilation and the endothelium-derived relaxing factor.** *Acta. Physiol. Scand.* 1990; **139**: 257-270.

Furchgott RF, Zawadzki JV. **The obligatory role of endothelial cells in the relaxation of arterial smooth muscle by acetylcholine.** *Nature* 1980; **288**: 373-376.

Galea E, Feinstein DL, Reis DJ. **Induction of calcium independent nitric oxide synthase activity in primary rat glial cultures.** *Proc. Natl. Acad. Sci. USA.* 1992; **89**: 10945-10949.

Galli-Taliadoros LA., Sedgwick JD, Wood SA, Korner H. **Gene knock-out technology: a methodological overview for the interested novice.** *J. of Immunology Methods* 1995; **181**: 1-15.

Gazzinelli RT, Eltoun I, Wynn TA, Sher A. **Acute cerebral toxoplasmosis is induced by *in vivo* neutralization of TNF- $\alpha$  and correlates with the down-regulated expression of inducible nitric oxide synthase and other markers of macrophage activation.** *J. Immunol.* 1993; **151**: 3672.

Geller DA, Nussler AK, Disilvio M, Lowenstein CJ, Shapiro RA, Wang SC, Simmons RL, Billiar TR. **Cytokines, endotoxin, and glucocorticoids regulate the expression of inducible nitric oxide synthase in hepatocytes.** *Proc. Natl. Acad. Sci. USA.* 1993; **90**: 522-526.

Geller, DA., Lowenstein DJ, Shapiro RA, Nussler AK, Disilvio M, Wang SC, Nakayama DK, Simmons RL, Snyder SH, Billiar TR. **Molecular cloning and expression of inducible nitric oxide synthase from human hepatocytes.** *Proc. Natl. Acad. Sci. USA.* 1993; **90**: 3491-3495.

Goureau O, Lepoivre M, Becquet F, Courtois Y. **Differential regulation of inducible nitric oxide synthase by fibroblast growth factors and transforming growth factor beta in bovine retinal pigmented epithelial cells inverse correlation with cellular proliferation.** *Proc. Natl. Acad. Sci. USA.* 1993; **90**: 4276-4280.

Green LC, Wagner DA, Ruisde lusuriaga K, Istfa N, Young VR, Tannenbaum SR. **Nitrate biosynthesis in man.** *Proc. Natl. Acad. sci. USA.* 1981; **78**: 7764-7768.

Green SJ, Meltzer MS, Hibbs JB, Nacy CA. **Activated macrophages destroy intracellular *Leishmania major* amastigotes by an L-arginine dependent killing mechnism.** *J. Immunol.* 1990; **144**: 278-283.

Green SJ, Nacy CA. **Antimicrobial and immunopathologic effects of cytokine-induced nitric oxide synthesis.** *Curr. Opin. Infect. Dis.* 1993; **6**: 384.

Griffith TM, Edwards DH, Lewis MJ, Newby AC, Henderson AH. **The nature of endothelium-derived vascular relaxant factor.** *Nature.* 1984; **308**: 645-647.

Gryglewski RJ, Moncada S, Palmer RMJ. **Bioassay of prostacyclin and endothelium derived relaxing factor (EDRF) from porcine aortic endothelial cells.** *Br J. Pharmacol.* 1986a; **87**: 685-694.

Gryglewski RJ, Palmer RMJ, Moncada S. **Superoxide anion is involved in the breakdown of endothelium-derived vascular relaxing factor.** *Nature* 1986; **320**: 454-456.

Gryglewski RJ, Palmer RMJ, Moncada S. **Superoxide anion is involved in the breakdown of endothelium-derived vascular relaxing factor.** *Nature.* 1986b; **320**: 454-456.

Hall AV, Antoniou H, Wang Y, Cheug AH, Arbus AM, Olson SL, Lu WC, kau CL, Marsden PA. **Structural Organization of the Human Neuronal Nitric Oxide Synthase Gene (NOS1).** *J. Bio.Chem.* 1994; **269**: 33082-33090.

Hasty P, Rivera-perez J, Bradley A. **The length of homology required for gene targeting in embryonic stem cells.** *Mol. Cell. Biol.* 1991; 11, 5586-5591.

Heck DE, Laskin DL, Gardner CR, Laskin JD. **Epidermal growth factor suppresses nitric oxide and hydrogen peroxide production by keratinocytes potential role for nitric oxide in the regulation of wound healing.** *J. Bio. Chem.* 1992; **267**: 21277-21280.

Hevel JM, White KA, Marletta MA. **Purification of the inducible murine macrophage nitric oxide synthase identification as a flavoprotein.** *J. Bio. Chem.* 1991; **266**: 22789-22791

Hibbs JB, Lambert LH, Remington JS. **Control of carcinogenesis: a possible role for the activated macrophage** *Science* 1972; **177**: 998-1000.

Hibbs JB, Taintor RR, Vavrin Z. **Macrophage cyto-toxicity-role for L-arginine deiminase and imino-nitrogen oxidation to nitrite.** *Science* 1987; **235**: 473-476.

Hibbs JB, Vavrin Z, Taintor RR. **L-arginine is required for expression of the activated macrophage effector mechanism causing selective metabolic inhibition in target-cells.** *J. Immunol.* 1987; 138, 550-565

Hibbs JB. **Nitric Oxide from L-arginine: a Bioregulatory System.** (Moncada, S. and Higgs, E.A., eds) 1990, pp.189-223, Excerpta Medica

Hoffman RA, Langrehr JM, Billiar TR, Curran RD, Simmons RL. **Alloantigen-induced activation of rat splenocytes is regulated by the oxidative metabolism of L-arginine.** *J. Immunol.* 1990; **145**: 2220-2226.

Holiday BJ, Sadick MD, Wang Z-E, Reiner SL, Heinzl FP, Parslow TG, Locksley RM. **Reconstitution of leishmania immunity in severe combined immunodeficient mice using Th1- and Th2-like cell line.** *J. Immunol.* 1991; **147**: 1653-1658.

Huang S, Hendriks W, Althage A, Hemmi S, Bluethmann H, Kamijo R, Vilcek J, Zinkernagel RM, Aguet M. **Immune-response in mice that lack the interferon-gamma receptor.** *Science* 1993; **259**: 1742-1745.

Ialenti A, Ianaro A, Moncada S, Di Rosa M. **Modulation of acute inflammation by endogenous nitric oxide.** *Eur. J. Pharmacol.* 1992; **211**: 177-182.

Ialenti A, Moncada S, DiRosa M. **Modulation of adjuvant arthritis by endogenous nitric oxide.** *Br. J. Pharmacol.* 1993; **110**: 701-706.

Ianaro A, O'donnell CA, Dirosa M, Liew FY. **A nitric oxide synthase inhibitor reduces inflammation, down-regulates inflammatory cytokines and enhances interleukin-10 production in carrageenin-induced oedema in mice.** *Immunology.* 1994; **82**: 370-375.

Ignarro LJ, Buga GM, Wood KS, Byrns RE, Chaudhuri G. **Endothelium-derived relaxing factor produced and released from artery and vein is nitric oxide.** *Proc. Natl. Acad. Sci. USA.* 1987; **84**: 9265-9269.

Imai T, Hirata Y, Kanno K, Marumo F. **Induction of nitric oxide synthase by cyclic AMP in rat vascular smooth muscle cells.** *J. Clin. Invest.* 1994; **93**: 543-549.

Imai T, Hirata Y, Marumo F. **Expression of brain nitric-oxide synthase messenger RNA in various tissues and cultured cells of rat.** *Biomed. Res.* 1992; **13**: 371-374.

Iyengar R, Stuehr DJ, Marletta MA. **Macrophage synthesis of nitrite, nitrate, and N-Nitrosamine-precursors and role of the respiratory burst.** *Proc. Natl. Acad. Sci. USA.* 1987; **84**: 6369-6373.

Jaenisch R. **Transgenic animals.** *Science* 1988; **240**: 1468-1475.

Jenefer M, Blackwell C, Barton H, Jacqueline K, Tamara W, Roach IA, Shaw MA, Shiteehed SH, Mock BA, Searle S, Williams H, Baker AM. **Genetic regulation of**

**leishmanial and mycobacterial infections: the *Lsh/Ity/Bcg* gene story continues.** *Immunology Letters* 1994; **43**: 99-107.

Jenkins DC, Charles IG, Thomson LL, Moss DW, Holmes LS, Baylis SA, Rhodes P, Westmore K, Emson PC, Mocada S. **Role of nitric oxide in tumor growth.** *Proc. Natl. Acad. Sci. USA.* 1995; **92**: 4392-4396.

Johnson RS, Sheng M, Greenberg ME, Kolodner RD, Papaioannou VE, Spiegelman BM. **Targeting of nonexpressed genes in embryonic stem cells via homologous recombination.** *Science* 1989; **245**: 1234-1236.

Kamijo R, Harada H, Matsuyama T, Bosland M, Gerecitano J, Shapiro D, Le J, Koh SI, Kimura T, Green SJ, Mak TW, Taniguchi T, Vilcek J. **Requirement for transcription factor IRF-1 in NO synthase induction in macrophages.** *Science* 1994; **263**: 1612-1615.

Keller R, Jones VE. **Role of activated macrophages and antibody in inhibition and enhancement of tumour growth in rats.** *The Lancet.* 1971; **22**: 842-849.

Kirk SJ, Regan MC, Barbul A. **Cloned murine T lymphocytes synthesize a molecule with the biological characteristics of nitric oxide.** *Biochem. Biophys. Res. Commun.* 1990; **173**: 660-665.

Kishimoto J, Spurr N, Liao M, Lizhi L, Emson P Xu WM. **Localization of brain nitric oxide synthase (NOS) to human chromosome 12.** *Genomics.* 1992; **14**: 802-804.

Kobzik L, Reid MB, Bredt DS, Stamler JS. **Nitric oxide in skeletal muscle.** *Nature.* 1994; **372**: 546-548.

Koide M, Kawahara Y, Tsuda T, Yokoyama M. **Cytokine induced expression of an inducible type of nitric oxide synthase gene in cultured vascular smooth muscle cells.** *FEBS Lett.* 1993; **318**: 213-217.

Kolb H, Kiesel U, Kroncke KD, Kolbbachofen V. **Suppression of low-dose streptozotocin induced diabetes in mice by administration of a nitric oxide synthase inhibitor.** *Life Sciences.* 1991; **49**: 213-217.

Korprowski H, Zheng YM, Heber-katz E, Fraser N, Rorke L, Fu ZF, Hanlon C, Dietzschold B. **In vivo expression of inducible nitric oxide synthase in experimentally induced neurologic disease.** *Proc. Natl. Acad. Sci. USA.* 1993; **90**: 3024.

Kuhn R, Lohler J, Rennick D, Jajewsky K, Muller W. **Interleukin-10-deficient mice develop chronic enterocolitis .** *Cell* 1993; **75**: 263

Kuhn R, Rajewsky K, Muller W. **Generation and analysis of interleukin-4 deficient mice.** *Science* 1992; **254**: 707.

Kwon NS, Nathan CF, Stuehr DJ. **Reduced biopterin as a cofactor in the generation of nitrogen-oxides by murine macrophages.** *J. Bio. Chem.* 1989; **264**: 19654-19658.

Langrehr JM, Hoffman RA, Billiar TR, Lee KKW, Schraut WH, Simmons RL. **Nitric oxide synthesis in the in vivo allograft response: a possible regulatory mechnism.** *Sugery* 1991; **110**: 335-342.

Lenardo MJ, Baltimore D. **NF-kappa-B a pleiotropic mediator of inducible and tissue specific gene control.** *Cell.* 1989; **58**: 227-229.

Liew FY, Cox FEG. **Nonspecific defense-mechanism: The role of nitric oxide.** *Immunol. Today* 1991; **12**: A17-A21.

Liew FY, Millott S, Parkinson C, Palmer RMJ, Moncada S. **Macrophage killing of leishmania parasite in vivo is mediated by nitric oxide from L-arginine.** *J. Immunol.* 1990; **144**: 4794-4797

Liew FY. **Regulation of Cell-Mediated Immuity in Leishmaniasis.** *Current Topics in Microbiology and Immunology* 1990; **155**: 53-64

Lin FL, Sperle K, Steernberg N. **Recombination in mouse L-cells between DNA introduced into cells and homologous chromosomal sequences.** *Proc. Natl Acad. Sci. U.S.A.* 1985; **82**: 1391-1395.

Lorsbach RB, Murphy WJ, Lowenstein CJ, Snyder SH, Russell SW. **Expression of the nitric oxide synthase gene in mouse macrophages activated for tumor cell killing molecular basis for the synergy between interferon gamma and Lipopolysaccharide.** *J. Bio. Chem.* 1993; **268**: 1908-1913.

Lorsbach RB, Murphy WJ, Lowenstein CJ, Snyder SH, Russell SW. **Expression of the nitric oxide synthase gene in mouse macrophages activated for tumor cell killing molecular basis for the synergy between interferon gamma and lipopolysaccharide.** *J. Bio. Xhem.* 1993; **268**: 1908-1913.

Lowenstein CJ, Alley EW, Raval P, Snowman AM, Snyder SH, Russell SW, Murphy WJ. **Macrophage nitric oxide synthase gene : 2 upstream regions mediate induction by intergeron gamma and lipopolysaccharide.** *Proc. Natl. Acad. Sci. USA.* 1993; **90**: 9730-9734.

Lowenstein CJ, Glatt CS, Bredt DS, Snyder SH. **Cloned and expressed macrophage nitric oxide synthase contrasts with the brain enzyme.** *Proc. Natl. Acad. Sci. USA.* 1992; **89**: 6711-6715.

Lukic ML, Stosicgrujicic S, Ostojic N, Chan WL, Liew FY. **Inhibition of nitric oxide generation affects the induction of diabetes by streptozocin in mice.** *Biochem. Biophys. Res. Commun.* 1991; **178**: 913-920.

Lyons CR, Orioff GJ, Cunningham JM. **Molecular cloning and functional expression of an inducible nitric oxide synthase from a murine macrophage cell line.** *The Journal of biological Chemistry.* 1992; **267**: 6370-6374.

Mackman N, Brand K, Edgington TS. **Lipopolysaccharide mediated transcriptional activation of the human tissue factor gene in THP-1 monocytic cells requires both**

**activator protein 1 and nuclear factor kappa B binding sites.** *J. Exp. Med.* 1991; **174**: 1517-1526.

Macmicking JD, Nathan C, Hom G, Chartrain N, Fletcher DS, Trumbauer M, Stevens K, Xie QW, Sokol K, Hutchinson N, Chen H, Mudgett JS. **Altered responses to infection and endotoxic shock in mice lacking inducible nitric oxide synthase.** *Cell* 1995; **81**: 641-650.

Mansour SL, Thomas KR, Capecchi MR. **Disruption of the proto-oncogene int-2 in mouse embryo-derived stem cells: a general strategy for targeting mutations to non-selectable genes.** *Nature* 1988; **336**: 348-352.

Mansour SL, Thomas KR, Deng CX, Capecchi MR. **Introduction of a Lac Z Reporter Gene into the Mouse int-2 Locus by homologous Recombination.** *Proc. Natl. Acad. Sci. U.S.A.* 1990; **87**: 7688-7692.

Marletta MA. **Nitric Oxide Synthase Structure and Mechanism.** *The Journal of Biological Chemistry.* 1993; **268**: 12231-12234.

Marletta MA. **Nitric oxide: biosynthesis and biological significance.** *TIBS* 1989; **14**: 488-492.

Marsden PA, Heng HHQ, Duff CL, Shi XM, Tsui LC, Hall AV. **Localization of the human gene for inducible nitric oxide synthase (NOS2) to chromosome 17q11.2-Q12.** *Genomics.* 1994; **19**: 183-185.

Marsden PA, Heng HHQ, Scherer SW, Stewart RJ, Hall AV, Shi XM, Tsui LC, Schappert KT. **Structure and chromosomal localization of the human constitutive endothelial nitric oxide synthase gene.** *J. Bio. Chem.* 1993; **268**: 17478-17488.

Martin GR. **Isolation of a Pluripotential Cell-line from Early Mouse Cultured in Medium Conditioned with Teratocarcinoma Cells.** *Proc. Natl Acad. U.S.A.* 1981; **78**: 7634-7639.

Martin W, Villani GM, Jothianandan D, Furchgott RF. **Selective blockade of endothelium-dependent and glyceryl trinitrate-induced relaxation by hemoglobin and by methylene blue in the rabbit aorta.** *J. Pharmacol. Exp. Ther.* 1985; **232**: 708-716.

Martin W, Villani GM, Jothianandan D, Furchgott RF. **Selective blockade of endothelium-dependent and glyceryl trinitrate-induced relaxation by hemoglobin and by methylene blue in the rabbit aorta.** *J. Pharmacol. Exp. Ther.* 1985; **232**: 708-716.

Mayer B, John M, Bohme E. **Purification of a Ca<sup>2+</sup>/calmodulin-dependent nitric oxide synthase from porcine cerebellum.** *FEBS Lett.* 1990; **277**: 215-219.

Mayer B, John M, Werner ER, Wachter H, Schultz G, Bohme E. **Brain nitric oxide synthase is a biopterin containing and flavin containing multifunctional oxidoreductase.** *FEBS letters* 1991; **288**: 187-191.

Middleton SJ, Shorthouse M, Hunter JO. **Increased nitric oxide synthesis in ulcerative colitis.** *Lancet.* 1993; **341**: 465-466.

Miller MJS, Sadowska-Krowicka H, Chorinaruemol S, Kakkis JL, Clark DA. **Amelioration of chronic ileitis by nitric oxide synthase inhibition.** *J. Pharmacol. Exp. Ther.* 1993; **264**: 11-16.

Mombaerts P, Clarke AR, Hooper ML, Tonegawa S. **Creation of a large Genomic Deletion at the T-cell Antigen Receptor-subunit Locus in Mouse Embryonic Stem Cells by Gene targeting.** *Proc. Natl. acad.Sci. U.S.A.* 1991; **88**: 3084-3087.

Moncada S, Higgs A. **The L-arginine-nitric oxide pathway.** *The New England Journal of Medicine.* 1993; **11**: 2002-2012.

Moncada S, Higgs EA. **Nitric Oxide from L-arginine: a Bioregulatory System.** *Excerpta Medica* 1990;pp19-33.

Moncada S, Palmer RMJ, Higgs EA. **Nitric Oxide: Physiology, Pathophysiology, and Pharmacology.** *Pharmacological Reviews* 1991; **43**: 109-142.

Moncada S, Palmer RMJ. **The L-arginine: nitric oxide pathway in the vessel wall.** In Nitric oxide from L-arginine: A bioregulatory system. ed. by S.Moncada and EA. Higgs, pp19-33. Elsevier. Amsterdam. 1990.

Moncada S. **The L-arginine: nitric oxide pathway.** *Acta. Physiol. Scand.* 1992; **145**: 201-227.

Morris L, Troutt AB, McLeod KS, Kelso A, Handman E, Aebischer T. **Interleukin 4 but not gamma interferon production correlates with the severity of murine cutaneous leishmaniasis.** *Infect. Immun.* 1993; **61**: 3459-3465.

Morris SM, Billiar TR. **New insights into the regulation of inducible nitric oxide synthesis.** *Am. Phys. Soc.* 1994; **94**: E829-838.

Mosmann TR, Coffman RL. **Th1-cell and Th2 cell different patterns of lymphokine secretion lead to different functional properties.** *Annu. Rev. Immunol.* 1989; **7**: 145-173.

Moss DW, Wei XQ, Liew FY, Moncada S, Charles IG. **Enzymatic characterisation of recombinant murine inducible nitric oxide synthase.** *Eru. J. Pharm.* 1995; **289**: 41-48.

Mossalayi MD, Pauleugene N, Ouaz F, Arock M, Kolb JP, Kilchherr E, Debre P, Dugas B. **Involvement of Fc-epsilon-RII CD23 and L-arginine-dependent pathway in IgE-mediated stimulation of human monocyte functions.** *Int. Immunol.* 1994; **6**: 931-934.

Mount SM. **A catalog of splice junction sequences.** *Nucleic Acids Research.* 1982; **10**: 459-472.

Mountford P, Zevnik B, Duwel A, Nichols J, Li M, Dani C, Robertson M, Chambers I Smith A. **Dicistronic Targeting constructs: Reporters and modifiers of mammalian gene expression.** *Proc. Natl. Acad. Sci. USA.* 1994; **91**: 4303-4307.

Mulligan MS, Hevel JM, Marietta MA, Ward PA. **Tissue injury caused by deposition of immune complexes is L-arginine dependent.** *Proc. Natl. Acad. Sci USA.* 1991; **88**: 6338-6342.

Mundel P, Bachmann S, Bader M, Fischer A, Kummer W, Mayer B, Kriz W. **Expression of nitric oxide synthase in kidney macula densa cells.** *Kidney International.* 1992; **42**: 1017-1019.

Murphy ED, Roths JB. **Autoimmunity and lymphoproliferation: induction by mutant gene *lpr*, and acceleration by a male-associated factor in strain BXSB mice.** In: Rose NR *et al.*, ed. *Genetic control of autoimmune disease.* Elsevier/North Holland, Amsterdam, 1979.

Nakayama DK, Geller DA, Lowenstein CJ, Chern HD, Davies P, Pitt BR, Simmons RL, Billiar TR. **Cytokines and lipopolysaccharide induce nitric oxide synthase in cultured rat pulmonary artery smooth muscle.** *Am. J. Resp. Cell. Mol. Bio.* 1993; **9**: 231.

Nathan C, Xie QW. **Nitric Oxide Synthases: Roles, Tolls, and Controls.** *Cell* 1994; **78**: 915-918.

Nickoloff JA, Reynolds RJ. **Transcription Stimulates Homologous Recombination in Mammalian Cells.** *Mol. Cell Biol.* 1990; **10**: 4837-4845.

Nickoloff JA. **Transcription Enhances Intrachromosomal Homologous Recombination in Mammalian Cells.** *Mol. Cell Biol.* 1992; **12**: 5311-5318.

Nunokawa Y, Ishida N, Tanaka S. **Cloning of inducible nitric oxide synthase in rat vascular smooth muscle cells.** *Bioch. Biophys. Res. Commun.* 1993; **91**: 89-94.

Nussler AK, Billiar TR, Liu ZZ, Morris SM. **Coinduction of nitric oxide synthase and argininosuccinate synthetase in a murine macrophage cell line implications for regulation of nitric oxide production.** *J. Bio. Chem.* 1994; **269**: 1257-1261.

Nussler AK, Disilvio M, Billiar TR, Hoffman RA, Geller DA, Selby R, Madariaga J, Simmons RL. **Stimulation of the nitric oxide synthase pathway in human hepatocytes by cytokines and endotoxin.** *J. Exp. Med.* 1992; **176**: 261-264.

Oswald IP, Eltoun I, Wynn TA, Schwartz B, Caspar P, Paulin D, Sher A, James SL. **Endothelial cells are activated by cytokine treatment to kill an intravascular parasite, *Schistosoma mansoni*, through the production of nitric oxide.** *Proc. Natl. Acad. Sci. USA* . 1994; **91**: 999-1003.

Palmer RMJ, Ashton DS, Moncada S. **Vascular endothelial cells synthesize nitric oxide from L-arginine.** *Nature* 1988; **333**: 664-666.

Palmer RMJ, Ferrige AG, Moncada S. **Nitric oxide release accounts for the biological activity of endothelium derived relaxing factor.** *Nature* 1987; **327**: 524-526.

Palmer RMJ, Moncada S. **A novel citrulline forming enzyme implicated in the formation of nitric oxide by vascular endothelial cells.** *Biochem. Biophys. Res. Commun.* 1989; **158**: 348-352.

Pearse RN, Feinman R, Ravetch JV. **Characterization of the promoter of the human gene encoding the high-affinity Ig G receptor transcriptional induction by Gamma interferon is mediated through common DNA response elements.** *Proc. Natl. Acad. Sci. USA.* 1991; **88**: 11305-11309.

Radomski MW, Palmer RMJ, Moncada S. **Glucocorticoids inhibit the expression of an inducible, but not the constitutive, nitric oxide synthase in vascular endothelial cells.** *Proc. Natl. Acad. Sci. USA.* 1990; **87**: 10043-10047.

- Rapoport RM, Murad F. **agonist induced endothelium-dependent relaxation in rat thoracic aorta may be mediated through cyclic GMP.** *Circ. Res.* 1983; **52**: 352-357.
- Rees DD, Celtek S, Palmer RMJ, Moncada S. **Dexamethasone prevents the induction by endotoxin of a nitric oxide synthase and the associated effects on vascular tone - an insight into endotoxin shock.** *Bioch. iophys. Res. Comm.* 1990; **173**: 541-547.
- Reiling N, Ulmer AJ, Duchrow M, Ernst M, Flad HD, Hauschildt S. **Nitric oxide synthase: mRNA expression of different isoforms in human monocytes/macrophage.** *Eur. J. Immunol.* 1994; **24**: 1941-1944.
- Riele HT, Maandag ER, Berns A. **Highly efficient gene targeting in embryonic stem cells through homologous recombination with isogenic DNA constructs.** *Proc. Natl. Acad. Sci. U.S.A.* 1992; **89**: 5128-5132.
- Robertson EJ. **In Teratocarcinomas and embryonic stem cells: a practical approach.** (ed. E>J. Robertson). *IRL Press, Oxford* 1987.
- Romagnani S. **Human Th1 and Th2 subsets-doubt no more.** *Immunol. Today* 1991; **12**: 256-257.
- Rubanyi GM, Vanhoutte PM. **Superoxide anions and hyperoxide inactivate endothelium-derived relaxing factor.** *Am. J. Physiol.* 1986; **250**: H822-H827.
- Sadlack B, Merz H, Schorle H, Schimpl A, Feller AC, Horak I. **Ulcerative colitis-like disease in mice with a disrupted interleukin-2 gene.** *Cell* 1993; **75**: 253.
- Schleifer KW, Mansfield JM. **Suppressor macrophages in African trypanosomiasis inhibit T cell proliferative response by nitric oxide and prostaglandins.** *J. Immunol.* 1993; **151**: 5492-5503.
- Schmidt HHHW, Gagne GD, Nakane M, Pollock JS, Miller MF, Murad F. **Mapping of neural nitric oxide synthase in the rat suggests frequent colocalization with NADPH diaphorase but not with soluble guanylyl cyclase, and novel paraneural**

**functions for nitrinergic signal transduction. *J. Histochem. Cytochem.* 1992; 40: 1439-1456.**

Schmidt HHHW, Smith RM, Nakane M, Murad F. **Ca<sup>2+</sup> /Calmodulin dependent NO synthase type 1: a biopteroflavoprotein with Ca<sup>2+</sup> /Calmodulin independent diaphorase and reductase activities. *Biochemistry* 1992; 31: 3243-3255.**

Schmidt HHHW, Walter U. **No at Work. *Cell* 1994; 78: 919-925.**

Schwartzberg PL, Goff SP, Robertson EJ. **Germ-line transmission of a *c-abl* mutation produced by targeted gene disruption in ES cells. *Science.* 1989; 246: 799-803.**

Scott P, Natovitz P, Coffman RL, Pearce E, Sher A., **Immunoregulation of cutaneous leishmaniasis. T cell lines that transfer protective immunity or exacerbation belong to different T helper subsets and respond to distinct parasite antigens. *J.Exp. Med.* 1988; 168:1675-1684.**

Shenkar R, Shen MH, Arnheim N. **DNase I-hypersensitive sites and transcription factor-binding motifs within the mouse E $\beta$  meiotic recombination hot spot. *Mol. Cell. Biol.* 1991; 11: 1813-1819.**

Sherman PA, Laubach VE, Reep BR, Wood ER. **Purification and cDNA sequence of an inducible nitric oxide synthase from a human tumor cell line. *Biochemistry.* 1993; 32: 11600-11605.**

Skamene E. **Genetic control of host resistance to infection and malignancy. *Prog. Leukoc. Biol.* 1985; 3: 111-559.**

Smithies O, Gregg RG, Boggs SS, Karalewski MA, Kucheriapati RS. **Insertion of DNA Sequences into the Human Chromosomal  $\beta$ -globin Locus by Homologous Recombination. *Nature* 1985; 317: 230-234.**

Stanton BR, Reid SW, Parada LF. **Germ line transmission of an inactive N-myc allele generated by homologous recombination in mouse embryonic stem cells.** *Mol. Cell. Bio.* 1990; **10**: 6755-6758.

Stenberg J., McGuigan F. **Nitric oxide mediates suppression of T cell response in murine *Trypanosoma Brucei* infection.** *Eur. J. Immunol.* 1992; **22**: 2741-2744.

Stenger S, Thuring H, Rollinghoff M, Bogdan C. **Tissue expression of inducible oxide synthase is closely associated with resistance to *Leishmania major*.** *J. Exp. Med.* 1994; **180**: 783-793.

Stuehr DJ, Cho HJ, Kwon NS, Weise MF, Nathan C. **Purification and characterization of the cytokine induced macrophage nitric oxide synthase an FAD containing and FMN containing flavoprotein.** *Proc. Natl. Acad. Sci. USA.* 1991; **88**: 7773-7777.

Stuehr DJ, Marletta MA. **Induction of nitrite nitrate synthesis in murine macrophages by BCG infection, lymphokine, or interferon gamma.** *J. Immunol.* 1987; **139**: 518-525.

Stuehr DJ, Marletta MA. **Mammalian nitrate biosynthesis: mouse macrophages produce nitrite and nitrate in response to *Escherichia coli* lipopolysaccharide.** *Proc. Natl. Acad. Sci. USA.* 1985; **82**: 7738-7742.

Tayeh MA, Marletta MA. **Macrophage oxidation of L-arginine to nitric-oxide, nitrite, and nitrate- tetrahydrobiopterin is required as a cofactor.** *J. Bio. Chem.* 1989; **264**: 19654-19658.

Taylor-Robinson AW, Phillips RS, Severn A, Moncada S, Liew FY. **The role of T(h)1 and T(h)2 cells in a rodent malaria infection.** *Science* 1993; **260**: 1931-1934.

Thomas KR, Capecchi MR. **Site-directed Mutagenesis by Gene Targeting in Mouse Embryo-derived Stem Cells.** *Cell* 1987; **51**: 503-512.

Thomas KR, Falger KR, Capecchi MR. **High Frequency Targeting of Genes to Specific Sites in the Mammalian Genome.** *Cell* 1986; **44**: 419-428.

Vidal SM, Malo D, Vogan K, Skamene E, Gros P. **Natural resistance to infection with intracellular parasites: Isolation of a candidate for BCG.** *Cell* 1993; **73**: 469-485.

Vodovotz Y, Bogdan C, Paik J, Xie QW, Nathan C. **Mechanisms of suppression of macrophage nitric oxide release by transforming growth factor beta.** *J. Exp. Med.* 1993; **178**: 605-613.

Vouldoukis I, Issaly F, Fourcade C, Pauleugene N, Arock M, Kolb JP, Dasilva OA, Monjour L, Poinot H, Tselentis Y, Dugas B, Debre P, Mossalayi MD. **CD23 and IgE expression during the human immune-response to cutaneous leishmaniasis possible role in monocyte activation.** *Res. in Immunol.* 1994; **145**: 17-27.

Vouldoukis I, Riverosmoreno V, Jugas B, Ouaz F, Becherel P, Debre P, Moncada S, Mossalayi MD. **The killing of leishmania major by human macrophages is mediated by nitric oxide induced after ligation of the Fc-epsilon-RII/CD23 surface-antigen.** *Proc. Natl. Acad. Sci. USA.* 1995; **92**: 7804-7808.

Weinberg JB, Granger DL, Pisetsky DS, Seldin MF, Misukonis MA, Mason SN, Phippen AM, Ruiz P, Wood ER, Gilkeson GS. **The role of nitric oxide in the pathogenesis of spontaneous murine autoimmune disease: increased nitric oxide production and nitric oxide synthase expression in MRL-*lpr/lpr* mice, and reduction of spontaneous glomerulonephritis and arthritis by orally administered N<sup>G</sup>-monomethyl-L-arginine.** *J. Exp. Med.* 1994; **179**: 651-660.

Wood ER, Berger H, Sherman PA, Lapetina EG. **Hepatocytes and macrophages express an identical cytokine inducible nitric oxide synthase gene.** *Biochem. Biophysic. Res. Commun.* 1993; **191**: 767-774.

Xie K, Huang SY, Dong S, Juang SH, Gutman M, Xie QW, Nathan C, Fidler IJ. **Transfection with the Inducible Nitric Oxide Synthase Gene Suppresses**

**Tumorigenicity and Abrogates Metastasis by K-1735 Murine Melanoma Cells.** *J. Exp. Med.* 1995; **181**: 1333-1343.

Xie QW, Cho HJ, Calaycay J, Mumford RA, Swiderek KM, Lee TD, Ding AH, Trosco T, Nathan C. **Cloning and characterization of inducible nitric oxide synthase from mouse macrophages.** *Science.* 1992; **256**: 225-228.

Xie QW, Whisnant R, Nathan C. **Promoter of the mouse gene encoding calcium-independent nitric oxide synthase confers inducibility by interferon gamma and bacterial lipopolysaccharide.** *J. Exp. Med.* 1993; **177**: 1779-1784.

Xu WM, Charles IG, Liu LH, Koni PA, Moncada S, Emson P. **Molecular genetic analysis of the duplication of human inducible nitric oxide synthase (NOS2) sequences.** *Bioch. Biophys. Res. Comm.* 1995; **212**: 466-472.

Yang Z, Sugawara M, Ponath PD, Wessendorf L, Banerji J, Li Y, Strominger JL. **Interferon gamma response region in the promoter of the human DPA gene.** *Proc. Natl. Acad. Sci. USA.* 1990; **87**: 9226-9230.

Zhang HB, Hasty P, Bradley A. **Targeting Frequency for Deletion Vectors in Embryonic Stem Cells.** *Molecular and Cellular Biology.* 1994; **14**: 2404-2410.

Zheng H, Wilson JH. **Gene targeting in normal and amplified cell lines.** *Nature* 1990; **344**: 170-173.